National Technical University of Athens
School of Applied Mathematical And Physical Science
Department of Mathematics

On Knotoids, Braidoids and Their Applications

Neslihan Gügümcü
Ph.D. Thesis

Advisor
Sofia Lambropoulou

Athens, December 2017

National Technical University of Athens
School of Applied Mathematical and Physical Sciences
Department of Mathematics

On Knotoids, Braidoids and Their Applications

Neslihan Gügümcü

Ph.D. Thesis

Advisory Committee: Sofia Lambropoulou
Louis H. Kauffman
Dimitrios Kodokostas

Examining Committee: Sofia Lambropoulou, *Prof., NTUA, Greece*
Louis H. Kauffman, *Prof., University of Illinois At Chicago, USA*
Dimitrios Kodokostas, *Ass. Prof., NTUA, Greece*
Vladimir Turaev, *Prof., Indiana University, USA*
Sam Nelson, *Prof., Claremont McKenna College, USA*
Oktay Pashaev, *Prof., Izmir Institute of Technology, Turkey*
Paolo Bellingeri, *Prof., University of Caen, France*

Athens, December 2017

Summary

In this present thesis, we study on the theory of knotoids that was introduced by V. Turaev in 2012, we introduce the theory of braidoids and lastly we apply the theory of knotoids to the study of proteins. In the first chapter of the thesis, after a detailed recollection of basic notions of knotoids, we construct new invariants of knotoids, including the arrow polynomial, the odd writhe, the parity bracket polynomial, the affine index polynomial, and also give an introduction to the theory of virtual knotoids. These invariants are defined for both classical (knotoids in S^2 or $\mathbb{R}^2$) and virtual knotoids in analogy to the corresponding invariants of virtual knots. We discuss on the virtual closure map that connects the classical knotoid theory to the virtual knot theory and show it is a non-injective and non-surjective map. We show that the arrow polynomial that is an oriented generalization of the bracket polynomial, provides a lower bound estimation for the height (or complexity) invariant of knotoids. We then introduce the affine index polynomial of knotoids and show that the afine index polynomial of a knotoid in S^2 is symmetric. We provide one more lower bound estimation for the height invariant via the affine index polynomial. We compare the two lower bounds for the height invariant provided by the arrow polynomial and the affine index polynomial with some examples. Additionally, we observe that knotoids are the first knotted objects to admit a non-trivial parity in the classical setting. We introduce parity invariants using the parity defined; such as the odd writhe and the parity bracket polynomial. We also give a geometric interpretation of planar knotoids in terms of open ended space curves. This interpretation later in the last chapter is used for the study of protein chains. This part covers the results of works with L.H. Kauffman.

In the second chapter, we introduce the theory of braidoids that forms a 'braided' counterpart theory for the theory of knotoids. We introduce notions of braidoid diagram and isotopy classes of braidoid diagrams, namely, braidoids, and we define a closure operation on a special class of braidoids namely labeled braidoid diagrams. We give two algorithms to turn a knotoid or a multi-knotoid into a labeled braidoid diagram whose closure is isotopic to the initial (multi-)knotoid. With our algorithms and defined closure, we obtain a theorem which is analogous to the classical Alexander theorem for knotoids. After this, we adapt the classical L-moves on braidoid and labeled braidoid diagrams that generate an extended equivalence relation on them, called the L-equivalence together with braidoid isotopy. e show that the L-equivalence provides a bijection between the set of multi-knotoids and the L-equivalence classes of labeled braidoid diagrams. This provides an analogous theorem to the L-move analogoue of the Markov theorem for braidoids that we give

a proof herein. We note that it would not be possible to have such a result without the concept of the L-moves, since we do not have in hand an algebraic structure for braidoids. We introduce a set of elementary blocks that any braidoid is composed of, and we give the defining relations for the 'multiplication' of these blocks that correspond to the braidoid isotopy moves. In this way, we show that braidoids can be encoded in terms of algebraic expressions. We end this chapter with a discussion on further questions and directions for braidoids with a small introduction to the theory of tangloids. This part of the thesis covers the results of the works with Lambropoulou.

Lastly, we study topological modelings of protein chains bu utilizing the geometric interpretation we give for planar knotoids. We observe that planar knotoids provide a finer way to understand the entanglement in protein chains than the using the spherical knotoids and classical modelings utilizing closures for protein chains. We introduce the notion of bonded knotoids for modelling bonded protein chains. We study the twist insertion at bonding sites and provide a detection for sequential, pseudoknot-like and nested bonds by using knotoid invariants, such as the Turaev loop polynomial and the arrow polynomial. We end the thesis with a proposal of an algebraic encoding of polymer chains by corresponding braidoids to their knotoid models. This chapter covers the results of the work with Kauffman, Lambropoulou, Stasiak, Goundaroulis and Dorier.

Acknowledgements

Everything started with a single word: 'Courage!'.
It was a difficult time of the year , the bureaucracy was heavy and as always some other technical difficulties of life surrounded us. I first and foremost would like to thank my advisor Prof. Sofia Lambropoulou for saying me this word, for her continous encouragement from the very beginning until this time, for being on my side in all manners, for being an advisor with whom I could have a cup of aromatic coffee and discuss mathematics at the same time, and for her admirable enthusiasm for mathematics and her surroundings. I am indebted for the things that I have learnt from her and I am hoping that I will continue to learn more. Then after almost one year from 'Courage' , I met with Prof. Louis Kauffman with whom I had met indeed years ago, not personally, but by his books that I discovered at my home university's library. It is still crystal clearly remembered by myself that I was particularly reading his 'orange' book and at the same time wishing to meet with him one day. I would like to thank Prof. Kauffman firstly for writing all those books and being the one why I chose to work on knot theory even though he did not know this, for explaining me all those crystal clear facts for him in great patience and resistance to 'virtual' conditions in our meetings, for being so generous in sharing his knowledge with me, and for being so much supportive and always kind so that I have not lost my track in this big forest.

I would also like to thank, to my professors at the department of mathematics of Middle East Technical University for giving me an attitude in mathematics when I was a bachelor student there, to Prof. Timur Karacay for his trust in me, to Prof. Spiros Argyros and Prof. Panagiotis Psarakos at National Technical University for their support in my survival in Greece, to all professors in the committee for accepting being in this committee, especially to Prof. Sam Nelson for his positive attitude and his hospitality during my visit in Southern California, and to Prof. Vladimir Turaev for introducing the beautiful theory of knotoids that has given rise to this thesis.

This difficult path would not be taken without my family's support. It is going to be left still missing regardless of how much I thank to my mother and father who have done anything for me to be at this point, -I believe the support and the reasons they have been providing to thank them are inexpressible in words-, and to my dear sisters; Yasemin and Sevcan, for always being instantaneously 'there' for me and leaving me never lonely even though we are all in different continents now physically, also I thank to the prettiest and the youngest element in the family; Pietro Deniz, for being an absolute joy for me. I should also admit that it was hard

to be a PhD student in Greece for the difficult times that it has been going through, but I need to say I am glad to be in this land since it has brought me back all my childhood memories that I had with my grandather and grandmother in the island of Kos, sometimes with 'gofrettas' and sometimes with a Greek word my grandfather used to say.

Of course, special thanks go to my friends and colleagues at the same time; Bahar Acu for her dignity and solidarity while sharing the same path with me (and lastly for the West Coaster ride), to Mehmet Oz for meeting me at weird places (of course, we are gonna save Princess Karya!) and Nicat Aliyev for our Sariyer coast memories that have recently expanded to some other coastal memories, to Aras Erzurumluoglu for sharing the same taste in music with me and for his never-fading 'mathematician' jokes, to my Athens friends; Nikos Stamatis for being next to me when everything began very hardly, Yelda Mouemin and Murat Varna for saving me from boredom at times of homesickness.

I lastly thank to Thalis Research Program for supporting my PhD financially.

This has been, sometimes hard mostly joyful but indeed a long path with all its magical events, nice encounterings, coincidences, with all great people and of course with a big course of patience for me. I am glad to walk this path.

Wake! The sky is light!
let us to the road
again . . .
Companion butterfly!
-Bash$\bar{o}$–

Contents

Chapter 1

Preliminaries

1.0 Introduction

In this chapter we recall the concepts of virtual knot theory that will be later consulted throughout the discussion in Chapter 2. The virtual knot theory was introduced by Louis Kauffman [28, 29] in 1996 as a generalization of the classical knot theory. The objects of virtual knot theory are virtual knots and links that are studied either in (thickened) surfaces of some genus up to an equivalence relation called the stable-equivalence or in the 2-sphere S^2 (equivalently in $\mathbb{R}^2$) with the concept of a virtual crossing up to a combinatorial equivalence relation called the virtual equivalence. See Figure 1.1 for two presentations of a virtual knot with respect to two different approaches.

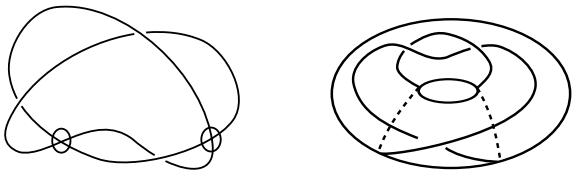

Figure 1.1: The diagrams of a virtual knot in a plane and in a torus

1.1 Basics on virtual knots

Definition 1.1. A *virtual link* k is an embedding of a finite union of disjoint unit circles S^1 in a thickened orientable surface $\Sigma_g \times [0,1]$, of some genus $g \geq 0$
The number of circles in this embedding denotes the *component number* of the virtual link k. A *virtual knot* is a one component virtual link.

Definition 1.2. A *diagram* of a virtual knot k in $\Sigma_g \times I$ is a generic projection of k in Σ_g with finitely many transversal double points that are endowed with over-

/under-data accordingly to the weaving of k and called *crossings* of the diagram.

Definition 1.3. Two virtual knots/links k_1 and k_2 in some thickened surfaces $\Sigma_{g_1} \times I$ and $\Sigma_{g_2} \times I$ are said to be *stably-equivalent* if their diagrams in surfaces Σ_1 and Σ_2 are related to each other by a finite sequence of three Reidemeister moves, orientation preserving homeomorphisms of the surfaces and addition/removal of 1- handles to surfaces in the complements of the diagrams.

The combinatorial way of studying virtual knot theory considers virtual knots/links as represented by *virtual knot diagrams* with finitely many classical (or real) crossings and *virtual crossings* that are neither over-crossings nor under-crossings. A virtual crossing is indicated by two crossing segments with a small circle placed around the crossing point as depicted in Figure 1.2.

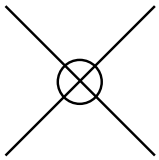

Figure 1.2: A virtual crossing

The equivalence moves on virtual knot/link diagrams, shown in Figure 1.4 are generated by the Reidemeister moves plus the detour move. The *detour move*, shown in Figure 1.3 allows a segment with a consecutive sequence of virtual crossings to be excised and replaced by any other such a segment with a sequence of virtual crossings.

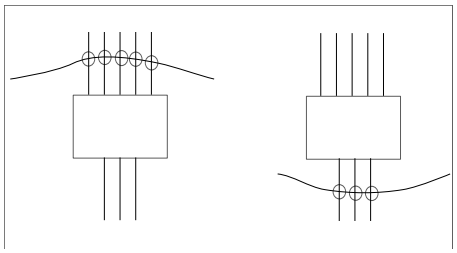

Figure 1.3: The detour move

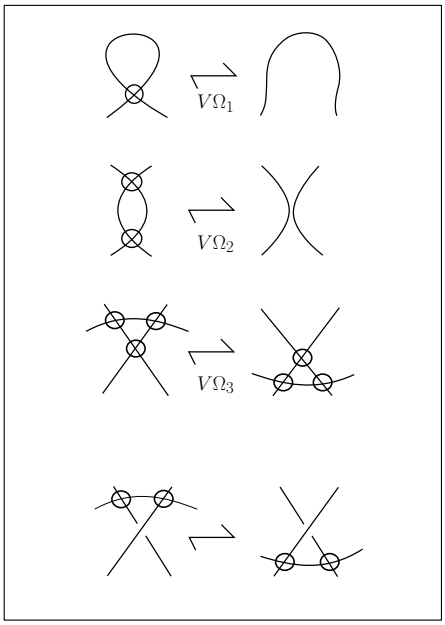

Figure 1.4: Virtual $\Omega_{i=1,2,3}$-moves and a partial virtual move

Definition 1.4. Virtual knot/link diagrams that can be related to each other by a finite sequence of the Reidemeister and detour moves are said to be *virtually equivalent* or *virtually isotopic*. A virtual equivalence class of virtual knot/link diagrams is called a *virtual knot/link*.

There is a one-to-one correspondence between the topological and the combinatorial approach to virtual knot theory. Just as non-planar graphs can be embedded in surfaces of some genus, a virtual knot in the plane can be represented by an embedding of the circle in thickened orientable surfaces without any virtual crossings, or in the opposite direction, an embedding of the circle in some thickened orientable surface can be represented by a virtual knot in the plane by regarding virtual crossings as artifacts of the projection of the relating surface to the plane. Precisely, we have the following theorem.

Theorem 1.5. *([4]) Two virtual link diagrams are virtually equivalent if and only if their surface embeddings are stably-equivalent.*

The proof of this theorem investigates the transition between the two approaches by utilizing abstract knot/link diagrams that are uniquely assigned to virtual knot/link diagrams and associating virtual knot/link diagrams to thickened surface embeddings. More details on abstract diagrams and their association with thickened surfaces appear in [4, 25, 28, 30, 31]. We shall discuss more on an analogous notion of abstract diagrams in relation with knotoid diagrams in Section 2.2.

Definition 1.6. The *genus* of a virtual knot is the minimum genus among the surfaces that the knot has a diagram without any virtual crossings. A diagram of a virtual knot lying in the minimum genus surface are called a *minimal representation* of the virtual knot.

Theorem 1.7. *([41]) (Kuperberg's theorem) Virtual knots/links admit a unique minimal representation.*

Considering classical knots/links in the virtual setting, it can be said that a classical knot/link is a virtual knot of genus 0 (a virtual knot in $S^2 \times I$). Moreover the following theorem resulting from Theorem 1.7, justifies the virtual knot theory is a natural extension of the classical knot theory.

Theorem 1.8. *([10, 28, 29]) If two classical knot diagrams are virtually equivalent to each other then they are equivalent in the classical setting, that is, there is a sequence of Reidemeister moves and planar isotopies taking one another.*

The minimal surface representation of virtual knots can be detected by the surface bracket polynomial introduced by H. Dye and L. Kauffman in [10].

Definition 1.9. Let (F, K) denote a representation of the virtual knot K in the surface F. A *surface state pair*, (F, s) is a collection of disjoint simple closed curves in F obtained by smoothing each crossing of K in A- or B- type. The collection of all state pairs is denoted by (F, S).

Definition 1.10. [10]. Let K be a virtual knot and (F, K) be a fixed representation of K. The *surface bracket polynomial* of K, denoted by $< (F, K) >_S$ is defined as follows.

$$< (F, K) >_S = \Sigma_{(F,s)\in(F,S)} < K|s > d^{|s|}[s],$$

where $< K|s > = A^{\#ofA-smoothings \ - \ \#ofB-smoothings}$, $|s|$ is the number of simple closed curves bounding a disk in F in state s , and $[s]$ is the sum of the isotopy classes of non-trivial curves in the state s up to orientation preserving homeomorphisms of the surface F.

1.1.1 Virtualization of classical crossings

A classical crossing in a classical knot diagram K is *virtualized* as follows. A tangle consisting of a single crossing is removed and replaced with a new tangle consisting

of the opposite crossing flanked by two virtual crossings. See Figure 1.5. This operation is called the *virtualization* of the crossing.

Figure 1.5: Virtualization of a crossing

It is shown in [29] that the Jones polynomial of a classical knot diagram is equal to the Jones polynomial of its virtualization of a crossing. This implies the existence of an infinite set of non-trivial virtual knot diagrams with unit (trivial) Jones polynomial. Precisely, a subset of crossings of a classical knot diagram K is chosen such that K is unknotted when these crossings are switched to opposite crossings. Letting $Virt(K)$ denote the virtual knot diagram obtained by virtualizing each crossing in S, it follows that the Jones polynomial of $Virt(K)$ is equal to unity. Nevertheless, $Virt(K)$ is a non-trivial knot as can be shown by using the involutary quandle invariant of knots [32]. Indeed, if K is non-trivial then its involutary quandle is not trivial [32] and the involutary quandle of $Virt(K)$ is equal to the involutary quandle of K [29].

Theorem 1.11. *(Dye & Kauffman) [10] If K is a classical knot diagram with unknotting number one and non-unit Jones polynomial then $Virt(K)$ is a genus 1 virtual knot.*

Dye and Kauffman utilize the surface bracket polynomial for detecting the resulting knots are indeed non-classical so to prove Theorem 1.11. Note that if K is a non-trivial classical knot with unit Jones polynomial and unknotting number one then the surface bracket polynomial would not detect $Virt(K)$. The following theorem is proved by an analysis of the fundamental group by Silver and Williams [56].

Theorem 1.12. *(Silver & Williams) [56] Let K be a non-trivial classical knot diagram. The virtualization of K, $Virt(K)$ is a non-trivial and non-classical virtual knot.*

Corollary 1. *[10, 56] There is an infinite set of virtual knots of genus* 1 *with unit Jones polynomial.*

1.1.2 Parity in virtual knots

Gauss introduced encoding of plane curves and this was generalized to encoding of knot diagrams with a sequence of labels corresponding to the crossings of an oriented diagram that are met during a full trip along the diagram. A *Gauss* or *chord diagram* of an oriented classical knot diagram consists of such labels that are placed upon a circle with an order of labels and oriented chords (arcs) connecting the same labels. The orientation on chords carries the information of the passages of crossings, that is, the orientation assigned to each chord heads from overpassing strands to underpassing strands. The Gauss diagram of an oriented virtual knot diagram is defined similarly, by placing labels corresponding to the classical crossings on an oriented circle and connecting the same labels via oriented chords. Virtual crossings are not represented on Guass diagrams. See for [28, 29, 47, 57] for Gauss diagrams for flat knots, free knots.

Definition 1.13. [46] A *Gaussian parity* is a rule assigning classical crossings of all knot diagrams of a knot theory to a value in the set of integers modulo two such that
i. the parity is invariant for crossings that do not take place in a Reidemeister move,
ii. for each of the Reidemeister moves, the sum of parities of crossings taking place in these moves is equal to zero modulo two.

The realization of knot diagrams via chord diagrams gives rise to a Gaussian parity in the following way. We say that two chords are linked if the ends of one chord lies on different components obtained by removing the ends of the other chord from the circle. A crossing of a knot diagram is said to be *even* if its corresponding chord is linked with an even number of chords, and *odd* otherwise. Any crossing of a classical knot diagram is even. In fact, it is proved that there is no non-trivial parity for classical knots. For virtual knots, and as we shall show in the next chapter for both classical and virtual knotoids, however, the parity starts being a non-trivial theme with the existence of odd crossings. In fact, it is known that not every Gauss diagram realizes a classical knot diagram, that is, one may need virtual crossings when drawing the corresponding knot diagram to a given Gauss diagram. It is shown [20, 28] that the theory of virtual knots is in one-to-one correspondence with the theory of Gauss diagrams taken up to the equivalence relation on Gauss diagrams induced by the Reidemeister moves. As studied in [26, 28, 29, 36, 46, 87],

the parity in knots gives rise non-trivial invariants of virtual knots. See for [58, 87] for other aspects of parity.

Here we recall the following theorems.

Theorem 1.14. *[46] Given a virtual knot diagram K. If its surface representation is not a minimal genus representation then there exists a knot diagram K' in the virtual equivalence class of K, whose Gauss diagram is obtained by deleting some chords of the Gauss diagram of K.*

Theorem 1.15. *(Nikonov) [46] There is a projection map pr from minimal genus virtual knot diagrams to classical knot diagrams, such that for every knot K, $pr(K)$ is obtained by deleting some chords of K and if two diagrams K_1 and K_2 are related by a Reidemeister move (within the given minimal genus surface) then $pr(K_1)$ and $pr(K_2)$ are related by a Reidemeister move.*

From the above theorems the following theorem follows.

Theorem 1.16. *(Manturov) [46] For every virtual knot diagram K there exists a classical knot diagram K^* such that*
i. *The Gauss diagram of K^* is obtained by deleting some chords of K.*
ii. *$K = K^*$ if and only if K is classical itself.*
iii. *If K and K' are virtually equivalent then the corresponding knots K^* and K'^* are equivalent.*
iv. *The map pr is a surjection when restricted to non-classical knots.*

Here is a corollary of these theorems which will be used in proving a conjecture of Turaev [57] in the next chapter (see for Section 2.3, Proposition 2).

Corollary 2. *[46] Minimal number of classical crossings of a virtual knot can be attained only in minimal genus representations of the knot.*

Chapter 2

On Knotoids

2.0 Introduction

Knotoid diagrams are open ended oriented knot diagrams in oriented surfaces, forming new diagrammatic theories, including an extension of the classical knot theory when the surface of the knotoid is considered to be the 2-sphere S^2 [57]. A standard 1-1 tangle or a long knot has its endpoints in a single region of the diagram. A knotoid diagram generalizes the notion of 1-1 tangle or long knot by allowing the endpoints to be in different regions of the diagram. This gives rise to many topological and algebraic properties of knotoids that are not observed in classical knots, and a more realistic insight for understanding the knottedness in physical structures. In this chapter, we first recollect fundamental notions of knotoids given by Turaev, give a geometric interpretation for planar knotoids, make a small introduction to the theory of virtual knotoid theory, then present and introduce invariants of knotoids, mostly focusing on spherical and planar knotoids given in [15, 57] and discuss about their relations to the height invariant of spherical knotoids. We also give a proof to a conjecture of Turaev on minimal diagrams of knot-type knotoids. The results of this chapter appear in [15–17].

2.1 Basics on knotoids

Definition 2.1. [57] A *knotoid diagram* K in an oriented surface $\Sigma_{g\geq 0}$ is a generic immersion of the unit interval $[0, 1]$ into $\Sigma_{g\geq 0}$

$$K : [0, 1] \to \Sigma_g \text{ such that}$$

i. K has finitely many singular points that are transversal double points. Each double point is endowed with over/under- crossing data and called a *classical crossing*

of the knotoid diagram.

ii. The images of 0 and 1 are two points distinct from each other and any of the crossings. They are regarded as the *endpoints* of a knotoid diagram and called the *tail* (or the *leg*) and the *head*, respectively.

iii. K is endowed with the natural orientation of $[0, 1]$, oriented from tail to head.

Some examples of knotoid diagrams are given in Figure 2.1. The *trivial knotoid diagram* is a knotoid diagram admitting no crossings, as depicted in Figure 2.1(a).

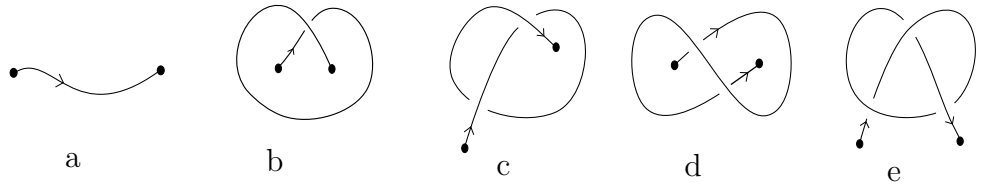

Figure 2.1: **Knotoid diagrams**

The Δ- moves of knot diagrams specifically the Reidemeister moves are adapted to knotoid diagrams as follows. The Reidemeister moves of knotoid diagrams modify a knotoid diagram as shown in Figure 2.2b within small disks surrounding the local the diagrammatic regions and not containing any of the endpoints. These moves are denoted as $\Omega_1, \Omega_2, \Omega_3$ moves, respectively. Together with the planar isotopy moves (moves having no intersecting arc in defining regions, see Figure 2.2a), they are referred as Ω-moves. Since pulling the strand adjacent to an endpoint over and under a transversal strand can turn any knotoid diagram into a trivial knotoid diagram, the moves Φ_+ and Φ_-, depicted in Figure 2.2c are forbidden and called *forbidden moves* of knotoids.

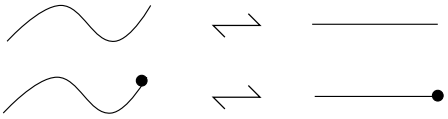

(a) Planar Ω- moves

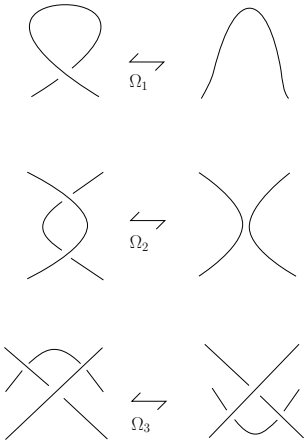

(b) $\Omega_{1,2,3}$- moves

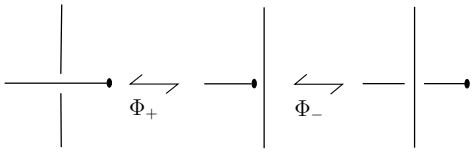

(c) Forbidden moves

Figure 2.2: The moves on knotoid diagrams

Definition 2.2. It is clear that the Ω-moves generate an equivalence relation on knotoid diagrams in a surface Σ_g. Two knotoid diagrams in Σ_g are said to be *equivalent* or *(conspiratorially) isotopic* if they are related to each other by a finite sequence of Ω-moves. The corresponding equivalence classes are called *knotoids* in Σ_g and the set comprising all knotoids in Σ_g is denoted by $\mathscr{K}(\Sigma_g)$. A knotoid diagram is said to *represent* a knotoid if it is in the equivalence class of the knotoid.

Definition 2.3. Let $\mathscr{M}$ be a category of mathematical structures (e.g. polynomials, Laurent polynomials, the integers modulo five, commutative rings, groups, $\cdots$). An *invariant* of knotoids is a mapping I: Knotoids $\to \mathscr{M}$ such that equivalent knotoids map to equivalent structures in $\mathscr{M}$.

2.1.1 Extending the definition of a knotoid

Definition 2.4. A *multi-knotoid diagram* is defined to be a knotoid diagram in an oriented surface Σ with multiple circular components [57]. The equivalence relation

on knotoid diagrams extends naturally to an equivalence relation on multi-knotoid diagrams and a *multi-knotoid* is defined to be an equivalence class of multi-knotoid diagrams.
A *linkoid diagram* is defined to be an immersion of a disjoint union of finitely many unit intervals whose images are knotoid diagrams. The equivalence relation on knotoid diagrams extends naturally to an equivalence relation on linkoid diagrams and a *linkoid* is defined to be an equivalence class of linkoid diagrams

2.1.2 Spherical and planar knotoids

We assume that the 2-sphere S^2 is endowed with the natural orientation extending the orientation on $\mathbb{R}^2$.

Definition 2.5. Knotoid diagrams in S^2 or in $\mathbb{R}^2$ are called *classical knotoid diagrams*. The equivalence classes of classical knotoids are specifically called *spherical knotoids* and *planar knotoids*, respectively.

The sets comprising all spherical and planar knotoids are denoted by $\mathscr{K}(S^2)$ and $\mathscr{K}(\mathbb{R}^2)$, respectively. There is a well-defined map between these two sets of classical knotoids, $\iota : \mathscr{K}(\mathbb{R}^2) \to \mathscr{K}(S^2)$, that is induced by the inclusion $\mathbb{R}^2 \hookrightarrow S^2 \cong \mathbb{R}^2 \cup \infty$ [57]. Any knotoid in S^2 can be represented by a knotoid diagram in $\mathbb{R}^2$ by pushing a representative diagram in S^2 away from $\infty \in S^2$. Considering the equivalence class of this planar representation in $\mathscr{K}(\mathbb{R}^2)$, there is also a well-defined map $\rho : \mathscr{K}(S^2) \to \mathscr{K}(\mathbb{R}^2)$. It is clear that $\iota \circ \rho = id$ so that the map ι is surjective. However, there are examples of nontrivial knotoids in $\mathscr{K}(\mathbb{R}^2)$ which are trivial in $\mathscr{K}(S^2)$. For instance, the knotoid diagram given in Figure 2.1(b) represents a nontrivial planar knotoid [57] whilst it represents the trivial knotoid in S^2. In fact, it can be turned into the trivial diagram by an isotopy of S^2 (pulling the lower arc across S^2 and bringing it back to the diagram side) followed by an Ω_1-move. This suffices to tell that the map ι is not an injective map and unlike the case of the classical knot diagrams, planar and spherical knotoid diagrams yield different theories.

Classical knots via knotoid diagrams

In [57], classical knotoid diagrams are suggested as a new diagrammatic approach to the study of knots in three-dimensional space. Precisely, the endpoints of a knotoid diagram in S^2 can be connected with an arc that is declared to go either under or over every strand it meets. A connection arc is called a *shortcut* of the knotoid diagram. In this way, one obtains an oriented classical knot diagram. One then

can regard the knotoid diagram as a knotoid representation of the corresponding classical knot. In fact, any classical knot can be represented by a knotoid diagram by cutting out an under- or over-passing strand from an oriented diagram of the knot. The connection types due to the passage information of the shortcut, are called the *underpass closure* and the *overpass closure*, respectively. A knotoid diagram may represent different knots depending on the type of the closure. For example, the knotoid in Figure 2.3 represents a trefoil via the underpass closure and represents the trivial knot via the overpass closure.

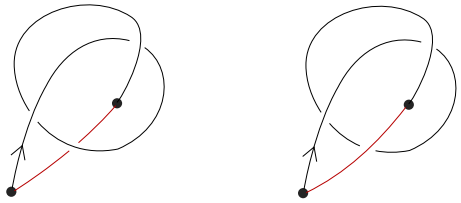

Figure 2.3: Two closures of a knotoid resulting in different knots

In order to have a well-defined representation of knots via knotoid diagrams, one fixes the closure type. In fact, assuming the closure type as the underpass closure induces a well-defined map ω_{-} [15, 57],

$$\omega_{-} :\{ \text{ Knotoids in } \mathrm{S}^2\} \rightarrow \{\text{Classical knots } \} \ .$$

The map ω_{-} is clearly a surjective but not an injective map, in fact we have the following proposition.

Proposition 2.6. *[57] Two knotoid diagrams in S^2 represent the same classical knot if and only if the knotoid diagrams are related to each other by finitely many Ω- moves, the forbidden Φ_{-}-moves and planar isotopy moves in S^2.*

As it is proposed in [57], any invariant of classical knots can be computed on knotoid representatives of knots. Indeed, the use of knotoid diagrams may ease the computation of many knot invariants since knotoid representatives of a knot may have fewer crossings than its knot diagrams. One direct application of this approach is shown on the computation of the knot group [57]. Precisely, a *knotoid group* of a knotoid is defined to be the group represented by generators associated to the overpassings of a knotoid diagram and the relations obtained by imposing Wirtinger relations [38] at each crossing of the diagram [57]. The knotoid group is invariant under the Ω- moves and the forbidden move Φ_{-}. The following lemma shows that the knot group of a knot can be computed on its knotoid representatives.

Lemma 2.7. *([57]) Let κ be a classical knot in $\mathbb{R}^3$ and K be a knotoid in S^2 representing k via the underpass closure. Let $\pi(K)$ denote the knotoid group of K. Then,*

$$\pi_1(\mathbb{R}^3 - \kappa) \cong \pi(K).$$

We see a similar situation [16] for the tricolorability invariant of a classical knot [24]. The tricolorability rules can directly be applied to knotoid diagrams as follows. A knotoid diagram K in S^2 is *tricolorable* if each overpassing strand of K (a strand of K can be colored with one of three colors with respect to the following rules.

- At least two colors must be used.
- At each crossing, the three incident strand should be colored either with the same color or with three different colors.

Clearly, tricolorability of a knotoid is invariant under the Ω- moves and the forbidden move Φ_-. From this it follows that a classical knot is tricolorable if and only if it admits a knotoid representative (via the underpass closure) which is tricolorable. See Figure 2.4 for a tricolorable knotoid diagram which implies the knot it represents, the trefoil knot, is also tricolorable.

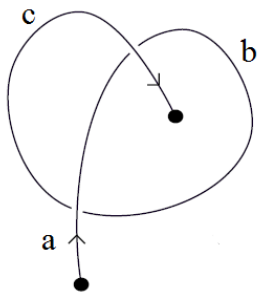

Figure 2.4: A knotoid colored with a, b, c

Spherical knotoids extending classical knot theory

Besides bringing a new diagrammatic approach for the study of classical knots, the theory of knotoids in S^2 is a natural extension of the theory of classical knots [57] in the following way. Let κ be a classical knot and D be an oriented knot diagram of κ in S^2. By cutting out an open arc of D which is disjoint from any of the crossings we obtain a knotoid diagram in S^2. This operation induces the injective map α [57]

$$\alpha\text{: } \{\text{Classical knots}\} \to \mathscr{K}(S^2),$$

defined by assigning κ to the resulting spherical knotoid type. It is shown in [57] that neither the choice of the knot diagram representing κ nor the choice of the open arc to be cut out from the chosen diagram alters the resulting knotoid. Therefore the map α is well-defined. For the injectivity of α, it suffices to see that underpass and overpass closures of any knotoid that is in the image of the map α, are equivalent knot diagrams [57].

Definition 2.8. The knotoids in S^2 that are in the image of the map α are called the *knot-type knotoids*, and otherwise, are called the *pure* or *proper knotoids*.

Let K be a classical knotoid diagram with n crossings. By ignoring the over/under information at each crossing of the diagram K and regarding crossings as vertices, we obtain a connected planar graph with $n+2$ vertices, n of which correspond to the crossings and two of which correspond to the endpoints of K. This graph is called the *underlying graph* of the knotoid diagram K. By Euler's formula, the underlying graph divides S^2 (or $\mathbb{R}^2$) into $n+1$ local regions. We call these regions the *regions of the knotoid diagram* K. Each knot-type knotoid has a knotoid diagram in its equivalence class whose endpoints are located in the same local region of the diagram. Such a knotoid diagram is called a *knot-type knotoid diagram*. The endpoints of a proper knotoid can be in any but different local regions of any of its representative diagrams. Figures 2.1(a),(b),(e), when they are considered in S^2, illustrate some examples of knot-type knotoid diagrams and Figures 2.1(c),(d),(f),(g) illustrate some examples of proper knotoid diagrams.

The set of knotoids, $\mathscr{K}(S^2)$ can be regarded as the union of the set of knot-type knotoids and the set of proper knotoids. The set of classical knots is in one-to-one correspondence with the set of knot-type knotoids via the map α. Note that a knot-type knotoid can be thought as a $1-1$ tangle or a long knot. It is well-known that a classical long knot carries the same knotting information as the classical knot obtained by closing the two endpoints of the long knot [6, 38, 47, 59]. From this it is immediate to conclude that a knot-type knotoid can be considered the same as the classical knot it represents. For proper knotoids this is no longer true. There are proper knotoids (so nontrivial) representing the trivial knot. The knotoid given by the diagram in Figure 2.1(d) is a nontrivial proper knotoid [57] but it represents the trivial knot (via the underpass closure map).

2.1.3 A geometric interpretation of planar knotoids

Let K be a knotoid diagram in $\mathbb{R}^2$. The plane of the diagram is identified with $\mathbb{R}^2 \times \{0\} \subset \mathbb{R}^3$. K can be embedded into $\mathbb{R}^3$ by pushing the overpasses of the

diagram into the upper half-space and the underpasses into the lower half-space in the vertical direction. The tail and the head of the diagram are attached to the two lines, t×ℝ and h×ℝ that pass through the tail and the head, respectively and are perpendicular to the plane of the diagram. Moving the endpoints of K along these special lines gives rise to open oriented curves embedded in $\mathbb{R}^3$ with two endpoints of each on these lines.

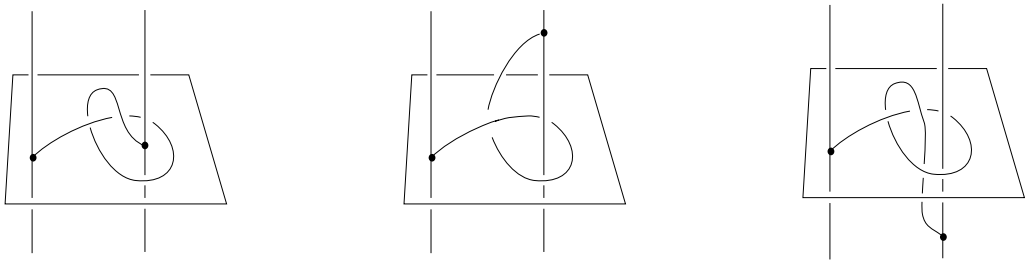

Figure 2.5: Space curves obtained by the knotoid diagram in Figure 2.1(c)

Definition 2.9. Two smooth open oriented curves embedded in $\mathbb{R}^3$ with the endpoints that are attached to two special lines, are said to be *line isotopic* if there is a smooth ambient isotopy of the pair $(\mathbb{R}^3 \setminus \{t \times \mathbb{R}, h \times \mathbb{R}\}, t \times \mathbb{R} \cup h \times \mathbb{R})$, taking one curve to the other curve in the complement of the lines, taking endpoints to endpoints, and lines to lines; $t \times \mathbb{R}$ to $t \times \mathbb{R}$ and $h \times \mathbb{R}$ to $h \times \mathbb{R}$.

Conversely, let be given an open oriented embedded curve in $\mathbb{R}^3$ with a generic projection to the xy- plane. The endpoints of the curve determine two lines passing through the endpoints and are perpendicular to the plane. The generic projection of the curve to the xy- plane along the lines with self-intersections endowed with over and under-crossing data of the curve, is a knotoid diagram in $\mathbb{R}^2$. We call a smooth open embedded curve in $\mathbb{R}^3$ that has a generic projection to the xy- plane a *generic curve with respect to the xy-plane*. Such a curve has a line isotopy class as described in the previous paragraph. We now prove the following theorem appearing in our paper [15].

Theorem 2.10. *[15] Two smooth open oriented curves in $\mathbb{R}^3$ that are generic with respect to the xy-plane are line isotopic with respect to the lines passing through the endpoints if and only if their generic projections to the xy-plane (along the lines) are equivalent knotoid diagrams, that is, they are related by Ω- moves in the plane.*

Proof. Since everything is set in the smooth category, we can switch to the piecewise linear category. Open curves are defined as *piecewise linear curves* in $\mathbb{R}^3$, that is, as

a union of finitely many edges: $[p_1, p_2]$,...,$[p_{n-1}, p_n]$ such that each edge intersects one or two other edges at the points, p_i, $i = 2,...,n-1$ and p_1 and p_n are the endpoints of the curve. We define the *triangle move* in 3- dimensional space. Given an open curve with endpoints on the lines, let $[p_i, p_{i+1}]$ be an edge of the curve and p_0 be a point in the complement of the curve and the two lines. The edge is transformed to two edges $[p_i, p_0]$ and $[p_0, p_{i+1}]$ which form a triangle, whenever this triangle is not pierced by another edge of the curve or by the lines. In the reverse direction, a consecutive sequence of two edges may be transformed to one edge by a triangle move. An ambient isotopy of a piecewise linear curve in the complement of the two lines can be expressed by a finite sequence of triangle moves.

By using triangle moves we can subdivide the edges into smaller edges as shown in Figure 2.6. Any triangle move can be factored into a sequence of smaller triangular moves by *subdividing* the triangles and the edges accordingly. Consider the projection of a curve to the plane, triangular regions that triangular moves take place are projected to non-singular triangles and these triangles possibly contain many strands which are the projection of other edges. The entire ambient isotopy of the curve can be reduced to the shadow cases in the plane shown in Figure 2.7, by subdivision. Inducting on the strands inside the triangles shows that triangle moves are generated by Ω- moves, shown in the left of the figure and the right side shows some cases that are finite combinations of Ω- moves. □

Corollary 3. *[15] There is a one-to-one correspondence between the set of knotoids in $\mathbb{R}^2$ and the set of line-isotopy classes of smooth open oriented curves in $\mathbb{R}^3$ with two endpoints attached to lines that pass through the endpoints and perpendicular to the xy-plane.*

It may be the case that a smooth open oriented curve embedded in $\mathbb{R}^3$ is not generic with respect to the xy-plane but is generic with respect to many other planes. Projecting the curve in the generic way to these planes gives a set of knotoid diagrams in the planes. The line isotopy can be generalized to all the curves that is generic with respect to some plane and Theorem 2.10 above generalizes as follows.

Theorem 2.11. *[15] Two open oriented curves embedded in $\mathbb{R}^3$ that are both generic to a given plane, are line isotopic (with respect to the lines determined by the endpoints of the curves and the plane) if and only if the projections of the curves to that plane are equivalent knotoid diagrams in the plane.*

We say that a knotoid in a plane *represents* an open oriented embedded curve in $\mathbb{R}^3$ if the knotoid is in the equivalence class of the generic projection of the curve to some plane.

The equivalence classes of knotoids in the planes all representing the same open curve embedded in 3-dimensional space, can vary with respect to the projection plane. For instance, the projection of the curve represented in Figure 3(b) to the yz-plane gives a knotoid diagram with the tail and the head in the unbounded region of the plane and one can see that it is equivalent to the trivial knotoid in the yz-plane. The projection to the xy- plane, however, is the knotoid diagram given in Figure 2.1(c) that is a nontrivial knotoid in S^2 as it can be verified by various knotoid invariants such as; the odd writhe, the bracket polynomial or the arrow polynomial (see Figures 2.23 and 2.27. Therefore it is also nontrivial in $\mathbb{R}^2$.

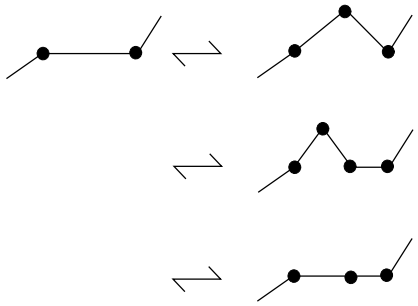

Figure 2.6: Subdivision of an edge

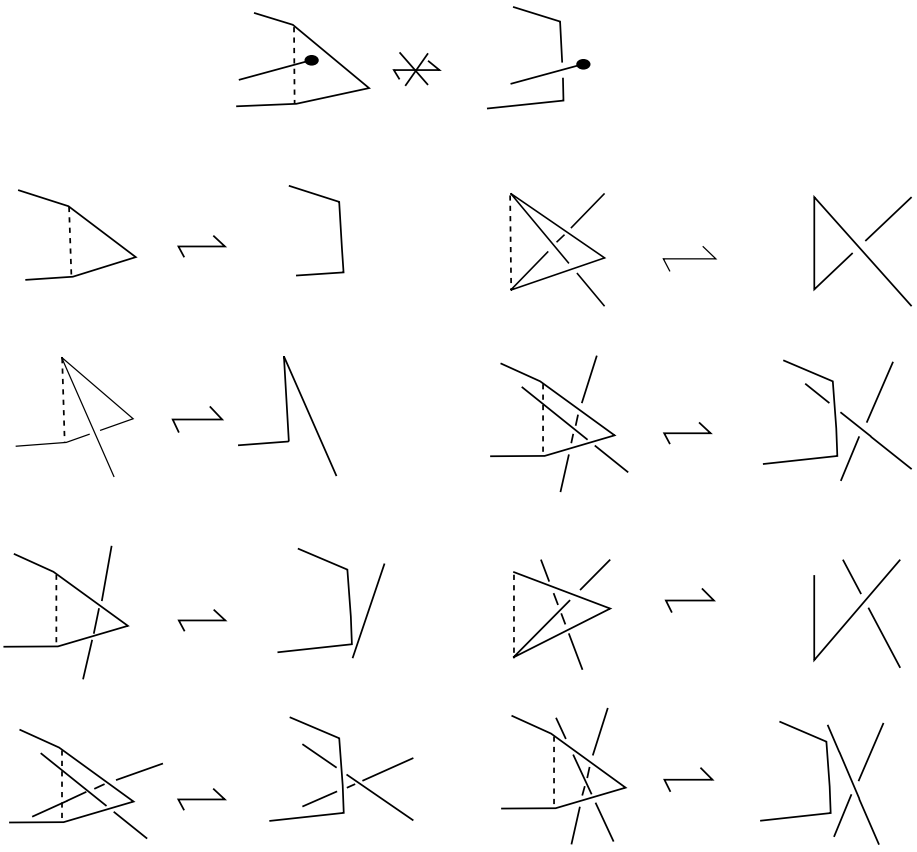

Figure 2.7: Shadow of Δ- moves

2.1.4 Involutions of knotoids

Two commuting operations; reversion and mirror reflection are defined on knotoids in Σ [57]. The *reversion* is induced by reversing the orientation of a knotoid diagram K. More precisely, the reversion operation exchanges the tail and the head. The resulting knotoid diagram is called the *inverse* of K, and is denoted by $\overline{K}$ or $\mathrm{rev}(K)$.
.

The *mirror reflection* is induced by changing overcrossings to undercrossings or vice versa of a knotoid diagram K. The resulting knotoid diagram is called the *mirror image* of K, and is denoted by K^* or $\mathrm{mir}(K)$.

There is another involution operation on spherical and planar knotoids, namely the symmetry [57]. The *symmetry* is induced by reflecting a knotoid diagram K in $\mathbb{R}^2$ with respect to the vertical line $\{0\} \times \mathbb{R}$. The symmetry extends to a self-homeomorphism of S^2 by sending ∞ to ∞ and induces an involution for spherical knotoids as well. The resulting knotoid diagram is said to be *symmetric* to K, and is denoted by $\mathrm{sym}(K)$.

Note 1. The involution operations defined above are also defined for classical knots and virtual knots.
For classical knots the mirror reflection and the symmetry operations coincide since the mirror reflections of a classical knot in any two orthogonal planes are isotopic.
It can be verified that for virtual knots the two operations do not coincide as in the case of knotoids.

2.1.5 Multiplication of knotoids

In [57], a multiplication operation is defined on knotoids in surfaces as follows. Let k_1, k_2 be two knotoids in Σ_1 and Σ_2 represented by two knotoid diagrams $K_1 \subset \Sigma_1$ and $K_2 \subset \Sigma_2$. Let $B_1 \subset \Sigma_1$, $B_2 \subset \Sigma_2$ be 2-disk neighborhoods of the head of K_1, and the tail of K_2, respectively, such that each disk intersects the diagrams along a radius. Such a disk neighborhood is called a *regular neighborhood of an endpoint.* We glue $\Sigma_1 - (B_1)$ to $\Sigma_2 - (B_2)$ through a homeomorphism taking ∂B_1 to ∂B_2 and carrying the single intersection point of ∂B_1 and K_1 to the single intersection point of ∂B_2 and K_2. Then $K_1 - (B_1)$ meets with $K_2 - (B_2)$ at one point and form a knotoid diagram $K1K2$ representing the knotoid k_1k_2 in a surface Σ. Note that the multiplication operation is well-defined up to the orientation preserving homeomorphisms of surfaces and if both Σ_1 and Σ_2 are connected surfaces then Σ is the connected sum of Σ_1 and Σ_2.

The multiplication operation is associative and the trivial knotoid in S^2 is the

identity element [57]. Since $S^2 \# S^2 = S^2$ the set of knotoids $\mathscr{K}(S^2)$ when endowed with the multiplication, forms a semigroup with identity element [57]. Note that the multiplication of spherical knotoids has a clear representation in terms of normal knotoid diagrams. A knotoid diagram in $\mathbb{R}^2$ is said to be *normal* if its tail lies in the outermost region (in the unbounded region of the plane) of the diagram. Any knotoid diagram in S^2 is equivalent to a normal knotoid diagram and the equivalence between two spherical knotoid diagrams is preserved between the coresponding normal knotoid diagrams [57]. A picture for the multiplication for spherical knotoids via normal knotoid diagrams is given in Figure 2.8.

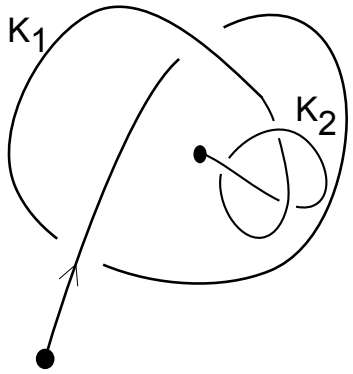

Figure 2.8: Multiplication of two knotoid diagrams

2.1.6 The height of knotoids

Now we present an invariant of knotoids given in [57]. The *height* (or the *complexity* with respect to Turaev's terminology in [57]) of a knotoid diagram K in S^2 is the minimum number of crossings that a shortcut creates during the underpass closure, and it is denoted by $h(K)$ [57]. The *height of a knotoid* k in S^2 is defined as the minimum of the heights, taken over all equivalent classical knotoid diagrams to k, and denoted by $h(k)$. The height is an invariant of knotoids in S^2 [57] that measures how far a knotoid is from being a knot. Precisely, a knotoid in S^2 is of knot-type if and only if its height is zero or equivalently, a knotoid in S^2 has nonzero height if and only it is a proper knotoid [57].

The height of a knotoid is preserved under the basic involutions of knotoid diagrams [57]. That is, for a knotoid K,

$$h(K) = h(\mathrm{mir}(K)) = h(\mathrm{sym}(K)) = h(\mathrm{rev}(K)).$$

Theorem 2.12 ([57, Theorem 4.3])**.** *The height is additive over the multiplication of knotoids, that is,* $h(k_1 k_2) = h(k_1) + h(k_2)$ *for any* $k_1, k_2 \in \mathscr{K}(S^2)$.

The height is also invariant under the isotopy of S^2 so that for the computation of the height one can work with planar representations of spherical knotoids and shortcuts in $\mathbb{R}^2$. The height invariant may get complicated to compute by a direct attack on knotoid diagrams. In Section 2.4.3 and 2.4.2, we will present two lower bounds for the height of a knotoid provided by two knotoid polynomials constructed in the same sections. We will see these lower bounds often ease the estimation of the height.

2.2 Virtual knotoids

As pointed out in [15,57], notions of virtual knot theory extend to knotoids naturally.

Definition 2.13. A *virtual knotoid diagram* is a knotoid diagram in S^2 with an extra combinatorial structure called *virtual crossings*. A virtual crossing is indicated by a circle around the crossing point of two strands, as in the case of virtual knots.

Figure 2.12 depicts an example of a virtual knotoid diagram.
The moves on virtual knot diagrams are generated by the Reidemeister moves and the detour move as for virtual knot diagrams. Similarly, the local moves generated are referred as the virtual $\Omega_{i=1,2,3}$-moves , the partial virtual move (see Figure 1.4) and the virtual Ω_v-move shown in Figure 2.9. The virtual Ω-move is a special case of the detour move that enables to slide back/forth the strand which is adjacent to the tail or the head, deleting/creating virtual crossings located consecutively on the strand. The virtual $\Omega_{i=1,2,3}$-moves, partial virtual moves and Ω_v-moves together with the (classical) Ω-moves are called the *generalized* Ω-moves of virtual knotoid diagrams.

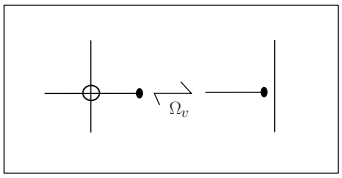

Figure 2.9: Ω_v-move

Definition 2.14. The generalized Ω- moves define an equivalence relation on virtual knotoid diagrams. We say that two virtual knotoid diagrams are *virtually equivalent* if one can be obtained from the other by a finite sequence of the generalized Ω-moves in S^2. The virtual equivalence is denoted by $\sim_{virt}$. A *virtual knotoid* is an equivalence class of virtual knotoid diagrams under this equivalence.

Definition 2.15. Let $\mathscr{M}$ be a category of mathematical structures. A virtual knotoid invariant is a mapping I: Virtual Knotoids $\rightarrow \mathscr{M}$ such that virtually equivalent knotoids map to equivalent structures in $\mathscr{M}$.

Note 2. *Note that any invariant of virtual knotoids is an invariant also of classical knotoids since the generalized* Ω*- moves include the* Ω*- moves.*

A topological interpretation of virtual knotoids

The theory of virtual knotoids has a topological interpretation as explained in our paper [15]. We give a detailed overview here.

Definition 2.16. Let K be a knotoid diagram in a compact connected and oriented surface F. The pair (F, K) is called an *abstract knotoid diagram* if $K \subset F$ is a deformation retract of F.

To any virtual knotoid diagram we can associate an abstract knotoid diagram. Let K be a virtual knotoid diagram. An abstract knotoid diagram associated to a virtual knotoid diagram can be considered to be a ribbon-neighborhood surface containing the knotoid diagram K. This surface is obtained by attaching a 2-disk to each classical crossing and the two endpoints of K such that the crossings and the endpoints are contained in the disks, and connecting these disks by ribbons, as depicted in Figure 2.10a. The virtual crossings are represented by ribbons that pass over one another. The abstract knotoid diagrams are pictured as embedded in 3-dimensional space, but they are not considered as particular embeddings. The ribbons containing virtual crossings can pass over one another in either way. In fact, there is a unique abstract knotoid diagram associated to a virtual knotoid diagram.

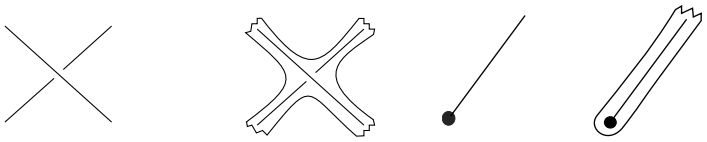

(a) Attaching disks to a classical crossing and to an endpoint

(b) Two ways of attaching bands to a virtual crossing

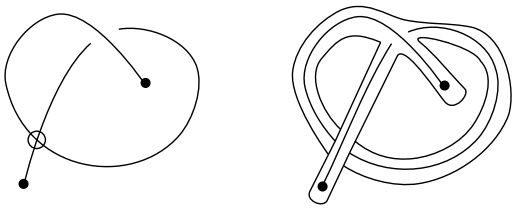

(c) A virtual knotoid diagram and the associated abstract knotoid diagram

Figure 2.10: Abstract knotoid diagrams

Definition 2.17. We say that two abstract knotoid diagrams are *abstractly equivalent* if one can be obtained from the other one by finitely many *abstract* Ω-moves that are shown in Figure 2.11. We denote the abstract equivalence by $\sim_{abst}$. Abstract Ω-moves are ribbon versions of the generalized Ω-moves. The abstract detour move is accomplished by the freedom of movement of the virtual crossings represented by non-interacting ribbon bands. An *abstract knotoid* is defined to be an equivalence class of abstract knotoid diagrams under these moves.

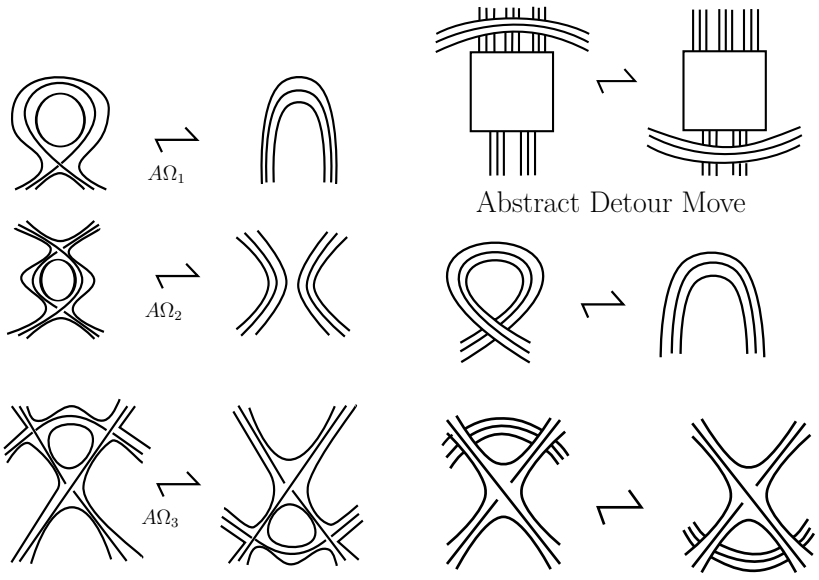

Figure 2.11: Generalized abstract moves

Proposition 2.18. *[15] The mapping*

$$f\text{: } \{\textit{Virtual knotoid diagrams }\} \to \{\textit{Abstract knotoid diagrams }\},$$

that is defined by assigning a virtual knotoid diagram K to the associated abstract knotoid diagram (F, K) induces a bijection

$$f_*\text{: } \{\textit{Virtual knotoid diagrams/} \sim_{virt} \to \{\textit{Abstract knotoid diagrams/}\sim_{abst} \}$$

Proof. Let K_1, K_2 be two virtually equivalent virtual knotoid diagrams and (F_1, K_1) and (F_2, K_2) be the assigned abstract diagrams, respectively. The Ω-moves between these diagrams transform to abstract Ω- moves between (F_1, K_1) and (F_2, K_2). If the given diagrams are related to each other by moves generated by the detour move then (F_1, K_1) and (F_2, K_2) are related by the moves generated by the abstract detour move. This shows the map f_* is well-defined.

Let (F, K) be an abstract knotoid diagram. (F, K) can be embedded in S^3 in a way that the 2- disks containing the classical crossings and the endpoints of K lie in $S^2 \subset S^3$. Being an orientable surface, the abstract knotoid diagram (F, K) can be projected to S^2 so that the projection is an immersion whose only singularities are the transversal intersection of bands. The segments through transversal ribbon bands are projected as transversal segments and the intersection points of the transversal segments are regarded as virtual crossings. So, the image of K under this projection is a virtual knotoid diagram and in fact this virtual knotoid diagram is taken to (F, K) under the map f. Therefore f so f_* are surjective.

It follows similarly as in the case of virtual knots [25] that projection taken with an embedding of the immersed abstract diagram, induces a well-defined map from the set of abstract knotoids to the set of virtual knotoids and this map forms the inverse of f_*. □

Abstract knotoid diagrams are associated to knotoid diagrams in surfaces of higher genus in the following sense. The abstract knotoid diagram (F, K) associated to a virtual knotoid diagram K is a closed connected orientable surface with boundary. The *underlying graph of a virtual knotoid diagram* is the graph that is obtained by turning the classical crossings and the endpoints of K into graphical vertices, and keeping the virtual crossings as they are. The underlying graph of a virtual knotoid diagram is sometimes called a *virtual graph*. A virtual graph is subjected to the detour move but not the Ω-moves.

Let $\Gamma(K)$ be the underlying graph of K. $\Gamma(K)$ is a connected graph with n four-valent vertices corresponding to classical crossings of K, two one-valent vertices corresponding to the endpoints of K, and with $2n+1$ edges. It is a consequence of the

construction of (F, K) that the graph $\Gamma(K)$ is a deformation retract of (F, K). We close the boundary components of (F, K) with 2-disks to have a representation of the virtual knotoid K in a closed connected orientable surface, denoted by $\overline{(F, K)}$. Let δ be the number of boundary components of (F, K). Then the Euler characteristic of $\overline{(F, K)}$ is equal to $(n + 2) - (2n + 1) + \delta = 1 - n + \delta$ and the genus of $\overline{(F, K)}$, g is equal to

$$g = 1 + ((n - 1) - \delta)/2.$$

The closure $\overline{(F, K)}$ is the least genus surface among the surfaces in which the knotoid diagram K can be immersed without any virtual crossings. We can add extra handles in the complement of K so that K is represented by a diagram without any virtual crossings in other surfaces with higher genus. On the other hand, let be given a knotoid diagram K in a surface of genus $\widetilde{g}$, $\Sigma_{\widetilde{g}}$. The regular neighborhood of the diagram $N(K)$ can be regarded as an abstract knotoid diagram $(N(K), K)$ immersed in $\Sigma_{\widetilde{g}}$. If the complement of $(N(K), K)$ has genus then we cut out this extra genus to reduce the genus $\tilde{g}$ to the genus of $\overline{(N(K), K)}$.

Definition 2.19. Let K_1, K_2 be two knotoid diagrams in surfaces Σ_{g_1}, Σ_{g_2}, respectively. These surface representations are denoted by (Σ_{g_1}, K_1) and (Σ_{g_2}, K_2), respectively. Two surface representations (Σ_{g_1}, K_1) and (Σ_{g_2}, K_2) are said to be *stably equivalent* if they can be obtained from each other by finitely many Ω-moves in the surfaces (that do not utilize the endpoints), isotopy of the surfaces and the addition/subtraction of empty handles in the complement of the diagrams. The stable equivalence is denoted by $\sim_{stable}$.

Proposition 2.20. *[15] The mapping*

$$\tilde{f}\text{: } \{\textit{Abstract knotoid diagrams}\} \to \{\textit{Knotoid diagrams in c.c.o. surfaces }\}$$

defined by assigning to (F, K) the knotoid diagram in the closure $\overline{(F, K)}$ induces a bijection
$\tilde{f}_*$*:{ Abstract knotoid diagrams/*$\sim_{abst}$*}* $\to$ *{Knotoid diagrams in c.c.o surfaces/*$\sim_{stable}$ *}*

Proof. It is easy to see that by filling the boundary components of an abstract knotoid diagram with 2-disks, abstract Ω_1 and Ω_3-moves are transformed to Ω_1- and Ω_3-moves between the knotoid diagrams represented in the resulting surfaces of the same genus. The genus does not change under these two moves. An abstract Ω_2-move may increase/decrease the genus of the surface by 1. In the case of a change

in the genus, an abstract Ω_2-move corresponds to Ω_2-move plus removal/addition of empty handles in the surface. Thus the map $\tilde{f}_*$ is well-defined.

Let K be a knotoid diagram in a surface Σ_g. The regular neighborhood of the diagram in Σ_g is an abstract knotoid diagram $(N(K), K)$. The closure of $(N(K), K)$ with 2-disks, $\overline{(N(K), K)}$ is stably equivalent to (Σ_g, K) since $\overline{(N(K), K)}$ is the least genus surface in which K is given without any virtual crossings. So, the map is surjective. Addition/removal of handles occur in the complement of K in the surface. Thus $(N(K), K)$ is not affected by these moves. An Ω-move on K transforms to an abstract Reidemeister move on $(N(K), K)$ as can be verified easily. Therefore the map $\tilde{f}_*$ is injective. This completes the proof of Proposition 2.20 □

The statement of the following theorem is due to Turaev [57]. We demonstrate a proof for the theorem [15] in the sequel.

Theorem 2.21. *The theory of virtual knotoids is equivalent to the theory of knotoid diagrams in higher genus surfaces considered up to Ω-moves in the surfaces, isotopy of the surfaces and addition/removal of handles in the complement of knotoid diagrams.*

Proof. The composition of the two bijections f_* and $\tilde{f}_*$ gives a bijection between the virtual knotoids and knotoids in higher genus surfaces up to the stable equivalence. □

Projecting a knotoid diagram that lies in a higher genus surface to S^2 results in virtual crossings. We make this projection canonical by forming the abstract knotoid diagram in the surface and then arranging a standard projection of the abstract diagram. Figure 2.12 depicts the projection process.

Definition 2.22. The *genus* of a knotoid is the least genus among the surfaces in which the knotoid can be immersed without any virtual crossings. Virtual knotoids that can be represented by a classical knotoid diagram are called *genus* 0- *knotoids*.

We end this section with the following conjecture.

Conjecture 1. *[15] If two classical knotoid diagrams in S^2 are virtually equivalent then they are equivalent to each other by finitely many Ω- moves in S^2.*

Remark 1. A *virtual multi-knotoid diagram* is defined to be an immersion of finitely many oriented circles and oriented unit intervals into S^2 with finitely many transversal double points that correspond to classical and virtual crossings. The virtual equivalence defined for virtual knotoids generalizes to an equivalence on virtual multi-knotoids in the obvious way.

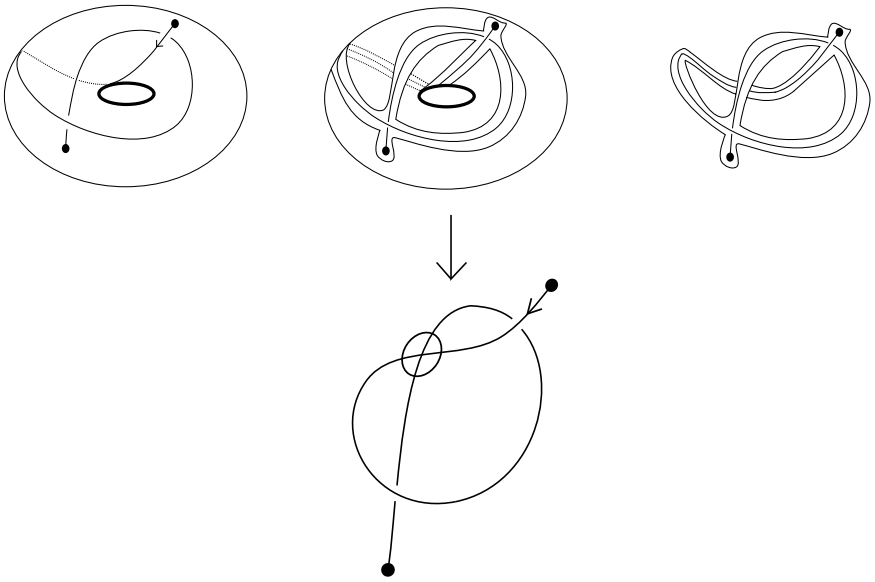

Figure 2.12: Canonical projection of a knotoid diagram

A digression on welded knotoids

There are two more moves on virtual knotoid diagrams, shown in Figure 2.13, which resemble the Reidemeister moves but do not result from any of the Ω-moves or the detour move. We call them *virtual forbidden moves*. The virtual forbidden moves slide either an underpassing or overpassing under/over a virtual crossing and they are denoted by Φ_{under} and Φ_{over}, respectively. These moves are the forbidden moves of virtual knots/links since allowing both of these moves trivializes the theory of virtual knots [51]. It can be shown that any virtual knotoid diagram can be transformed to the trivial knotoid diagram by observing the effect of allowing both virtual forbidden moves on the corresponding chord diagrams of knotoid diagrams (see Section 2.4.4 for chord diagrams). On the other hand, allowing only the over-forbidden move, Φ_{over}, yields a nontrivial theory called *welded knot theory* [28,54]. We introduce the corresponding *welded knotoid theory* [15].

Definition 2.23. Two virtual knotoid diagrams are said to be *w-equivalent* if they can be obtained from one another by a finite sequence of the generalized Ω-moves, the over-forbidden move Φ_{over} and the forbidden move Φ_{-} (see Figure 2.2c). The corresponding equivalence classes are called *welded virtual knotoids*.

S. Satoh [55] defines *w-equivalence* on virtual knotoid diagrams (named as *virtual arc diagrams* in [55]) just in the same way. The fundamental group of a virtual knotoid diagram is given by the generators associated to the overpasses of the diagram and at each classical crossing there is a relation defined in the same way with

the relations of Wirtinger presentation [13] of knot groups. Note that the fundamental group of any knotoid diagram K in S^2 is invariant under the Ω-moves and the $\Phi_{\_}$-move, and the fundamental group of K is isomorphic to the fundamental group of the classical knot represented by the underpass closure of K, see [57] for more details and also [55] in which this concept was given in terms of w-equivalences of classical arc diagrams. Satoh shows that any two w-equivalent virtual knotoid diagrams represent equivalent ribbon 2-knots in $\mathbb{R}^4$ and the fundamental group of the complement of any ribbon 2-knot is isomorphic to the fundamental group of the associated welded virtual knotoid.

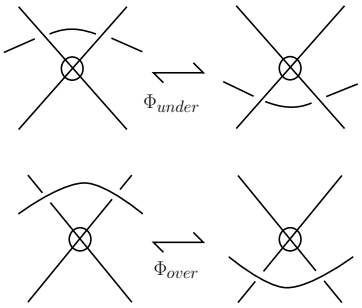

Figure 2.13: Virtual forbidden moves

2.2.1 Flat knotoids

Definition 2.24. A *flat knotoid diagram* in an oriented surface Σ is a generic immersion of the unit interval into Σ with finitely many *flat crossings* that are the transversal double intersection points without any under/over-crossing information or further data. The two endpoints of a flat knotoid diagram that are the images of 0 and 1, are distinct from each other and from any of flat crossings. The endpoints are named analogously with endpoints of knotoids, as the *tail* and the *head* of the diagram.

Flat Ω_1,Ω_2,Ω_3- *moves* on flat knotoid diagrams in S^2 or $\mathbb{R}^2$, are defined by ignoring the under/over- crossing information at the crossings of the move patterns Ω_1, Ω_2 and Ω_3, respectively. These moves are referred as *flat* Ω-*moves*. The flat Ω-moves and planar isotopy moves induce an equivalence relation on flat knotoid diagrams that is called the f-equivalence.

Definition 2.25. A *flat knotoid* is defined to be an equivalence class of flat knotoid diagrams with respect to the f-equivalence.

The analogue of the forbidden moves of knotoids, that allows pulling the strand

adjacent to the tail or the head across a transversal strand so that creating/removing a flat crossing, remains as forbidden for flat knotoids.

Definition 2.26. A *flat virtual knotoid diagram* is defined to be a flat knotoid diagram in S^2 with also *virtual crossings* as we have described them.

The detour move is defined in the same way as it is defined for virtual knotoid diagrams. The rules for changing flat crossings among themselves are identical with the rules for changing virtual crossings. A special case of the detour move, a *flat partial virtual move* is available for virtual crossings with respect to flat crossings when classical crossings in the partial virtual moves are replaced by flat crossings. The moves obtained by replacing classical crossings in the forbidden moves given in Figure 2.13 by flat crossings, remain forbidden for flat virtual knotoid diagrams. The moves on flat knotoid diagrams that are generated by flat Ω-moves and the detour move, are called *generalized flat* Ω- *moves.*

Definition 2.27. Two flat virtual knotoid diagrams are said to be *f-equivalent* if there is a finite sequence of generalized flat Ω- moves together with the planar isotopy moves taking one diagram to the other. A *flat virtual knotoid* is defined to be an equivalence class of flat knotoids diagrams with respect to this equivalence.

We say that a virtual knotoid diagram K *overlies* a flat virtual knotoid diagram if it is obtained from the flat diagram by choosing a crossing type as over or under for each flat crossing. The flat virtual diagram that K overlies, is the *underlying flat diagram* of K and denoted by $F(K)$. It is clear that any generalized Ω-move on K induces a flat generalized Ω-move on the underlying flat diagram $F(K)$. It follows that if K and $\widehat{K}$ are two virtually equivalent virtual knotoid diagrams then the underlying flat diagrams, $F(K)$ and $F(\widehat{K})$ are f-equivalent. Thus, a virtual knotoid diagram is necessarily nontrivial if it overlies a nontrivial flat virtual knotoid. Clearly, this argument holds for flat knotoid diagrams in S^2 or in $\mathbb{R}^2$. A classical knotoid diagram is nontrivial if it overlies a montrivial flat knotoid diagram.

It is well-known that any flat classical knot diagram is equivalent to the trivial knot diagram. This property of flat classical knots generalizes to flat knotoid diagrams in S^2 as we [15] explain in the sequel.

Proposition 2.28. *[15] Any flat knotoid in S^2 is f-equivalent to the trivial knotoid.*

Proof. A flat knotoid diagram in $\mathbb{R}^2$ is said to be *normal* if its tail in the outermost region of the diagram. Similarly with the argument for knotoids in S^2, any flat knotoid diagram in S^2 can be represented by a flat normal knotoid diagram. It is clear that two flat normal knotoid diagrams represent the same flat knotoid in S^2 if

and only if they are related to each other by a finite sequence of flat Ω-moves and planar isotopy.

An *ascending knotoid diagram* is a classical knotoid diagram that consists of crossings encountered firstly as an undercrossing while traversing the diagram from its tail to its head. Clearly, a flat normal knotoid diagram is f-equivalent to the trivial knotoid diagram if and only the ascending normal knotoid diagram overlying this flat diagram is equivalent to the trivial knotoid diagram. We claim that any ascending normal knotoid diagram is equivalent to the trivial knotoid diagram. To prove our claim, we first show that any open-ended space curve corresponding to a normal ascending knotoid diagram, is line isotopic to the trivial space curve with two endpoints attached to the special lines. Then by Theorem 2.11, it follows that an ascending normal knotoid diagram represents the trivial knotoid in $\mathbb{R}^2$, so in S^2.

Let K be an ascending normal knotoid diagram. Let l_1 and l_2 be the two lines that are passing through the tail and the head, respectively, and perpendicular to the xy-plane. We fix the tail at the point $(x, y, 0)$ (on the plane) on l_1 and start raising K in the vertical direction by pulling the head up along the line l_2. The head is pulled up until K becomes a helical space curve $c(K)$. See Figure 2.14 for an illustration of this.

Notice that the curve $c(K)$ is isotopic to a curve that does not wind around the line l_1 since K is a normal diagram. Then the curve $c(K)$ is line isotopic to a curve with one endpoint on the line l_1 and the rest winds around l_2, where the other endpoint is attached. The part of the curve $c(K)$ that winds around the line l_2 together with the line l_2 that is oriented upwards, can be regarded as a 2-braid. By the line isotopy the parts that correspond to a braid word $\sigma_1\sigma_1^{-1}$, are eliminated so that the curve $c(K)$ corresponds to a braid word $\sigma_1^n \in B_2$, for some $n \geq 0$. We start unwinding $c(K)$ from the top by a rotation of 180-degrees in the counterclockwise direction around the line l_2. Applying n consecutive rotations around the line l_2 transforms the curve $c(K)$ into the trivial curve. In other words, the curve $c(K)$ is line isotopic to the trivial curve. Then the projection of $c(K)$ to $\mathbb{R}^2$ is the trivial knotoid diagram by Theorem 2.11. This proves that any ascending normal knotoid diagram is equivalent to the trivial knotoid. Therefore, by the argument above, any flat normal knotoid diagram is f-equivalent to the trivial knotoid diagram. Since any flat knotoid diagram in S^2 can be represented by a flat normal diagram, the statement follows. □

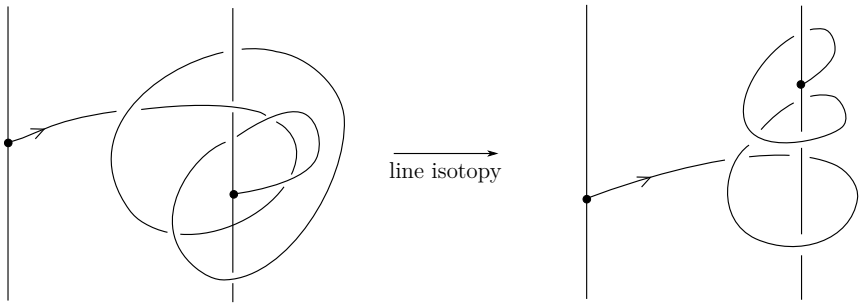

Figure 2.14: A space curve corresponding to an ascending knotoid diagram

Note 3. Proposition 2.28 does not hold for flat knotoids in $\mathbb{R}^2$. For instance, the ascending knotoid diagram shown in Figure 2.1b, when considered in the plane, is not equivalent to the trivial knotoid [57]. It follows that the underlying flat diagram of the diagram K is not f-equivalent to the trivial knotoid diagram. Also, there are flat virtual knotoids that are non-trivial. See Section 2.4.4 for a discussion on this.

2.3 The virtual closure

Every knotoid diagram in S^2 represents a virtual knot as discussed in [15, 57]. The endpoints of a knotoid diagram can be connected with an embedded arc in S^2 but this time a virtual crossing is created every time the connection arc crosses a strand of the diagram, as depicted in Figure 2.15a. In this way one obtains a virtual knot diagram. Let B_1, B_2 be regular neighborhoods of the tail and the head of the knotoid diagram, respectively. The virtual knot diagram resulting from the above connection can be represented in a torus in the following way. The disks B_1, B_2 are cut out from S^2 and a 1-handle that holds the connection arc is attached to the resulting tube via an orientation reversing homeomorphism identifying the boundary circles of the tube and the handle in a way that the endpoints of the connection arc are identified with the intersection points of the disks with the strands adjacent to the endpoints. Such a representation of the resulting virtual knot in the torus is called the *standard torus representation* of the knot, see Figure 2.15b.

Connecting the endpoints of a knotoid in the virtual fashion explained above induces a map from the set of spherical knotoids to the set of virtual knots of genus at most 1 that is called the *virtual closure map* and denoted by $\overline{v}$,

$$\overline{v} : \mathscr{K}(S^2) \to \{ \text{ Virtual knots of genus} \leq 1 \ \}.$$

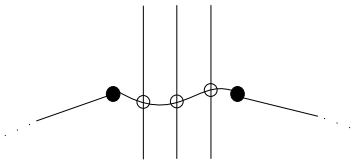

(a) The virtual closure of a knotoid diagram

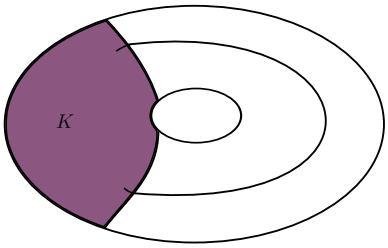

(b) Standard torus representation of the virtual closure

The connection arc is unique up to isotopy of S^2. The isotopy between any two connection arcs induces detour moves between the corresponding virtual knot diagrams. So, the choice of a connection arc does not alter the isotopy class of the resulting virtual knot. Also, an Ω-move on a knotoid diagram is transformed to a combination of generalized Reidemeister moves on the resulting knot diagram. Therefore, the virtual closure map is a well-defined map. The virtual knot assigned to a knotoid K in S^2 via the virtual closure map is called the *virtual closure* of K, and it is denoted by $\overline{v}(K)$.

Having its endpoints in the same region, a knot-type knotoid diagram can result in a classical knot diagram when its endpoints are connected virtually. Then since the map $\overline{v}$ is well-defined, the virtual closure of a knot-type knotoid is a classical knot. Moreover the converse also holds as shown in [39].

Theorem 2.29. *[39] A knotoid is knot-type (or of height* 0*) if and only if its virtual closure admits destabilization.*

Note 4. *The classical closures (underpass/overpass closure) and the virtual closure of a knot-type knotoid are isotopic classical knots.*

Lemma 2.30. *[15, 16] The virtual closure map is not injective.*

Proof. It can be shown that the knotoid diagrams given in Figure 2.16 with the same virtual closure, are nonequivalent, by using many knotoid invariants. One way can be the following. It can be shown that the knotoid group of the left hand-side knotoid diagram has the presentation $< x, y | x^2 = y^3 >$ (it is isomorphic to the knot group of the trefoil knot). On the other hand, the knotoid group of the right hand side knotoid diagram is isomorphic to $\mathbb{Z}$. Since the knotoid group is a knotoid invariant [57], we conclude that these two diagrams are nonequivalent knotoid diagrams. One another way is to utilize the tricolorability of knotoids. One can verify easily that the right hand-side knotoid diagram is not tricolorable but the left hand-side knotoid is tricolorable (recall Figure 2.4).

□

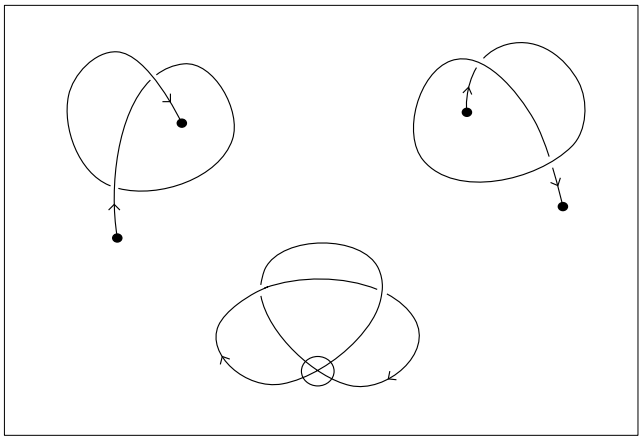

Figure 2.16: A pair of nonequivalent knotoids with the same virtual closure

The virtual closure map is also non-surjective as we show in [17].

Theorem 2.31. *[17] If a virtual knot of genus* 1 *lies in the image of the virtual closure map* $\overline{v}$ *then any torus representation of the knot contains a surface bracket state curve that is homologous to the curve* $h_*([\lambda]+n[\mu])$ *where* λ *and* μ *are generators of* $H_1(T^2,\mathbb{Z})$*, where* h_* *is the isomorphism on* $H_1(T^2,\mathbb{Z})$ *induced by an orientation preserving homeomorphism* h *of the torus* T^2*.*

Proof. Let k be a virtual knot of genus 1 that lies in the image of $\overline{v}$ and K be a knotoid diagram in S^2 such that $\overline{v}(K) = k$. Consider the standard torus representation of the virtual knot $\overline{v}(K)$. Let $[\lambda], [\mu]$ be the generators of $H_1(T^2,\mathbb{Z})$ corresponding to the longitude and the meridian of T^2, respectively. By the construction of the standard representation, the surface bracket states consist of components that are homologous to the curves $[\lambda] + n[\mu]$ and $m[\mu]$, $n, m \in \mathbb{Z}$, for some choice of orientation assigned to state curves. Standard torus representation of $\overline{v}(K)$ is a minimal representation. Then by Kuperberg's theorem, there is an orientation preserving homeomorphism of the torus taking the standard representation to any torus representation of the knot k. Then it follows that at least one of the surface state components of any torus representation of k is homologous to $h_*([\lambda] + n[\mu])$ where h_* is the isomophism on $H_1(T,\mathbb{Z})$ induced by an orientation preserving homeomorphism h.

□

Corollary 4. *[17] Let* k *be a virtual knot of genus* 1 *and* (T,k) *denote a torus representation of* k*. If the nontrivial isotopy classes of state curves of* (T^2,k) *are only of the form (for some choice of orientation)* $a[\lambda]$ *and* $b[\mu]$ *for some* $a, b \in \mathbb{Z}-\{0\}$*,* $|a|, |b| \neq 1$ *then* k *does not lie in the image of* $\overline{v}$*.*

Proof. Suppose k lies in the image of $\overline{v}$ then by Theorem 2.31, (T, k) has a state curve, when oriented, that is homologous to $h_*([\lambda] + n[\mu])$ for some $h \in Aut^+(T)$. Then $h_*([\lambda] + n[\mu]) = a[\lambda]$ or $h_*([\lambda] + n[\mu]) = b[\mu]$. Since $\lambda + n\mu$ is a connected curve, there is no homeomorphism taking $\lambda + n\mu$ to $a\lambda$ or $b\mu$ for some a, b $\neq 1$. □

Claim 1. *The virtual knot represented by the diagram K given in Figure 2.17 is not the virtual closure of a knotoid in S^2.*

Proof. The surface bracket states of the representation of K in the torus consist of the curves shown in Figure 2.17. When the curves are oriented in an all possible ways, it is observed that there are only two states that contribute to the polynomial in a nontrivial way. The isotopy classes of the non-trivial state curves are of the form (homologous to) $[2a]$ and $[2b]$. Then by Corollary 4, it is deduced that K cannot be turned into (by any orientation preserving homeomorphism of T^2) a virtual knot diagram that is the virtual closure of a knotoid diagram in S^2. □

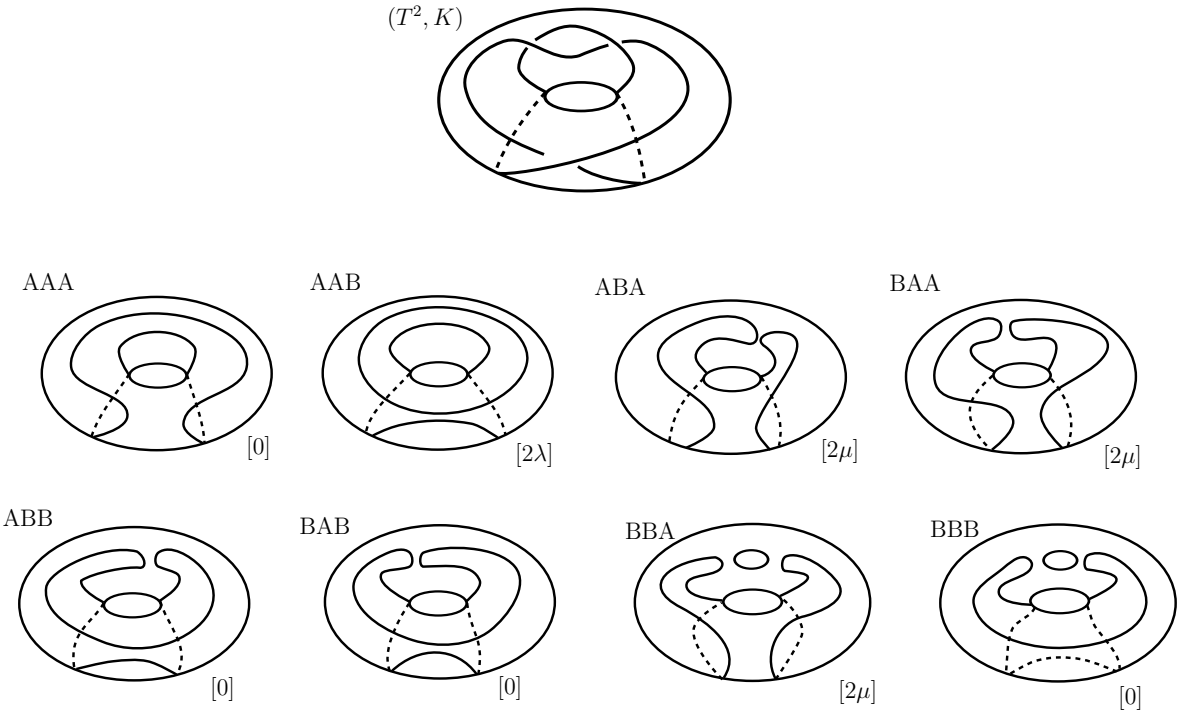

Figure 2.17: Surface state loops of K

More generally we have the following theorem appearing in [17].

Theorem 2.32. *[17] Let K be a non-trivial classical knot diagram with unknotting number* 1*. Then the genus* 1 *virtual knot $Virt(K)$ that is obtained by virtualizing of a crossing which turns K into unknot when switched, does not lie in the image of the virtual closure map.*

Proof. We analyze the surface state curves of the torus representation of $Virt(K)$ depicted in Figure 2.18. Note that trivial state curves bounding a disk in torus may appear in the circled region. We see that non-trivial state curves of this representation are only of the form $2[\mu]$ and $2[\lambda]$. Then by Corollary 4 the theorem follows. □

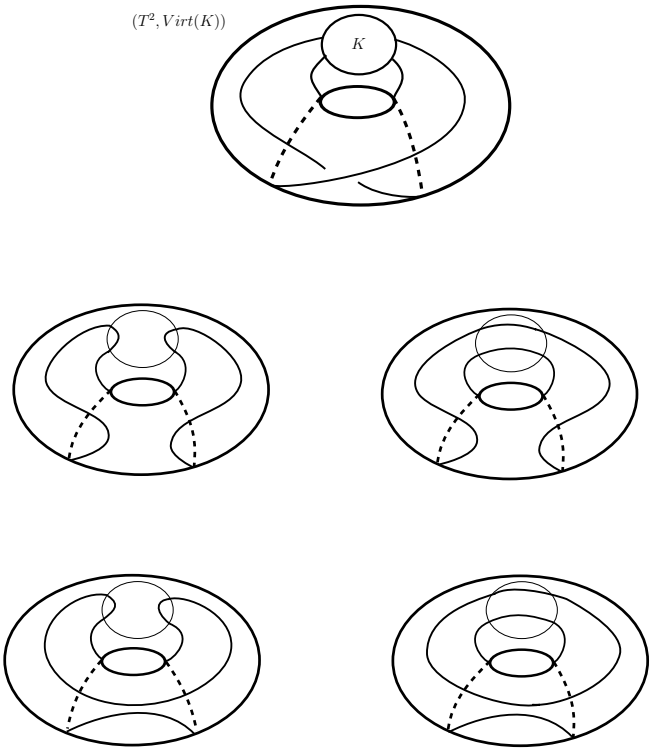

Figure 2.18: The homology classes of surface state curves of $Virt(K)$ in torus (up to an orientation)

Corollary 5. *The virtual closure map is not surjective.*

The following conjecture appearing in [57] is due to Turaev. We now give a proof for this conjecture that also appears in [17]. In the following, a minimal diagram refers to a diagram (a classical knotoid diagram or classical/virtual knot diagram) with minimal number of classical crossings, and recall that genus g of the abstract knotoid diagram associated to a virtual knot diagram is:

$$g = 1 + (n - \delta)/2.$$

Conjecture 2. *[57] Minimal diagrams of non-trivial knot-type knotoids have zero height.*

Proof. Let k be a knot -type knotoid and assume to the contrary that k admits

a minimal diagram with non-zero height. Let K_1 denote such diagram with the minimal number of classical crossings, say $n > 0$.

Since k is a knot-type knotoid, the virtual closure of k, $\overline{v}(k)$ is a classical knot. On the other hand, the diagram K_1 has nonzero height so its virtual closure $\overline{v}(K_1)$ is a virtual knot diagram with a number of virtual crossings that is equal to the height of K_1 and with n classical crossings. The virtual closure map is well-defined. From this it follows that the virtual knot diagram $\overline{v}(K_1)$ represents the classical knot $\overline{v}(k)$.

Claim 2. *The genus of the abstract knot diagram associated with $\overline{v}(K_1)$ is 1 (that is the surface representation of $\overline{v}(K_1)$ is 1).*

Proof. The abstract knotoid diagram associated with K_1 has genus 0 since it is a planar diagram. In fact we have

$$0 = g = 1 + ((n-1) - \delta)/2,$$

where n is the crossing number of K_1 and δ is the number of boundary components of the abstract diagram associated with K_1.

The number of boundary components is equal to the the number of regions of the diagram K_1. The boundary components that are adjacent to the endpoints, are actually different components since the endpoints are in different regions. Closing K_1 virtually does not change the number of classical crossings but reduces the number of boundary components by one since the two different boundary components become the same. Then by Equation (2.2) we have,

$$g(\overline{v}(K_1) = 1 + (n - (\delta - 1))/2 = 1$$

. □

Since $\overline{v}(k)$ is a classical knot then by Manturov's theorem 2, minimal number of classical crossings can be attained only in a classical diagram of $\overline{v}(k)$. let $\overline{K}$ be such diagram of $\overline{v}(k)$ with m crossings. It is clear that $\overline{K}$ is virtually equivalent to $\overline{v}(K_1)$ for representing the same knot $\overline{v}(k)$. Then we have

$$m < n.$$

On the other hand, the image of $\overline{K}$ under the α-map (recall Section 2.1.2), $\alpha(\overline{K})$ is a knot-type knotoid diagram with m crossings. It is clear that the underpass closures of $\alpha(\overline{K})$ and the knotoid diagram K_1 are both equivalent to the knot $\overline{v}(k)$. This implies that both knotoid diagrams are equivalent to each other since the

underpass closure is a bijection map when restricted to the knot-type knotoids. By assumption K_1 is a minimal diagram of k, that is we have,

$$n \leq m,$$

which contradicts with the above inequality. □

Remarks.

1. Being a well-defined map, the virtual closure map gives a way to construct many invariants for knotoids in S^2 which can be generalized to a virtual knotoid invariant. In fact, for any invariant of a virtual knot, denoted by Inv, an invariant on knotoids in S^2 denoted by I, can be defined through the following formula,

   $$I(K) = \text{Inv}(\overline{v}(K)),$$

   where K is knotoid in S^2.

   This makes virtual knot theory a natural domain for the study of knotoids in S^2. Note also that as we will do in the sequel, many virtual knot invariants can be constructed directly on knotoid diagrams without need of closing the endpoints in the virtual fashion. We observe that this approach often gives more strength to the defined invariants.

2. The virtual closure map extends to a well-defined map from the set of virtual knotoids to the set of virtual knots. We call this map *extended virtual closure map*. It is clear that the extended virtual closure map is a surjective map. Any virtual knotoid diagram whose endpoints can be connected by an embedded arc without creating any type of crossings (either classical or virtual), can be regarded as a long virtual diagram. The virtual knotoid shown in Figure 2.19 is a nontrivial virtual knotoid as we show in Section 2.4.4 by the parity bracket polynomial of knotoids. It can be verified by the figure that the extended virtual closure of this virtual knotoid is the trivial knot. Obviously, trivial virtual knotoid diagrams are also sent to the trivial knot by the map. Thus, the extended virtual closure map is not injective.

3. The underpass closure map cannot be extended to a well-defined map on virtual knotoids. Figure 2.20 depicts a virtual knotoid diagram that represents two virtual knots via the underpass closure map. The arrow polynomial which will be discussed in Section 2.4.2, detects that these knots are not equivalent.

In fact, to transform one diagram to the other one, we require the virtual forbidden move, Φ_{under} which is shown in Figure 2.13.

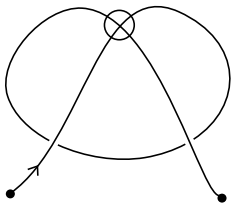

Figure 2.19: A nontrivial virtual knotoid with trivial virtual closure

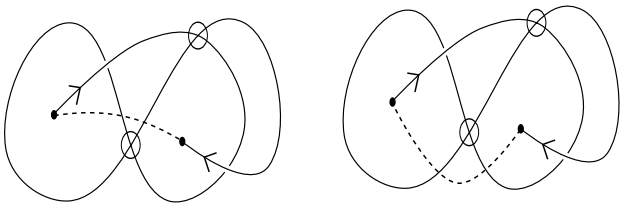

Figure 2.20: A virtual knotoid diagram representing different knots via ω_{-}

2.4 Invariants of knotoids

2.4.1 The bracket polynomial

The bracket polynomial of a knotoid in an oriented surface Σ is introduced by Turaev in [57]. The bracket polynomial of a knotoid is defined by extending the state expansion of the bracket polynomial of knots [32, 34, 35] as follows. Each classical crossing of a classical knotoid diagram K is smoothed either by A- or *B-type smoothing*, as shown in Figure 2.21. A smoothing site is labeled by 1 if A-smoothing is applied and labeled by -1 if B-smoothing is applied at a particular crossing. A *state* of the knotoid diagram K is a choice of smoothing each crossing of K with the labels at smoothing sites. Each state of K consists of disjoint embedded circular components and a single long segment component with two endpoints. The initial conditions given in Figure 2.21 are sufficient for the skein computation of the bracket polynomial of classical knotoids.

Definition 2.33. [57] The bracket polynomial of a knotoid diagram K is defined as

$$< K >= \sum_S A^{\sigma(S)} d^{\|S\|-1},$$

where the sum is taken over all states, $\sigma(S)$ is the sum of the labels of the state S, $\|S\|$ is the number of components of S, and $d = -A^2 - A^{-2}$.

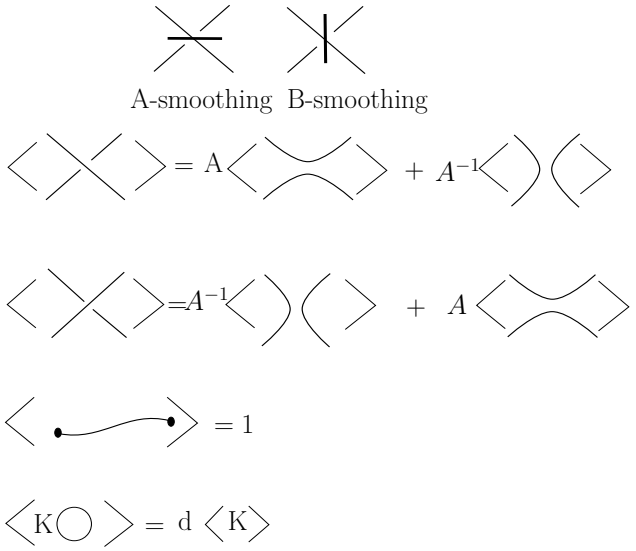

Figure 2.21: Skein relations of the bracket polynomial

The *writhe* of a classical or virtual knotoid diagram K, $\mathrm{wr}(K)$ is the number of positive crossings (the classical crossings with sign $+1$, see Figure 2.22) minus the number of negative crossings (the classical crossings with sign -1, see Figure 2.22) of K [57]. The writhe is invariant under the generalized Ω-moves except the Ω_1-move [57].

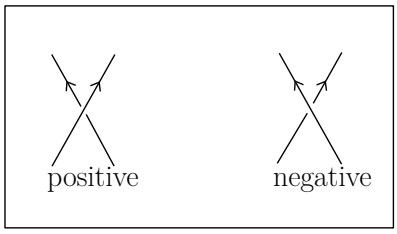

Figure 2.22: Crossing signs

An Ω_1-move changes the writhe by ± 1. The bracket polynomial turns into an invariant for classical knotoids with a normalization by the writhe. The *normalized bracket polynomial* of a classical knotoid K, f_K is defined as the multiplication,

$$f_K = (-A^3)^{-\mathrm{wr}(K)} < K > [57].$$

The normalized bracket polynomial of knotoids in S^2 generalizes the Jones polynomial of classical knots with the substitution $A = t^{-1/4}$ [57] . Note that by connecting the endpoints of the long segment components of states of a knotoid in S^2, K by an embedded arc in the virtual fashion, we obtain the bracket state components

of the virtual knot $\overline{v}(K)$. This gives us the equality, $V(K) = V(\overline{v}(K))$, where $V(K)$ denotes the Jones polynomial of K.

Example 1. Let K_1 be the knotoid diagram in S^2 illustrated in Figure 2.23. As can be seen by the figure, the normalized bracket polynomial of K_1, $f_{K_1} = (-A^3)^{-2}(A^2 + 1 - A^{-4}) = A^{-4} + A^{-6} - A^{-10}$. Having a nontrivial normalized bracket polynomial, K_1 is a non-trivial knotoid.

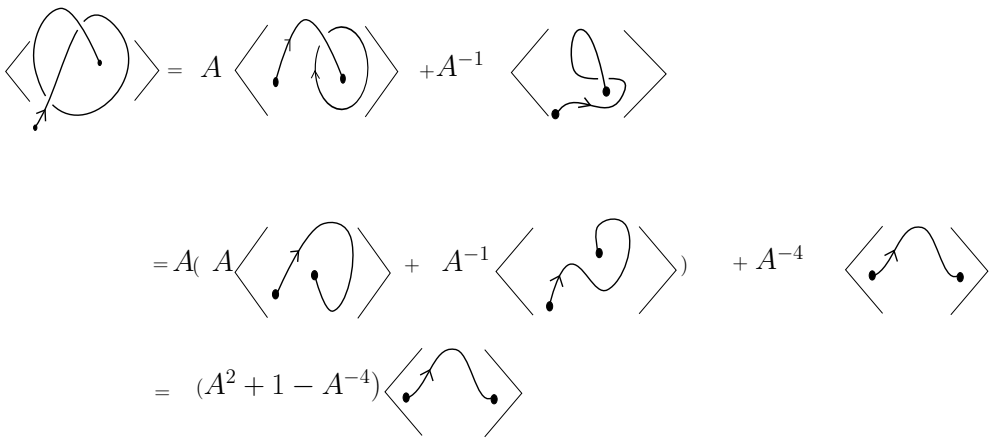

Figure 2.23: Computation of the bracket polynomial of K_1

We extend the well-known Jones polynomial conjecture to the following conjecture [15].

Conjecture 3. *[15] The normalized bracket polynomial of knotoids in S^2 (or the Jones polynomial) detects the trivial knotoid.*

Note 5. *The bracket polynomial for multi-knotoids can be extended naturally using the bracket state sum expansion.*

2.4.2 Generalizations of the bracket polynomial

The arrow polynomial

We define the arrow polynomial for knotoids [15] in analogy with the arrow polynomial of virtual knots and links which was defined by H.A. Dye and L.H. Kaufman [10] and independently by Y. Miyazawa [50]. The construction of the arrow polynomial of knotoids both for classical and virtual, is based on the *oriented state expansion* of the bracket polynomial of knotoids which is shown in Figure 2.24.

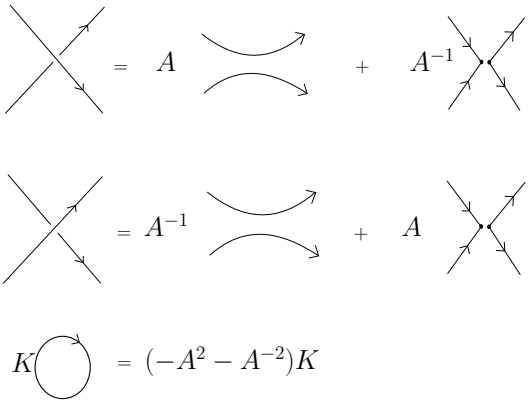

Figure 2.24: Oriented state expansion

Oriented state expansion of knotoids involves *oriented and disoriented smoothings* of all classical crossings that result in *oriented states* circular components and one long state component or only a single long state component. The state components which are obtained by disoriented smoothings include an extra combinatorial structure in the form of *paired cusps*. Each cusp has two arcs either going into the cusp or going out from the cusp. A cusp can be denoted by an angle which locally divides S^2 into two parts. One part is the span of the acute angle and the other part is the span of the obtuse angle. We call the part which is the span of the acute angle as *inside* of the cusp and the part which is the span of the obtuse angle as *outside* of the cusp.

There is a list of rules which reduce the number of cusps in a state component that are generated accordingly to the virtual equivalence that is generated by the isotopy of S^2 or $\mathbb{R}^2$ and the detour move (only isotopy of S^2 or $\mathbb{R}^2$ for the classical case). This list is given in Figure 2.25. The basic reduction rule consists of cancellation of two consecutive cusps both with insides on the same side of the segment connecting them. Two consecutive cusps on a state component which have insides on the opposite sides of the segment connecting them, are not canceled out. Specifically, any two consecutive cusps on a circular component are canceled if they have insides in the same local region that the component forms. Therefore, a circular component with two such cusps turns into an embedded circular component which contributes to the polynomial as $d = -A^2 - A^{-2}$. Any two consecutive cusps on a long state component which have insides on the same side of the segment connecting them, are canceled out as well. Such a long state component turns into an embedded arc in S^2 and contributes to the polynomial with the same value of an embedded circular state, as $d = -A^2 - A^{-2}$. Two cusps on a circular component with insides on the opposite local sides of the circle are kept as graphical nodes. This component is regarded as

a circular graphical state. Two cusps on a long state component whose insides are on opposite sides of the segment connecting them, are not reduced as well. Such a long state component is regarded as a graphical state. The graphical components contribute to the polynomial as extra variables. A circular graph component with surviving cusps can be turned into a circular graph without any virtual crossings by the detour move so that it can be depicted as a circular graph with cusps forming zig-zags on the component. A circular component with two cusps forming a zig-zag contributes as K_1 to the polynomial. In general, a circular graph with zig-zags formed by $2i$ alternating cusps, contributes as a variable, K_i to the arrow polynomial. A long state component with zig-zags formed by $2i$ alternating cusps contributes as an additional variable, as Λ_i to the arrow polynomial.

Definition 2.34. We define the *arrow polynomial* of a virtual or classical knotoid diagram K as,

$$\mathscr{A}[K] = \sum_S A^{i-j}(-A^2 - A^{-2})^{\|S\|-1} < \hat{S} >,$$

where the sum runs over the oriented bracket states, i is the number of state markers touching A labels and j is the number of state markers touching A^{-1} labels in the state S, as in the usual the bracket sum, $\|S\|$ is the number of components of the state S and $< \hat{S} >$ is the product of variables, ${K_{i_1}}^{j_1}...{K_{i_n}}^{j_n}\Lambda_i$, associated to the components of S with surviving cusps.

The variables K_i and Λ_i constitute an infinite set of commuting variables, commuting with each other also with the variable A of the arrow polynomial. It can be seen by Figure 2.26, an Ω_1- move changes the arrow polynomial of a virtual knotoid by $-A^{\pm 3}$.

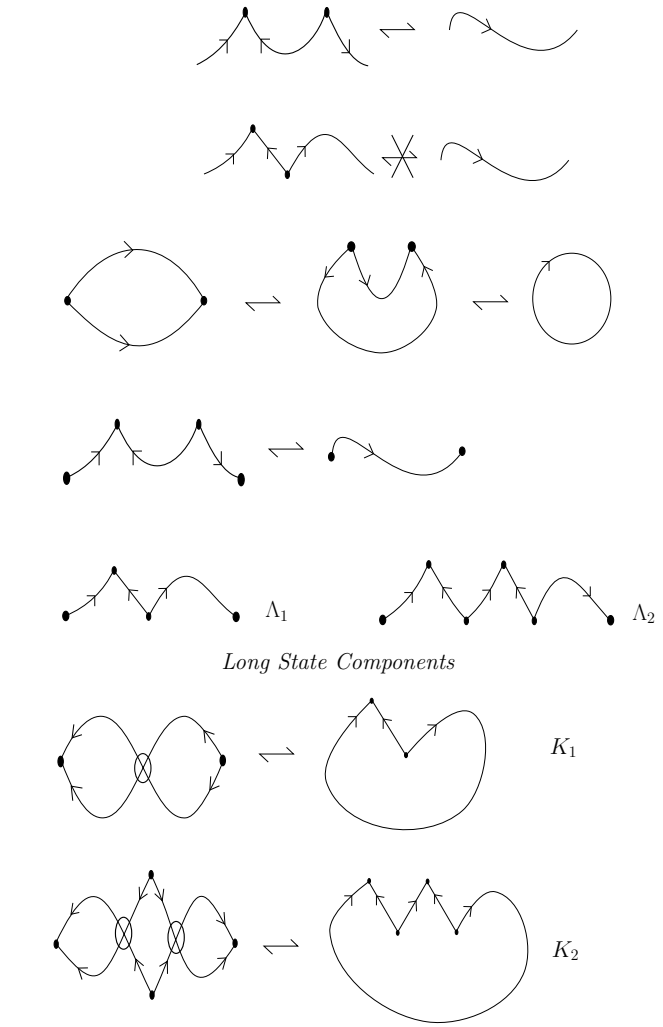

Figure 2.25: Reduction rules for the arrow polynomial

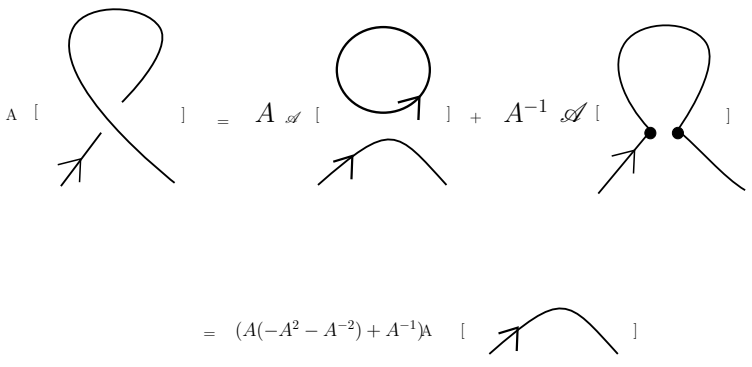

Figure 2.26: The arrow polynomial change by an Ω_1-move

Theorem 2.35. *[15] The normalization of arrow polynomial by* $(-A^3)^{-\operatorname{wr}(K)}$*, where* $\operatorname{wr}(K)$ *is the writhe of* K*, is a virtual and classical knotoid invariant.*

Proof. Since Ω- moves take place far away from the endpoints, the proof follows similar as the proof of the invariance of the arrow polynomial for virtual knots/links. See [10, 29]. □

See Figure 2.27 for an example of a knotoid with nontrivial arrow polynomial.

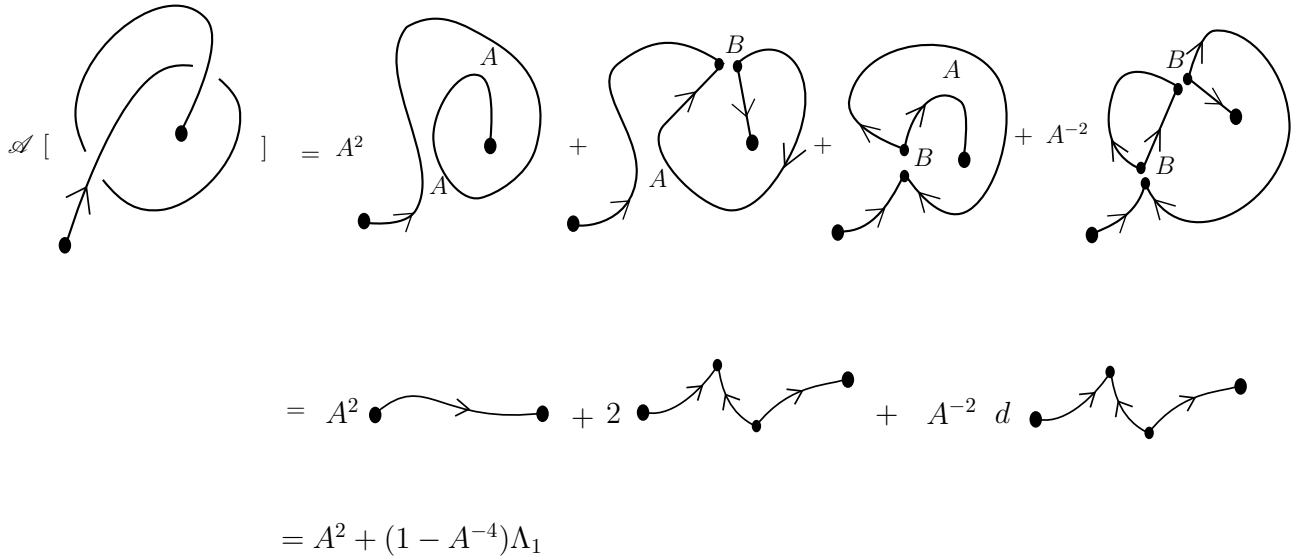

Figure 2.27: A knotoid with non-trivial arrow polynomial

Definition 2.36. The *K-degree* of a summand of the arrow polynomial of a virtual knotoid which is of the form, $A^m({K_{i_1}}^{j_1}{K_{i_2}}^{j_2}...{K_{i_n}}^{j_n})\Lambda_i$, is equal to

$$i_1 \times j_1 + ... + i_n \times j_n.$$

The *K-degree* of the arrow polynomial of a virtual knotoid is defined to be the maximum K- degree taken among the K-degrees of summands of the arrow polynomial of the knotoid.

Note that the K-degree of the arrow polynomial of a virtual knot/link is defined in a similar way, as the maximum K-degree among the K-degrees of the summands of the arrow polynomial [10].

Definition 2.37. The Λ-degree of a summand of the arrow polynomial of a virtual knotoid which is in the form, $A^m({K_{i_1}}^{j_1}{K_{i_2}}^{j_2}...{K_{i_n}}^{j_n})\Lambda_i$ is equal to i. The Λ-*degree* of the arrow polynomial of a virtual knotoid is defined to be the maximum Λ- degree among the Λ-degrees of all the summands of the polynomial.

Note 6. For a classical knotoid diagram in S^2 or a virtual knotoid diagram K, the oriented state components of the virtual closure of K, $\overline{v}(K)$, is obtained by connecting the endpoints of each long state component in the oriented state expansion of

K in the virtual fashion (with an embedded arc creating virtual crossings whenever it meets with the component). Therefore, instead of assigning Λ_i to long state components with $2i$ cusps which are not reduced by the reduction rules, if we assigned K_i as a variable, we would have

$$\mathscr{A}[K] = \mathscr{A}[\overline{v}(K)].$$

The arrow polynomial gets more effective as an invariant of virtual knotoids by assigning to long state components with $2i$ irreducible cusps, the variable Λ_i, $i \in \mathbb{Z}^+$. Figure 2.28 depicts the oriented state expansion of the knotoid diagram given before in Figure 2.19. It is visible that the virtual closure of this knotoid is the trivial knot and the arrow polynomial of the resulting virtual knot is trivial. In the direction of the discussion, it can be said that assigning K_1 to the long state components of this knotoid results in trivial arrow polynomial. Assigning Λ_1 to the long state components, however, results in a non-trivial arrow polynomial, as shown in Figure 2.28. The arrow polynomial extended with Λ-variables detects the non-triviality of this knotoid.

Another example is the virtual knotoid represented by the knotoid diagram K, shown in Figure 2.29. The virtual closure of this knotoid is the Slavik's Knot [10] whose normalized arrow polynomial is trivial. The arrow polynomial of the knotoid K is

$$\mathscr{A}[K] =$$
$$(A^{-9}+A^{-7}+3A^{-5}+5A^{-1}+A+6A^3++2A^5+3A^7)+(-A^3-A^{-1}+A^{-3}+A+A^5)\Lambda_1.$$

This implies that the normalized arrow polynomial is non-trivial and shows that the non-triviality of this virtual knotoid is detected by the normalized arrow polynomial defined by assigning Λ_1-variable to the long state components.

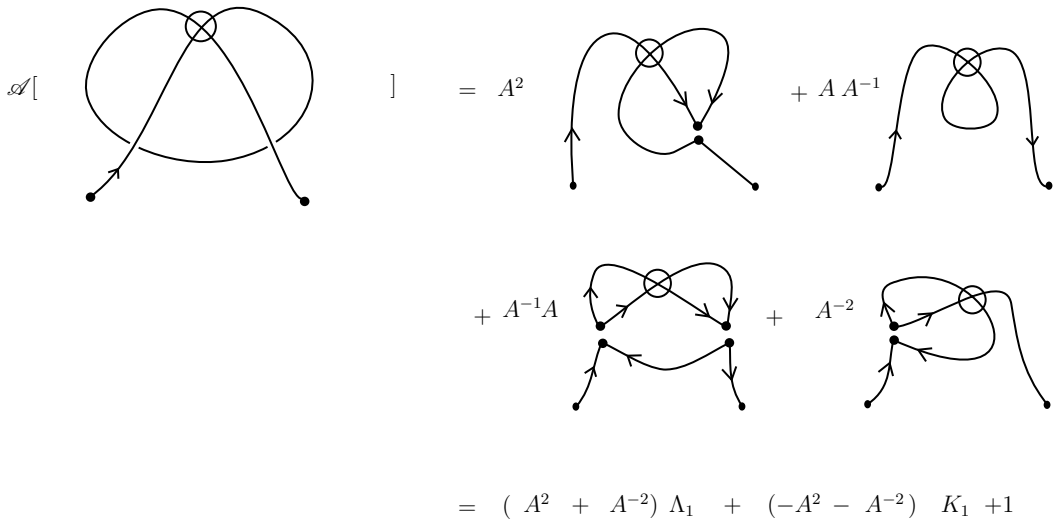

Figure 2.28: The arrow polynomial of the knotoid in Figure 2.19

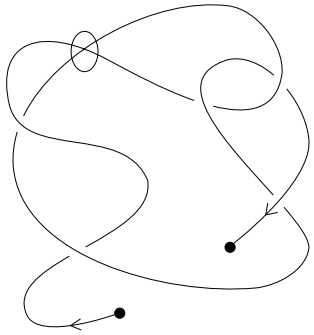

Figure 2.29: A knotoid closing to Slavik's knot

Theorem 2.38 ([29])**.** *In a classical knot or link diagram, all state components of the arrow polynomial reduce to loops that are free from cusps.*

Proof. The proof follows by Jordan curve theorem. For the details the reader is directed to [29]. □

As it has been discussed in Section 2.3, the virtual closure of a knot-type knotoid diagram is a classical knot diagram. The oriented state components of a knot-type knotoid diagram become the oriented state components of a classical knot diagram when the endpoints of long components are connected virtually. Then it follows by the Theorem 2.38 that cusps do not survive in any of the state components of a knot-type knotoid diagram, and we have the following corollary.

Corollary 6. The normalized arrow polynomial of a knot-type knotoid coincides with the normalized bracket polynomial of the knotoid.

On the other hand, cusps may survive in a long state component of a proper knotoid diagram as seen in Figure 2.27. If the Λ-degree of the arrow polynomial of a knotoid is nonzero then it is immediate to conclude by the discussion above that it not a knot-type but a proper knotoid, in other words a knotoid with nonzero height. For example, the knotoid diagram shown in Figure 2.27 represents a proper knotoid since the arrow polynomial of the knotoid has Λ- degree 1.

The circular components of an oriented state of any classical knotoid diagram are all free of cusps. This follows by the same reasoning with the proof of Theorem 2.38. As a conclusion, the K-degrees of any summand of the arrow polynomial of a classical knotoid is zero.

For virtual knotoids, cusps may survive in circular state components as well as they can survive in long state components. It means that both the K- and Λ- degrees of the arrow polynomial of a virtual knotoid may be nontrivial. We know that the knotoid diagram, given in Figure 2.28 is not virtually equivalent to a classical knotoid since the K-degree of the arrow polynomial is 1.

Remark 2. Direct computation shows that the arrow polynomial of the knotoids represented by the diagrams K_1 and K_2 given in Figure 2.20, are respectively,

$$\mathscr{A}[K_1] = 1 - A^{-4} + A^4 + (-A^{-2} + A^2)\Lambda_1$$

,

$$\mathscr{A}[K_2] = 2 - A^{-4} - A^4 + A^8 + (-A^{-6} + A^{-2})\Lambda_1$$

. It can be easily verified that the normalized arrow polynomials of K_1 and K_2 are different. Therefore K_1 is not equivalent to K_2 and the underpass closure is not well-defined on virtual knotoids.

Note 7. The arrow polynomial generalizes to a virtual multi-knotoid invariant directly as follows. All crossings including the crossings shared by two components of a given oriented virtual multi-knotoid diagram are smoothed in the same way. The resulting oriented state components, including oriented circular components and oriented long state components, are labeled by either A or A^{-1} at each smoothing site. The arrow polynomial for multi-knotoids is defined as the summation of all products of labels assigned to oriented state components. If K is a multi-knotoid diagram without any virtual crossings then it follows by a reasoning similar to the the proof of Theorem 2.38 that the circular components of K are free of cusps, and cusps can survive only on the long state components.

An estimation of the height by the arrow polynomial

The arrow polynomial can be used for estimating the height of a knotoid in S^2 as we show in [15]. Before demonstrating this result, we shall firstly recall more from virtual knot theory.

Definition 2.39. The *virtual crossing number* of a virtual knot/link is the minimum number of virtual crossings over all representative diagrams.

The problem of determining the virtual crossing number of a virtual knot or link is a fundamental problem in virtual knot theory. There is a relation between the virtual crossing number and the maximal K-degree of the arrow polynomial of a virtual knot, as stated by the following theorem.

Theorem 2.40. *[10] The virtual crossing number of a virtual knot/link is greater than or equal to the maximal K-degree of the arrow polynomial of that virtual knot/link.*

Let K be a knotoid in S^2. The oriented state components of the virtual closure of K, $\overline{v}(K)$ are the same with the oriented state components of K when the long state components are closed in the virtual fashion. Therefore the Λ_i-variables assigned to long state components with surviving cusps of a knotoid transform to K_i-variables assigned to the circular components with surviving cusps in the arrow polynomial of the virtual knot which is the virtual closure of the knotoid. Using this idea, we show that the Λ-degree of the arrow polynomial can be used as a lower bound for the height of knotoids in S^2.

Theorem 2.41. *[15] The height of a knotoid in S^2 is greater than or equal to the Λ-degree of its arrow polynomial.*

Proof. Let K be a knotoid in S^2. By Theorem 6.3 and the discussion above we have the following inequality,

$$\text{The } \Lambda\text{-degree of } \mathscr{A}[K] \leq \text{The virtual crossing number of the knot } \overline{v}(K).$$

It is clear that the least number of virtual crossings obtained by closing a classical knotoid diagram virtually, is equal to the height of that diagram. Let $\tilde{K}$ be a classical knotoid diagram representing K. Then the height of the knotoid diagram $\tilde{K}$, $h(\tilde{K})$ is equal to the number of virtual crossings of $\overline{v}(\tilde{K})$. So, the virtual crossing number of the virtual knot $\overline{v}(K)$ is less than or equal to $h(\tilde{K})$. By this and the first inequality, we have the following.

$$\text{The } \Lambda\text{-degree of } \mathscr{A}[K] \leq h(\tilde{K}).$$

The inequality above holds for any classical knotoid diagram equivalent to K since the Λ-degree of the polynomial is invariant under the Ω-moves. Therefore we have,

$$\text{The } \Lambda\text{-degree of } \mathscr{A}[K] \leq h(K),$$

where $h(K)$ denotes the height of the knotoid K. □

A 3-variable bracket polynomial

Turaev defines a 3-variable polynomial invariant $[]_o$ [57] for knotoids in $\mathbb{R}^2$ with values in $Z(A^{\pm 1}, u^{\pm 1}, v)$ as follows. Each crossing of a planar knotoid diagram K are smoothed in two ways as in the bracket state expansion. We obtain states each consisting of a number of circular components and a long segment component. Given any state s, any circular state component bounds a disk in $\mathbb{R}^2$ which is either disjoint from the long segment component of the state or contain this long segment component. Let $p(s)$ be the number of the circular components of the former type and $q(s)$ be the number of the circles of the latter type. Then,

$$[K]_o = (-A^3)^{-wr(K)} u^{K.a} \Sigma_{s \in S(K)} A^{\sigma_s} u^{-k_s.a} (-A^2 - A^{-2})^{p(s)} v^{q(s)},$$

where $K.a$ is the algebraic intersection number of K with a chosen shortcut a and $k_s.a$ is the algebraic intersection number of the long segment of the state s, k_s with the shortcut a.

The polynomial $[]_o$ is the extended 2-variable bracket polynomial [57] when $v = -A^2 - A^{-2}$ and the normalized bracket polynomial when we also set $u = 1$.

We set $u = 1$ and keep the v- variable and call the polynomial as *Turaev loop polynomial*. The Turaev loop polynomial is a knotoid invariant as it can be verified in a routine way. It will be discussed later in Section 4 that we use the Turaev loop polynomial for detecting types of planar knotoids obtained by projecting a protein chain in to planes.

2.4.3 The affine index polynomial

The affine index polynomial was initially constructed for virtual knots and links by Kauffman [33]. In [15], we construct the affine index polynomial for knotoids. analogously. The affine index polynomial of a knotoid, either classical or virtual, is based on an integer labeling assigned to flat knotoid diagrams in the following way. A flat knotoid diagram, classical or virtual, is associated with a graph (virtual graph in the case of flat virtual diagrams) where the flat classical crossings and the endpoints are regarded as the vertices of the graph. An *arc* of an oriented flat

knotoid diagram is an edge of the graph it represents, that extends from one vertex to the next vertex. Note that tail and the head of the diagram are considered to be vertices of the graph). Given a knotoid diagram K, the labeling of each arc of the underlying flat knotoid diagram of K, $F(K)$, begins with the first arc which connects the tail and the first flat crossing. The integer labeling rule at a flat crossing is illustrated in Figure 2.30. At each flat crossing, the labels of the arcs change by one; if the incoming arc labeled by a, $a \in \mathbb{Z}$ crosses the crossing towards left then the next arc is labeled by $a+1$, if the incoming arc crosses the crossing towards right then it is labeled by $a-1$. There is no change of labels at virtual crossings. Note that the numbers at c, $w_+(c)$ and $w_-(c)$ are defined as differences of labels so that the weights are well-defined. Since the weights are well-defined up to this integer labeling, it is convenient to label the first arc with 0.

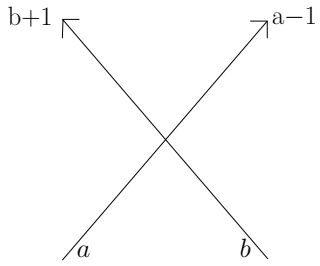

Figure 2.30: Integer labeling at a flat crossing

Let c be a classical crossing of K. We define two numbers at c resulting by the labeling of $F(K)$. These numbers that are denoted by $w_+(c)$ and $w_-(c)$, are defined as follows.

$$w_+(c) = a - (b+1)$$
$$w_-(c) = b - (a-1),$$

where a and b are the labels for the left and the right incoming arcs at the corresponding flat crossing to c, respectively. the numbers $w_+(c)$ and $w_-(c)$ are called *positive* and *negative* weights of c, respectively.
The *weight* of c is defined as

$$w_K(c) = \begin{cases} w_+(c), & \text{if the sign of } c \text{ is a positive crossing} \\ w_-(c), & \text{if the sign of } c \text{ is a negative crossing.} \end{cases}$$

Definition 2.42. The *affine index polynomial* of a virtual or classical knotoid diagram K is a Laurent polynomial in variable t that is defined by the following

equation.

$$P_K(t) = \sum_c \text{sign}(c)(t^{w_K(c)} - 1),$$

where the sum is taken over all classical crossings of a diagram of K.

The underlying flat diagram of the virtual closure of a knotoid diagram is labeled as the same as the knotoid diagram since virtual crossings do not add any new arcs or labels. In fact, we have $P_K(t) = P_{\overline{v}(K)}(t)$, where K is a knotoid diagram in S^2 and $\overline{v}(K)$ is the virtual closure of K.

Theorem 2.43. *[15] The affine index polynomial is a virtual and classical knotoid invariant.*

Proof. The polynomial $P_K(t)$, by its definition, is independent of the moves generated by the detour move. It is left to check the invariance under oriented Ω- moves. Note that for the verification of invariance of oriented virtual knot invariants, it is sufficient to check the oriented Reidemeister moves given in Figure 2.31 that include two types of the first move, one type of the second move and one type of the third move where there is a cyclic triangle in the middle and two of the crossings have the same sign and the third crossing has the opposite sign [52]. It can be verified easily that this argument applies directly to verification of virtual knotoid invariants. The integer labeling is uniquely inherited under these moves. The local changes (inside the disks where the move pattern lies) in labels is shown in Figure 2.31. It can be seen in the figure that the Ω_1-move adds a crossing with zero weight. The Ω_2-move adds/removes two crossings with opposite signs but with same weights. The Ω_3-move does not change weights or signs of the three crossings in the move pattern. Therefore, the affine index polynomial remains unchanged under these moves. □

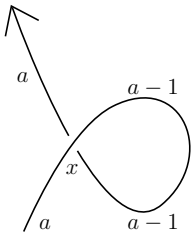

$w_+(x) = w_-(x) = 0$

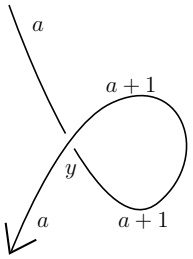

$w_+(y) = w_-(y) = 0$

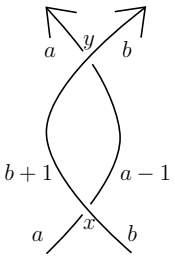

$w(x) = w_-(x) = b - a + 1$
$w(y) = w_+(y) = b - a + 1$

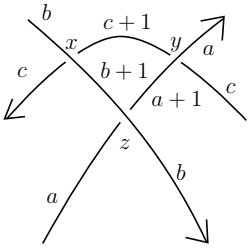

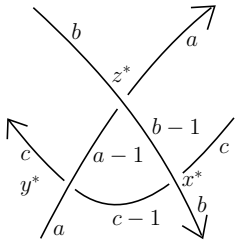

$w_+(x) = c - b = w_+(x^*)$
$w_+(y) = a - c = w_+(y^*)$
$w_+(z) = b - a = w_+(z^*)$

Figure 2.31: The invariance of the affine index polynomial under the oriented moves

A comparison of affine index polynomials: Knotoids vs Knots

The affine index polynomial of a knotoid in S^2 is the same as the affine index polynomial of its virtual closure that is a virtual knot as we noted before. We show in the following that the affine index polynomial has different properties for classical knotoids than the polynomial has for virtual and classical knots.

1. It is shown in [33] that any classical knot has trivial affine index polynomial. Similarly knot-type knotoids have trivial affine index polynomial. In fact,

any crossing of a knot-type knotoid diagram is even by Theorem 2.50, and so the weights of crossings are zero. Since a knot-type knotoid can always be represented by a knot-type knotoid diagram, the statement follows. On the other hand, proper knotoid diagrams have odd crossings that have nonzero weights. Following this, a proper knotoid may have nontrivial affine index polynomial if the contributions to the polynomial coming from the crossings do not cancel each other.
This difference may be used to determine whether a knotoid is proper or knot-type knotoid: If a given classical knotoid diagram has nonzero affine index polynomial, then we conclude that this knotoid diagram represents a proper knotoid.

2. Let k be a virtual knot. Then we have,

$$P_K(t) = P_{\overline{K}}(t^{-1}) \text{ [33]},$$

where K is an oriented diagram of k and $\overline{K}$ is the inverse of K (see Section 2.1.4). Therefore, the affine index polynomial may be used to distinguish a virtual knot from its inverse.
The affine index polynomial fails to distinguish a knotoid diagram from its inverse as we explain in the sequel.

Definition 2.44. The weights of crossings of a knotoid diagram K are said to be *symmetric* if for any classical crossing of K, c_1 with a nonzero positive weight $w_+(c_1)$, there is another classical crossing c_2 with a nonzero positive weight $w_+(c_2)$ such that $w_+(c_2)=-w_+(c_1)$. Such two crossings with opposite positive weights are said to be *paired* crossings.

Lemma 2.45. *[15] The weights of the crossings of a flat knotoid diagram in S^2 are symmetric.*

Proof. Proposition 2.28 implies that any flat knotoid diagram in S^2 can be obtained from the trivial knotoid diagram by a finite sequence of the flat Ω-moves, and also by isotopy of S^2. Using this fact, we proceed by induction on flat knotoid diagrams in S^2. The trivial diagram has no crossings so conventionally it satisfies the lemma. The flat diagrams shown in Figure 2.32, are obtained by applying one or two Ω_i-moves to the trivial knotoid diagram. The weights of crossings of these diagrams are symmetric, as can be seen in the figure. Let us assume that the weights of crossings of any flat classical knotoid diagrams that are obtained by applying $n > 0$ flat Ω_i- moves to the

trivial knotoid diagram are symmetric. Let K be such a flat knotoid diagram and K_1, K_2, K_3 be flat knotoid diagrams that are obtained by applying one flat Ω_1, Ω_2 and Ω_3-move to K, respectively. A flat Ω_2 move adds/removes two crossings to K. Since the weights of the other crossings outside the move region are not affected, the symmetry of weights of K is not destroyed. If the crossings located in the move region are even then they both have zero weights. If the crossings are odd then they are paired crossings. Thus, the weights of crossings of K_2 are symmetric. A flat Ω_3- move does not change the weights of the three crossings, A, B, C that are located in the triangular region of the move or the weights of the crossings outside the move region. If A, B, C are even crossings then they have zero weight and they are taken to crossings with zero weight by a flat Ω_3-move. If two of these crossings are odd and one of them is even, it is assumed that the odd crossings are paired with some other crossings of K (either two of them with each other or with other crossings in the rest of the diagram). Thus the weights of K_3 are symmetric. A flat Ω_1- move adds/removes one crossing with zero weight to the given diagram K and does not change the weights of the remaining crossings. Therefore, the weights of the crossings of K_1 are symmetric. This completes the induction and proves that the weights of crossings of any flat knotoid diagram in S^2 are symmetric. □

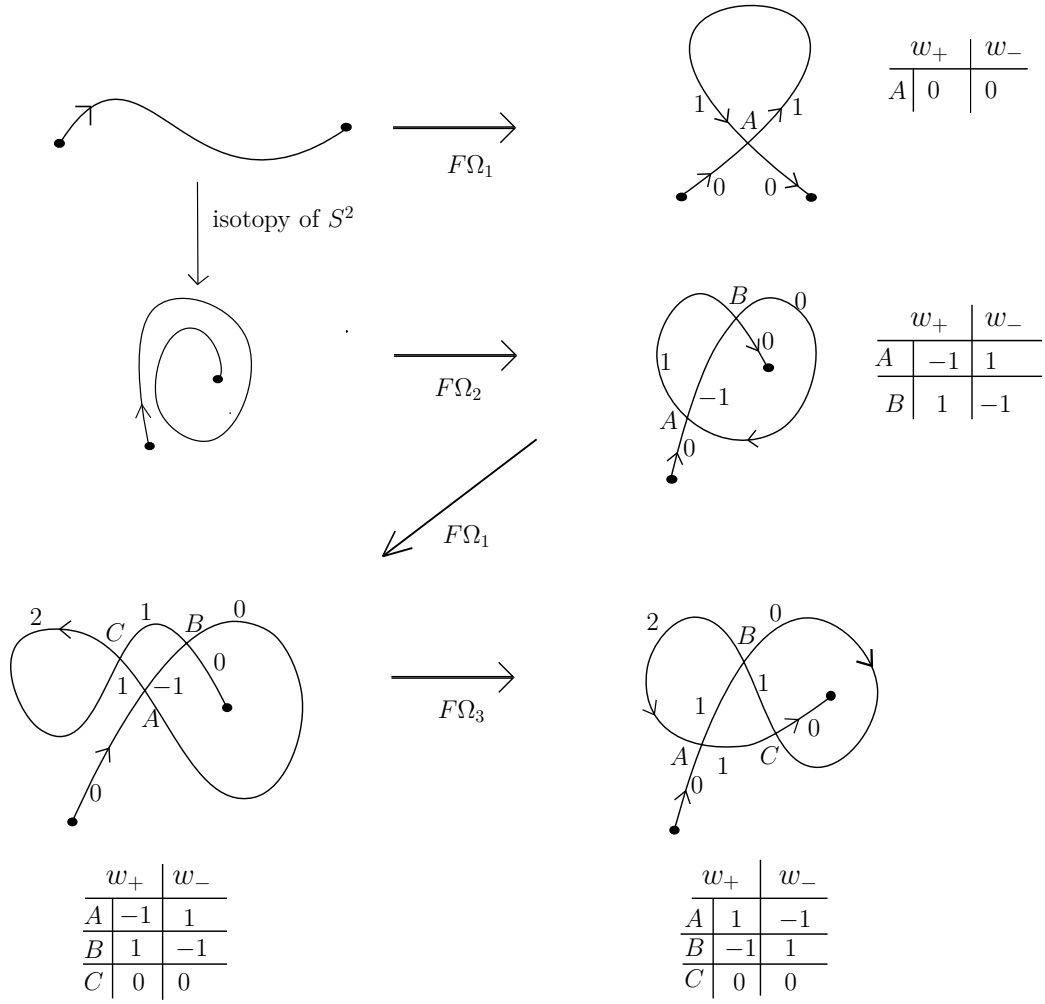

Figure 2.32: Induction step

Theorem 2.46. *[15] The affine index polynomial of a knotoid K in S^2 is symmetric with respect to $t \leftrightarrow t^{-1}$. Therefore, $P_K(t) = P_{\overline{K}}(t)$, where $\overline{K}$ denotes the inverse of K.*

Proof. Lemma 2.45 shows that any crossing of a knotoid diagram in S^2 with a nonzero positive weight, is paired with another crossing. If the signs of paired crossings are different then the contributions of these crossings to the polynomial are canceled out. Let c_1 and c_2 be two paired crossings with the same sign, then they contribute to the polynomial either as the summands $(t^n - 1)$ and $t^{-n} - 1$ or $-t^n + 1$ and $-t^{-n} + 1$, respectively, where n is the weight of c_1 and $-n$ is the weight of c_2. Since the affine index polynomial is a classical knotoid invariant, the symmetry of the affine index polynomial follows. It can be verified easily by the reader that reversing the orientation of K only permutes the set of crossings and the weight chart of K. The

affine index polynomial remains the same by reversing the orientation of K. Therefore we have $P_K(t) = P_K(t^{-1}) = P_{\overline{K}}(t^{-1}) = P_{\overline{K}}(t)$. □

3. The mirror reflection on a virtual knot and a knotoid diagram does not change weight chart since the underlying flat diagrams appear the same. But this operation changes the signs of (classical) crossings of diagrams and so reverses the attributed weight to a crossing. For an oriented virtual knot diagram K, this results in the following equality.

$$P_K(t) = -P_{K^*}(t^{-1}) \text{ [33]}$$

Therefore if the affine index polynomial of a virtual knot is non-trivial then the polynomial distinguishes the knot from its mirror reflection .
On the other hand, since the weights of a knotoid in S^2 are symmetric by the above argument, the affine index polynomial changes only by sign. That is we have,

$$P_K(t) = -P_{K^*}(t)$$

This shows non-trivial affine index polynomials are able to distinguish a knotoid from its inverse.

Note 8. *There are virtual knotoids with non-symmetric affine index polynomial. For instance, it can be verified that any virtual knotoid diagram whose underlying flat diagram and the corresponding weight chart are as given in Figure 2.33, has non-symmetric affine index polynomial. Consequently, none of these virtual knotoid diagrams is virtually equivalent to a classical knotoid diagram.*

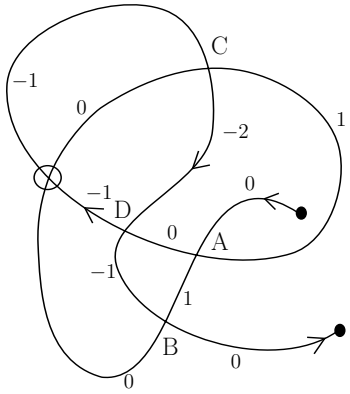

	w_+	w_-
A	0	0
B	1	−1
C	−2	2
D	1	−1

Figure 2.33: A flat virtual knotoid diagram with non-symmetric weights

Theorem 2.47. *[15] If the affine index polynomial of a virtual knot is not symmetric with respect to $t \leftrightarrow t^{-1}$ then it is not the virtual closure of a knotoid in S^2.*

Proof. The affine index polynomial remains unchanged by the virtual closure map since the virtual crossings added via the map, do not change the weights of any of the (classical) crossings and have no contribution to the polynomial. Thus, we have $P_K(t) = P_{\overline{v}(K)}(t)$, where K is a knotoid in S^2. The statement follows by this equality and by Theorem 2.46. □

Estimation of the height of a knotoid via the affine index polynomial

Now, we demonstrate a lower bound for the height of a knotoid by using the affine index polynomial.

Theorem 2.48. *[15] Let K be a knotoid in S^2. The height of K is greater than or equal to the maximum degree of the affine index polynomial of K.*

Proof. Let $\tilde{K}$ be a knotoid diagram representing K. We label the underlying flat knotoid diagram of $\tilde{K}$ with respect to the labeling rule given in Figure 2.30. The *algebraic intersection number* of a loop at a crossing C, $l(C)$ (see Section 2.4.4 for the definition of the loop at a crossing) with a strand of $\tilde{K}$ is defined to be the total number of times that the strand intersects the loop from right to left minus the total number of times that the strand intersects the loop from left to right. Figure 2.34 illustrates two possible types of loops at the crossing C one of which is oriented in the counterclockwise, and the other in the clockwise direction. The algebraic intersection numbers of the loop at C with the piece of strand shown in the figure, are $+1$ and -1, respectively. In both pictures, the incoming arcs towards the crossing C are labeled by some integer a. Assuming that the strand shown is the only one intersecting the loops, it can be verified that $+1$ is equal to the negative weight of the crossing C of the first loop and -1 is equal to the positive weight of the crossing C of the second loop. Then the following generalization is clear. If the sum of the algebraic intersection numbers of the loop $l(C)$ at the crossing C with intersecting strands is equal to n then n is equal to either $w_-(C)$ or $w_+(C)$, depending on the orientation of the loop $l(C)$.

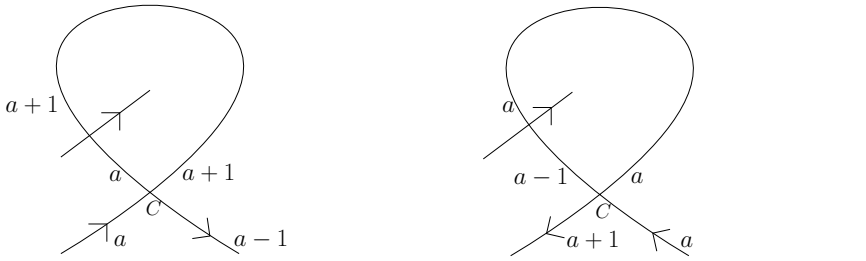

Entering Value − Exit Value $= w_-(C)$ Entering Value − Exit Value $= w_+(C)$

Figure 2.34: The weights with respect to the orientation of the loop at C

Let m be the maximum degree of the affine index polynomial of K. Then there exists a crossing of $\tilde{K}$ with weight m. In fact, m is the maximal weight among the weights of crossings of $\tilde{K}$. Let $\tilde{C}$ be one of the crossings of $\tilde{K}$ with weight m and $l(\tilde{C})$ be the loop at $\tilde{C}$.

Figure 2.35 shows the oriented smoothing of a classical crossing of a knotoid diagram. Each crossing which are met twice while traversing along the loop $l(\tilde{C})$, including the crossing $\tilde{C}$ itself, are all smoothed accordingly to the orientation. This implies that each self-intersection of the loop $l(\tilde{C})$ is smoothed. Smoothing the self-intersections of the loop $l(\tilde{C})$ results in oriented disjoint oriented embedded circles (in S^2), so called *Seifert circles*, and a long oriented segment containing the tail and the head of $\tilde{K}$. The long segment may intersect the resulting circles and itself. The *algebraic intersection number* of a Seifert circle with the long segment is defined as the total times of the segment intersects the circle from right to left minus the total times of the segment intersects the circle from left to right. Let $I_{\tilde{K}}$ denote the sum of the algebraic intersection numbers of resulting Seifert circles with the long segment.

Figure 2.35: Smoothing a crossing in the oriented way

The crossings of $\tilde{K}$ that contributes to non-trivially to the total algebraic intersection number are not smoothed since such crossings are met only once. As a result, $I_{\tilde{K}}$ is equal to the sum of algebraic intersection numbers of the loop $l(\tilde{C})$ with the strands intersecting $l(\tilde{C})$. This shows that the sum of algebraic intersection numbers of the Seifert circles with the long segment is equal to either $w_-(\tilde{C})$ or $w_+(\tilde{C})$. Thus, the absolute value of $I(K)$ is equal to the , $|I(K)| = m$.

On the other hand, it is easy to verify that the number $|I_K|$ can be at most as large as the number of the Seifert circles that are enclosing the endpoints (the tail

or the head). In particular, $|I_K|$ is equal to the number of the Seifert circles if all intersections are positive. Thus we have that m is at most as the number of circles enclosing the endpoints.

The height of the diagram $\tilde{K}$ is at least as large as the number of the Seifert circles enclosing the endpoints, by the Jordan curve theorem. With this we have $h(\tilde{K}) \geq m$.

The affine index polynomial is a knotoid invariant so m appears as the maximum degree of the affine index polynomial of any classical knotoid diagram equivalent to $\tilde{K}$. This implies that there is a crossing with weight m in each representative knotoid diagram of K. Applying the same procedure explained above to the loops at the crossings with weight m in each representative diagram gives us the inequality, $h(K) \geq m$ for any representative classical diagram K and the statement follows. □

Figure 2.36 gives an illustration for the proof of Theorem 2.48. In the figure the affine index polynomial of the knotoid K given in Figure 2.1(g), is computed. We see that C is one of the maximal weight crossings of K. Smoothing all the twice-met crossings on the loop at C in the oriented way results in two Seifert circles and an oriented long segment intersecting the circles.

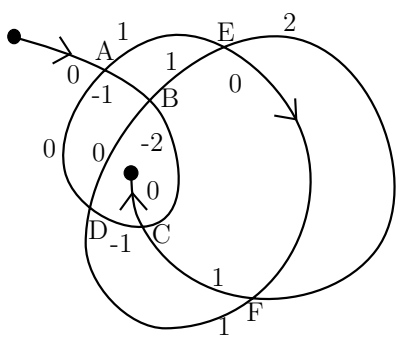

	w_+	w_-
A	(-1)	1
B	(-2)	2
C	(2)	-2
D	(1)	-1
E	(-1)	1
F	(1)	-1

$$P_K(t) = t^2 + 2t + 2t^{-1} + t^{-2} - 6$$

(a) $F(K)$ with integer labels

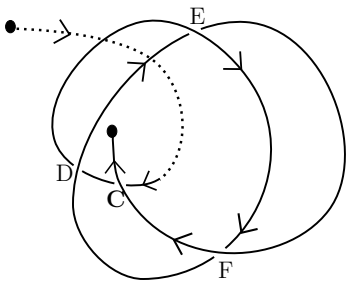

(b) The loop at the crossing C

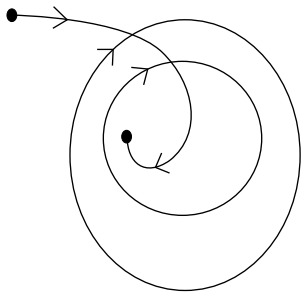

(c) Resulting Seifert circles and the long segment

Figure 2.36: An illustration for the proof of Theorem 2.48

One immediate consequence of Theorem 2.48 is that we are able to tell the height of the knotoids that can be represented with a spiral diagram with positive crossings. In particular, the affine index polynomials of the knotoids each represented by a diagram overlying the flat diagrams in 2.37 with positive crossings are the following. $P_{K_1}(t) = t + t^{-1} - 2$, $P_{K_2}(t) = t^2 + t + t^{-1} + t^{-2} - 4$ and $P_{K_3}(t) = t^3 + t^2 + t + t^{-1} + t^{-2} + t^{-3} - 6$. The heights of the given diagrams are 1, 2 and 3, respectively. Then by the theorem, it is concluded that the heights of the knotoids are 1, 2 and 3, respectively. This is generalized as follows. The affine index polynomial of a classical knotoid represented by an n- fold spiral knotoid diagram has a term of the form $t^n + t^{-n}$ if all crossings of the diagram are positive. The maximum degree of the affine index polynomial is n and the height of the spiral diagram is n. By Theorem 2.48, we conclude that the height of the knotoid is n. This shows that we have an infinite set of knotoids whose height is given by the affine index polynomial.

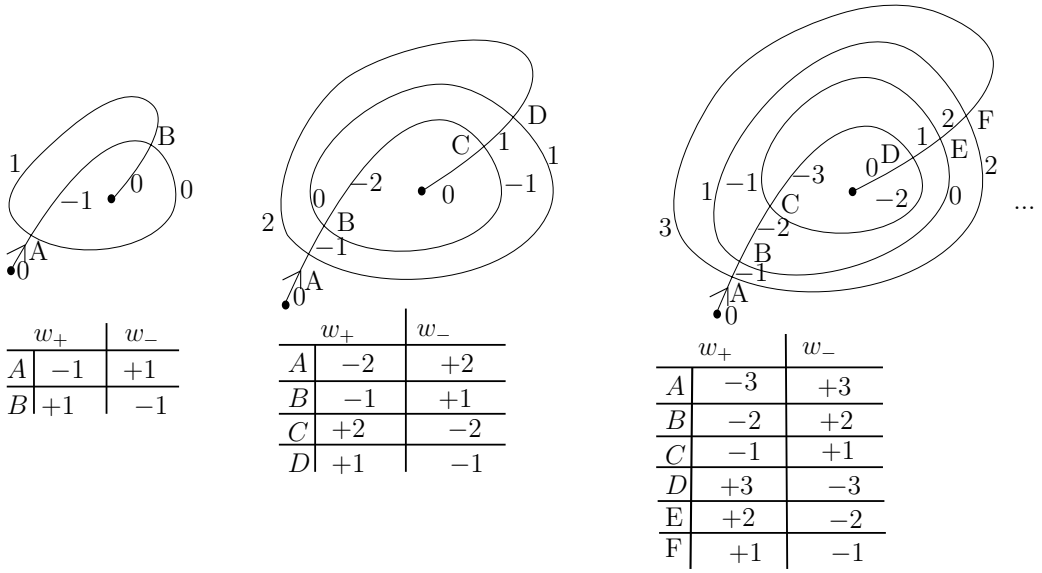

	w_+	w_-
A	-1	$+1$
B	$+1$	-1

	w_+	w_-
A	-2	$+2$
B	-1	$+1$
C	$+2$	-2
D	$+1$	-1

	w_+	w_-
A	-3	$+3$
B	-2	$+2$
C	-1	$+1$
D	$+3$	-3
E	$+2$	-2
F	$+1$	-1

Figure 2.37: Flat spiral knotoid diagrams

A discussion on the arrow polynomial and the affine index polynomial

The presented two tools for the estimation of the height of a knotoid, namely, the arrow polynomial and the affine index polynomial differ from each other conceptually. The arrow polynomial coincides with the bracket polynomial of knotoids [15, 16, 57] if the Λ_i-variables assigned to long segment components of oriented states are set to be equal to 1. In other words, the arrow polynomial is a generalization of the bracket polynomial of knotoids as we have already mentioned. The affine index polynomial on the other hand, uses the biquandle structure [12, 31] on flat knotoid diagrams.

In terms of height estimation, the strengths of the two polynomials also differ. There are cases that both of the polynomials give the same estimation for the height and there are cases in which one of the polynomials give a more accurate estimation. We give some examples here.

Example 2. The arrow polynomial of the knotoid K, represented by the diagram given in Figure 2.1(g) is equal to

$$\mathscr{A}[K] = A^6 - (A^{-4} - A^4)\Lambda_1 - (A^{-2} - A^2)\Lambda_2.$$

The Λ-degree of the arrow polynomial of the knotoid K is 2. As can be computed by the weight chart given in Figure 34(a), the affine index polynomial of K is equal to

$$P_K(t) = t^2 + 2t + 2t^{-1} + t^{-2} - 6,$$

Thus the maximal degree of the affine index polynomial of K is also equal to 2. So both the affine index polynomial and the arrow polynomial give the same lower bound for the height. It is easy to check that the height of the knotoid diagram in the figure is 2. Since K can be represented by a diagram with height 2, we conclude that the height of K is 2.

Example 3. The affine index polynomial of the knotoid K which is overlying the flat 3-fold spiral knotoid diagram given in Figure 2.37 with negative crossings B, C and D and positive crossings A, E and F, is trivial since the contributions by the crossings cancel each other. Direct computation shows that the arrow polynomial of the knotoid is equal to

$$\mathscr{A}[K] = 1 + (-A^{-3} + A^{-2} + A^2 + A^6)\Lambda_1 + (-2A^{-4} - 2A^4 + 4)\Lambda_2 + (-A^{-6} + A^{-2} + A^2 + A^6)\Lambda_3.$$

The Λ- degree of the arrow polynomial is 3 so by Theorem 2.41, the height of the knotoid K is at least 3. It is visible by the figure that the height of the given diagram is also 3. Therefore the height of the knotoid K is 3.

Example 4. Figure 2.38 illustrates a knotoid diagram representing the knotoid **5.7** [68] and the corresponding weight chart. It can be verified easily that the affine index polynomial of knotoid **5.7** is trivial. Direct computation shows that the arrow polynomial of the knotoid is equal to

$$\mathscr{A}[K_{5.7}] = (-A^{-3} + A - 2A^5 + A^9) + (A^{-9} - 2A^{-5} + 2A^{-1} - 2A^3 + A^7)\Lambda_1.$$

Thus it is a non-trivial arrow polynomial with Λ-degree 1. By Theorem 2.41 it follows that the height of the knotoid 5.7 is at least 1. It is seen by the figure that the height of the knotoid diagram is 1. Since the knotoid 5.7 is represented by a diagram with height 1, we conclude that the height of the knotoid 5.7 is 1.

Example 5. The reader can see that the height of the knotoid diagram K given in Figure 2.1(f) is equal to 2. We want to find out if there exists an equivalent knotoid diagram to K with less height. The affine index polynomial of K is equal to

$$P_K(t) = 2t + 2t^{-1} - 4$$

as can be verified by Figure 2.39. Direct computation shows that the arrow polynomial of K is equal to

$$\mathscr{A}[K] = (-A^{-5} + 2A^{-1} - A^3 - A^7) + 2(A - A^5)\Lambda_1.$$

The affine index polynomial and the arrow polynomial both assure that the height of K is at least 1. Therefore we have, $1 \leq h(K) \leq 2$. This is a case where our tools discussed here cannot give an exact estimation for the height.

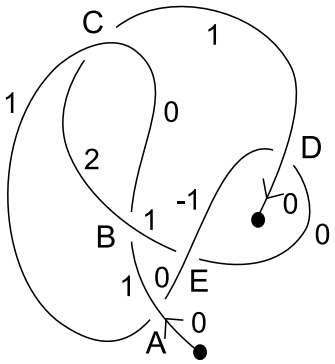

	w_+	w_-
A	0	⓪
B	-1	①
C	1	-①
D	①	-1
E	-①	1

Figure 2.38: The weight chart of knotoid 5.7

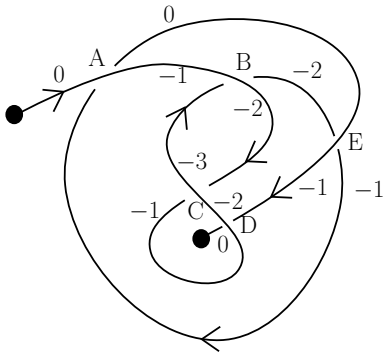

	w_+	w_-
A	⓪	0
B	①	-1
C	-①	1
D	①	-1
E	-①	1

Figure 2.39: The weight chart of K

2.4.4 Parity in knotoids

Gauss codes/diagrams

We introduce the Gauss code and Gauss diagram for knotoids [15]. The *Gauss code* of a knotoid diagram K (classical, virtual or flat) is a linear code that consists of a sequence of labels each of which is assigned to the classical (or flat for flat diagrams) crossings encountered during a trip along K from its tail to the head. Since any crossing of K is traversed twice, each label in the code appears twice. Thus, the length of the code is $2n$, where n is the number of classical crossings (flat crossings for flat diagrams) of K. We keep the information of the passage through a crossing either as an overcrossing or an undercrossing by adding the symbols O and U, respectively, to the code, and we keep the signs of the crossings by putting

+ or − next to the label accordingly to the sign of the crossing. The resulting code is referred as the *signed Gauss code* of K. Note that the symbols O and U and the signs of crossings are omitted in the Gauss codes of flat knotoid diagrams.

Gauss codes have a diagrammatic representation as follows. Each label in the Gauss code is represented by $2n$ points placed upon a segment which is oriented from left to right. The points are labeled as the corresponding labels in the code. A signed and oriented chord connects each pair of the labeled points. The orientation of a chord heads from the overcrossing to the undercrossing. That is, during a travel along the knotoid diagram K starting from the tail, if a crossing is first encountered as an overcrossing then the arrow of the corresponding chord heads towards the second appearance of the label. The sign of the chord is the sign of the associated crossing. For flat knotoid diagrams, we have the notion of right and left at each flat crossing as follows. If a crossing is first encountered as going to the right then the head of the arrow on the corresponding chord heads towards the first appearance of the label. We call such a diagram with chords that represents the Gauss code of a knotoid diagram the *chord diagram* or the *Gauss diagram* of the knotoid diagram. Each knotoid diagram, including classical, virtual and flat knotoid diagrams, has a unique Gauss code and chord diagram. Figure 2.40 depicts the chord diagram of the knotoid diagram K that is given in Figure 2.1(g).

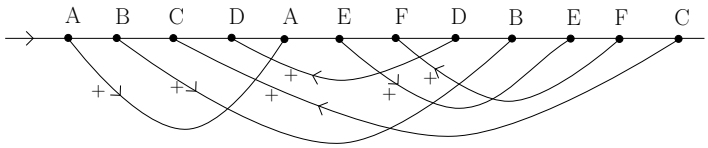

Figure 2.40: Chord diagram of K

Definition 2.49. A single component Gauss code is said to be *evenly intersticed* if there is an even number of labels between two appearances of any label.

Any classical knot diagram has evenly intersticed Gauss code [53]. The Gauss codes of classical knotoid diagrams are not necessarily evenly intersticed. For instance, the Gauss code of K shown in Figure 2.40, is $OA + OB + UC + UD + UA + OE + UF + OD + UB + UE + OF + OC+$, which is not an evenly-intersticed Gauss code. This fact gives rise to a well-defined parity for the crossings of classical knotoid diagrams taking values in $\mathbb{Z}_2$. A crossing of a classical, virtual or flat knotoid diagram is called *odd* if there is an odd number of labels in between the two appearances of the crossing otherwise it is called an *even* crossing. For the knotoid diagram K, the crossings A, D, E and F of the knotoid diagram K are odd, and the

crossings B, C are even. Note that for the purpose of parity we may use the Gauss code of the underlying flat diagram of a knotoid diagram.

Theorem 2.50. *[15] The Gauss code of a knotoid diagram in S^2 is evenly intersticed if and only if it is a knot-type knotoid diagram.*

Proof. *The loop* at a (classical) crossing of a knotoid diagram in S^2 is defined to be the path obtained by traversing the knotoid diagram starting and ending at that crossing, accordingly to the orientation. There is a loop at each crossing of a knotoid diagram. Let K be a proper knotoid diagram. Then one of the endpoints of K is separated from the other endpoint by at least one loop at a crossing of K, that is, one of the endpoints is located inside at least one loop. All the strands entering the loop except the one that is adjacent to the endpoint, leave the loop by Jordan curve theorem. Thus each such strand contributes with a pair of labels to the Gauss code of the diagram. The Gauss code of K along this loop is in the following pattern: $...c...\ d\ a\ e\ ...\overline{a}...\ \overline{e}\ c...$, where c represents the crossing that forms the loop containing the endpoint, d represents the crossing of the strand adjacent to the endpoint with the loop, and $a, \overline{a}$ and $e, \overline{e}$ for the pairs of crossings created by the transversally intersecting strands which enter and leave the loop. Thus, between the two appearances of the label c, we have an odd number of labels so that the Gauss code of K is not evenly-intersticed. For a knot-type diagram K, we can assume that the tail and head lie in the outermost region of the diagram (where the ∞-point is located) so that none of the loops at crossings encloses them. Again by Jordan curve theorem, all the strands passing through any of the loops of K enter and leave the loop so that they contribute with a pair of labels to the Gauss code of K. This shows that each crossing is even, that is, the Gauss code of K is evenly-intersticed. □

Lemma 2.51. *[15] The Gauss code of a knotoid diagram in S^2 is the same as the Gauss code of its virtual closure.*

Proof. The virtual closure map adds virtual crossings to a given knotoid diagram then it is clear that the map does not have any effect on the Gauss code of the diagram. □

Odd writhe

Using the parity of crossings of knotoid diagrams, we introduce the odd writhe of knotoids [15] in analogy with the odd writhe of virtual knots/links [36].

Definition 2.52. The *odd writhe* for both classical and virtual knotoid diagrams is defined to be the sum of the signs of the odd crossings,

$$\textit{Odd Writhe of } K = J(K) = \sum_{c \in (K)}(c),$$

where K is a knotoid diagram and Odd(K) is the set of odd crossings in K.

Theorem 2.53. *[15] Odd writhe is a virtual and classical knotoid invariant.*

Proof. The virtual moves that are induced by the detour move do not have an effect on the Gauss code of a virtual knotoid diagram. As a result, the set of odd crossings of the virtual knotoid diagram remains the same under these moves. The odd writhe is invariant under the virtual moves. It is left to verify the invariance under the Ω-moves. The changes in Gauss codes under some of the classical moves are illustrated in Figure 2.41. In this figure, A, B, C denote the labels of the crossings lying in the move patterns, and τ, γ and ω denote the words consisting of the labels of crossings that are met outside of the move patterns during a trip along a knotoid diagram. We observe the following. An Ω_1-move adds/removes two consecutive labels in the Gauss code. The parity of the crossings outside the move region remains the same and being an even crossing, the added/removed crossing by an Ω_1-move does not affect the odd writhe.

An Ω_2-move adds/removes either a pair of even crossings or a pair of odd crossings with opposite signs for any orientation type of the move. In the former case the even crossings do not have any effect on the odd writhe. In the latter case, the two odd crossings will be canceled out in the odd writhe summation for they have opposite signs. The parity of the crossings located outside the Ω_2 move region, remains the same since the labels which are added/removed by one Ω_2-move are located as consecutive pairs in the the Gauss code.

The triangular move pattern of Ω_3-move can contain either three even crossings or two odd crossings and one even crossing. In the former case, these even crossings are taken to even crossings by an Ω_3-move and the parity of other crossings outside the move pattern remains the same thus the odd writhe is not affected. In the latter case, an Ω_3- move permutes the order of the odd crossings in the Ω_3-move region. The parity and the sign of the odd crossings remain the same. It is not hard to see that the parities of crossings outside the move pattern do not change and the arguments above hold for the other cases of the oriented Reidemeister moves. Therefore, the odd writhe is an invariant of both virtual and classical knotoids. □

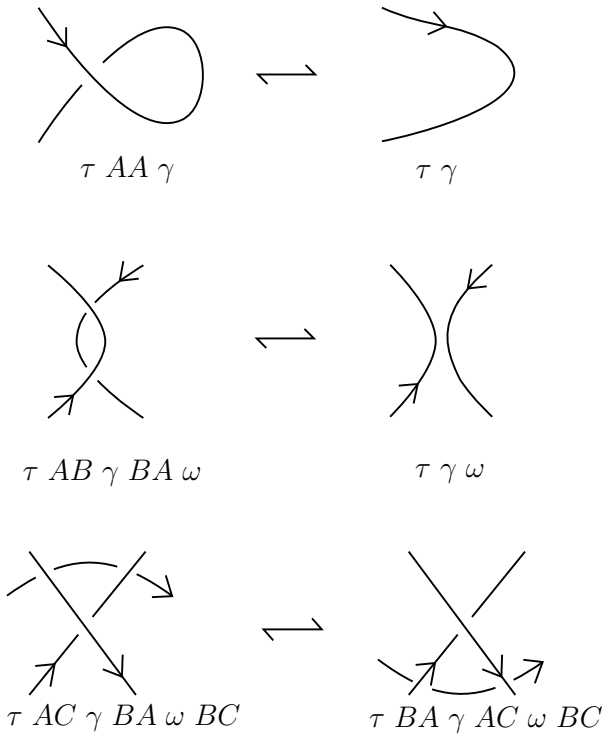

Figure 2.41: Change in Gauss codes under the oriented Ω- moves

Corollary 7. If a knotoid K is a knot-type knotoid then the odd writhe of K is zero.

Proof. It follows by Theorem 2.50 and Theorem 2.53. □

Note 9. The crossings shared by any two components of a multi-knotoid diagram obstruct extending the parity to multi-knotoids. For instance, the Gauss code of the multi-knotoid diagram given in Figure 2.42 is $O1-U2-O3-O4+U1-O2-U3-/U4+$. Crossings $1, 2$ and 3 are even crossings in the circular component. These crossings become odd when the second component is considered.

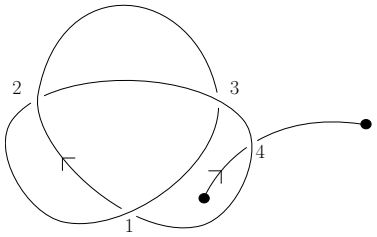

Figure 2.42: A multi-knotoid diagram

To define a well-defined parity for crossings of multi-knotoid diagrams, we apply the same method used in [26, 27, 87] to extend the parity to a parity of virtual

links [15]. The idea is to regard the crossings of a multi-knotoid diagram that are shared by two components as *link crossings*. The parity remains the same for self-crossings of each component, as odd or even crossings. In particular for the diagram given in Figure 2.42, the crossings 1, 2, 3 are even and the crossing 4 is a link crossing.

Parity bracket polynomial

The parity bracket polynomial of Manturov [87] is a modification of the bracket polynomial that uses the parity of crossings in virtual knots and links. With the existence of even and odd crossings in knotoid diagrams, we define the parity bracket polynomial for both classical and virtual knotoid diagrams [15] as follows. For a knotoid diagram K, either classical or virtual, a *parity state* is defined to be a labeled graph (a virtual graph for virtual diagrams). A parity state of a virtual knotoid diagram K is obtained by smoothing the even crossings of K by A- and B-smoothing type of the usual bracket polynomial and labeling the smoothing sites by A or A^{-1}, respectively, and replacing the odd crossings of K by graphical nodes. Note that circular and long segment components of parity states are regarded as graphs.

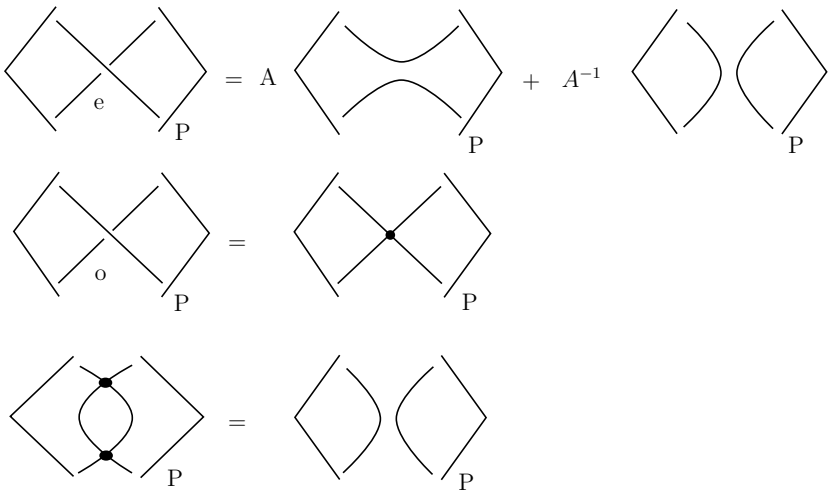

Figure 2.43: Parity bracket expansion

The resulting states are taken up to the virtual equivalence (isotopy of S^2 and detour moves) and up to the *reduction rule*, shown in Figure 2.43. The reduction rule is simply a Reidemeister two- move that eliminates two graphical nodes forming the vertices of a bigon. The state components that still contain nodes after applying the reduction rule, are called *irreducible state components*. Each irreducible state

component contributes to the polynomial as a graphical coefficient.

Definition 2.54. The *parity bracket polynomial* of a virtual or classical knotoid diagram K, is defined as

$$< K >_P = \sum_S A^{n(S)}(-A^2 - A^{-2})^{l(S)}G(S),$$

where $n(S)$ denotes the number of A-smoothings minus the number of B-smoothings, $l(S)$ is the number of components without any nodes of the parity state S and $G(S)$ is the union of irreducible state components.

Definition 2.55. The *normalized parity bracket polynomial* of a knotoid diagram (classical or virtual) K is defined as

$$\overline{< K >_P} = (-A^3)^{-\operatorname{wr}(K)} < K >_P.$$

Theorem 2.56. *[15] The normalized parity bracket polynomial is a virtual and a classical knotoid invariant.*

Proof. It can be verified by the reader that one Ω_1-move adds/removes an even crossing and changes the polynomial by $-A^{\pm 3}$. Then the writhe normalization makes the parity polynomial invariant under an Ω_1- move. An Ω_2-move may add two crossings that are both even crossings. In this case the parity bracket polynomial is invariant under this move since the bracket polynomial is invariant under Ω_2-move. If the crossings in the move pattern are both odd crossings, the reduction rule applies and eliminates the crossings. So, the polynomial does not change by an Ω_2- move. It is clear that the invariance under Ω_3- move, if three of the crossings in the triangular region are even, follows from the bracket polynomial invariance, and if two of them are odd and one is an even crossing then the invariance follows by an isotopy of the state component. □

The parity bracket polynomial can be defined for flat virtual knotoids and flat knotoids [15] as follows. Let K be a flat diagram. Odd crossings of K are replaced by graphical nodes and even crossings are smoothed out in two ways, and the smoothing sites are labeled by $A = -1$. If K is a virtual flat diagram, virtual crossings of K are kept as they are. In this way, we obtain the parity states of K. The reduction rule applies the same on the parity states of K for the elimination of nodes. The *parity bracket polynomial* of K is defined as,

$$< K >_P = \sum_S -2^{l(S)}G(S),$$

where $l(S)$ is the number of components without any nodes of the parity state S and $G(S)$ is the union of irreducible state components.

Theorem 2.57. *[15] The parity bracket polynomial is an invariant of flat virtual knotoids and flat knotoids. The parity bracket polynomial of a flat knotoid in S^2 is trivial.*

Proof. The invariance of the parity bracket polynomial for flat knotoids can be seen easily by checking of the invariance of the polynomial under the generalized flat Ω-moves. Since any flat knotoid in S^2 is f-equivalent to the trivial knotoid, the second statement follows. □

Proposition 2.58. *[15] There is no irreducible state component in the parity state expansion of a knotoid diagram in S^2.*

Proof. Let K be a knotoid diagram in S^2. If K is a knot-type knotoid diagram then none of its crossings is odd, as a result of Jordan curve theorem. Therefore, there is no graphical coefficient contributing to the parity bracket polynomial of K. In fact, the parity bracket polynomial of K coincides with its usual bracket polynomial. On the other hand, if K is a proper knotoid diagram then K has odd crossings by Theorem 2.50. Thus the parity states of K have components with nodes each corresponding to an odd crossings of K. It is clear that the set of odd crossings of K is the same with the set of odd crossings of $F(K)$ where $F(K)$ is the underlying flat knotoid diagram of K. For this reason, the existence of any irreducible state component in parity states of K would cause an irreducible state component in the parity states of $F(K)$. Thus to prove the theorem it is sufficient to show that any graphical state component of a flat knotoid diagram can be reduced to a component that is free of nodes. Proposition 2.28 implies that any flat knotoid diagram in S^2 can be obtained from the trivial knotoid diagram by finitely many flat Ω-moves. We induct on the flat knotoid diagrams.

The trivial knotoid diagram has no crossing so it has no irreducible state component. We assume that graphical state components of all flat diagrams that are obtained from the trivial diagram by an application of n flat Ω- moves, can be reduced to a component without any nodes. Let $\tilde{K}$ be such a flat knotoid diagram. A single flat Ω_2-move adds/removes either two odd or even crossings to $\tilde{K}$. Two crossings added/removed do not change the parity of the crossings outside the flat Ω_2-move pattern, as explained in the proof of Theorem 2.53. If the crossings are even crossings then they increase/decrease the number of state components but there is no resulting graphical component. If the crossings (added) are odd crossings, they are located as the vertices of a bigon (they are paired up) that can be eliminated by the reduction rule. Two paired up odd crossings are removed by the move, and since the rest of the odd crossings are assumed to be paired up so that they can be eliminated, there is no irreducible state component created. Thus a flat knotoid diagram

which is obtained by applying one Ω_2- move to $\tilde{K}$, does not have any irreducible graphical state components in its parity states.

The flat Ω_3- move does not add/remove any odd or even crossings or change the parity of the crossings outside the move pattern. Thus, the parity states of a flat knotoid diagram obtained by applying one flat Ω_3-move to $\tilde{K}$ are isotopic to the parity states of $\tilde{K}$.

The flat Ω_1-move adds/removes an even crossing which does not change the parity of the crossings outside the move pattern and does not add any nodes to the diagram, so there are no resulting graphical state components. This completes the induction argument. The parity state components of any flat knotoid diagram are reduced to state components that are free of nodes. Therefore, the parity state components of a knotoid diagram in S^2 are reducible. □

Lemma 2.59. *[15] Let K be a knotoid in S^2. Then we have $< K >_P = < \overline{v}(K) >_P$.*

Proof. Let $\tilde{K}$ be a classical knotoid diagram representing K. The classical crossings of $\overline{v}(\tilde{K})$ are the same with the classical crossings of $\tilde{K}$. Neither the skein relations nor the reduction rule of the parity bracket polynomial are applied to the virtual crossings of a virtual knot diagram, so to the virtual crossings of $\overline{v}(\tilde{K})$. By Proposition 2.58 , all nodes in a parity state component of $\tilde{K}$ are eliminated so that each parity state of $\tilde{K}$ is reduced to consist of disjoint simple closed curves and a long segment component. If any of the virtual crossings of $\overline{v}(\tilde{K})$ passes through a bigon whose vertices are reducible graphical nodes of a parity state of $\tilde{K}$ then we can move these virtual crossings out of the bigon by the detour move that is available for the parity states. After moving the virtual crossings out of the bigon, we can eliminate the nodes by the reduction rule as we do for the parity state of $\tilde{K}$. Therefore, any parity state component of $\overline{v}(\tilde{K})$ can be obtained by connecting the endpoints of the long segment component of the corresponding parity state component of $\tilde{K}$ in the virtual fashion. This shows that $< K >_P = < \overline{v}(K) >_P$. □

Corollary 8. *[15] If there are graphical coefficients in the parity bracket polynomial of a virtual knot K then K is not the virtual closure of a knotoid in S^2.*

Proof. It follows by Proposition 2.58 and Lemma 2.59. □

We give a combinatorial explanation for the reducibility of a parity state in S^2. We label each edge of a given state of which we illustrate a small portion in Figure 2.44. The nodes that share exactly two edges (labeled as b and e in the figure) form a reducible bigon if and only if the edges appear in the order $e\ b\ f\ c$ during a full tour in the counterclockwise direction around one of the nodes and in the order

$b\ e\ a\ d$ around the other node. More precisely, the shared edges b and e appear in cyclic order around the nodes. Note that the detour moves do not change the labels. Then up to detour moves, a parity state of a virtual knotoid diagram will have a removable bigon between the nodes.

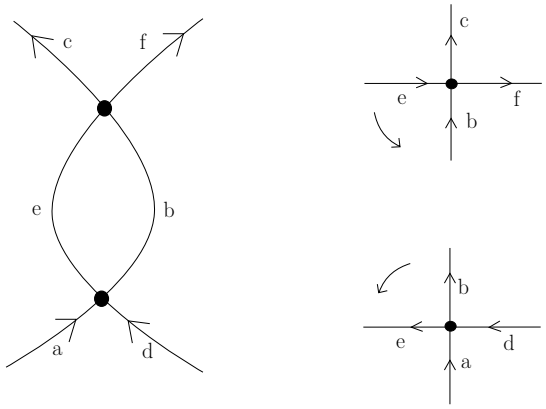

Figure 2.44: Labels at the nodes of a reducible bigon

Example 6. Both of the classical crossings of the virtual knotoid diagram given in Figure 2.19 are odd crossings. There is only one parity state of this diagram that is a graphical state, obtained by replacing these crossings by nodes. As seen in Figure 2.45, the two nodes have orders: $a\ c\ b\ d$ and $e\ b\ d\ c$, respectively. Since the shared edges b and d do not appear in the required order, the state is not reducible. We conclude that the parity bracket polynomial consists of one summand that is a graphical coefficient. Thus, the non-triviality of this virtual knotoid whose virtual closure is trivial, is verified by the parity bracket polynomial. Moreover, by Proposition 2.58, this virtual knotoid diagram is not virtually equivalent to a classical knotoid diagram, and in fact, it represents a genus one virtual knotoid.

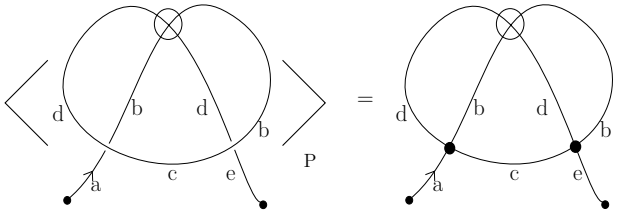

Figure 2.45: 1st node: *acbd* 2nd node: *ebdc*

The condition given above that is necessary for the elimination of the nodes of a graphical state component applies in the same way to the flat case. The parity bracket polynomial of the underlying flat diagram of the knotoid diagram given in

Figure 2.19 is the same as the polynomial of the overlying virtual knotoid, consisting of one graphical coefficient. Therefore, the parity bracket polynomial of this flat virtual knotoid diagram is not trivial. This completes the argument in Section 2.2.1 that flat virtual knotoids are not necessarily trivial.

Nothe that considering planar knotoid diagrams and parity states up to the isotopy of $\mathbb{R}^2$, the above condition does not apply anymore and we may observe irreducible parity states even though the condition holds. See Figure 2.46 for the parity state of the knotoid given. The crossings of K are both odd and the parity bracket polynomial of K is equal to the graphical state with two nodes.

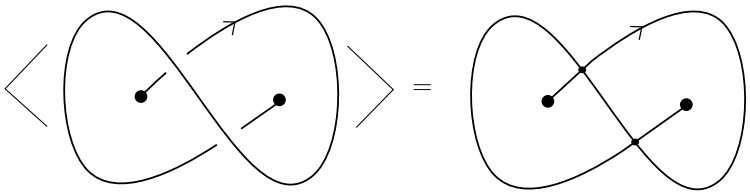

Figure 2.46: A planar knotoid with an irreducible parity state

Note 10. The normalized parity bracket polynomial extends to an invariant for virtual multi-knotoids. Even crossings of a multi-knotoid diagram are smoothed in the usual way. Together with odd crossings, also link crossings (crossings between distinct components) of a multi-knotoid diagram are replaced by graphical nodes. We extend the procedure for calculation of the parity bracket polynomial to include the link crossings as follows. The graphical state components containing the nodes corresponding to link crossings are eliminated by the same reduction rule. Irreducible graphical state components contribute to the polynomial as graphical coefficients. The parity bracket polynomial of a virtual multi-knotoid is defined in the same way by expanding the state summation, and the normalization of the polynomial with writhe is a virtual multi-knotoid invariant.

We have showed that the graphical components of a classical knotoid diagram are all reduced by the reduction rule, in other words, they are free of nodes. The parity states of a classical multi-knotoid diagram may contain irreducible graphical states. Figure 2.47 depicts a multi-knotoid diagram with two components and one link crossing. It is clear that the diagram has a nontrivial parity bracket polynomial that is equal to one graphical coefficient. Thus, the multi-knotoid represented by this diagram is a nontrivial multi-knotoid.

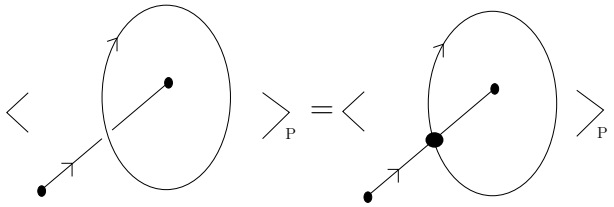

Figure 2.47: A multi-knotoid with nontrivial parity bracket

Chapter 3

On Braidoids

3.0 Introduction

Braidoids are geometric objects extending the notion of a classical braid with 'free strands' and analogously to the relation of classical braids with classical knots, forming a counterpart 'braided' theory to the theory of knotoids. In this chapter we first introduce the notions of a braidoid diagram and discuss on the isotopy moves of braidoid diagrams. We then give two algorithms turning any given (multi-)knotoid into a braidoid diagram and define a closure operation on braidoid diagrams back to (multi)-knotoids which is consistent with the braidoiding algorithms, so we obtain an analog of the classical Alexander theorem for knotoids. We adapt the classical L-moves that, together with braidoid isotopy, generate an equivalence relation on braidoid diagrams and provide our closure map to be a bijection, in other words, we obtain a geometrical analogue of the Markov theorem for knotoids. We provide a list of generating blocks or braidoiding diagrams and we give a set of relations on these blocks, reflecting the braidoid isotopy. Lastly, we make a short introduction to the theory of tangloids.
The results of this chapter are mainly based on the techniques in [21, 82–84], while they appear in [18, 19].

3.1 Basics on braidoids

3.1.1 The definition of a braidoid diagram

Definition 3.1. [18,19] Let I denote the unit interval $[0, 1] \subset \mathbb{R}$. A *braidoid diagram* B is a system of a finite number of arcs embedded in $I \times I \subset \mathbb{R}^2$ that are called the *strands* of B. There are only finitely many intersection points among the strands,

which are transversal double points endowed with over/under data, and are called *crossings*. We identify $\mathbb{R}^2$ with the xt-plane with the t-axis directed downward. Following the orientation of I, each strand is naturally oriented downward, with no local maxima or minima, so that it intersects a horizontal line at most once. A braidoid diagram has two types of strands, the classical strands and the free strands. A *classical strand* is as a braid strand connecting two points, the top one that lies in $I \times \{0\}$ and the bottom one that lies in $I \times \{1\}$. A *free strand* is a strand that either connects a point in $I \times \{0\}$ or in $I \times \{1\}$ to a point located anywhere in $I \times I$, called an *endpoint* of B, or it connects two endpoints that are not necessarily lying in $I \times \{0\}$ or $I \times \{1\}$. Thus a braidoid diagram has either one free strand (see for example Figure 3.1(a)) or two free strands (see for example Figure 3.1 (b), (c), (d), (e)) and exactly two endpoints, which are called the *leg* and the *head*, denoted by l and h respectively, in analogy with the endpoints of a knotoid diagram. The head is the endpoint that is terminal for a free strand with respect to the orientation, while the leg is the starting endpoint for a free strand with respect to the orientation.
The ends of the strands of B that are not the two endpoints of B are named *braidoid ends*.

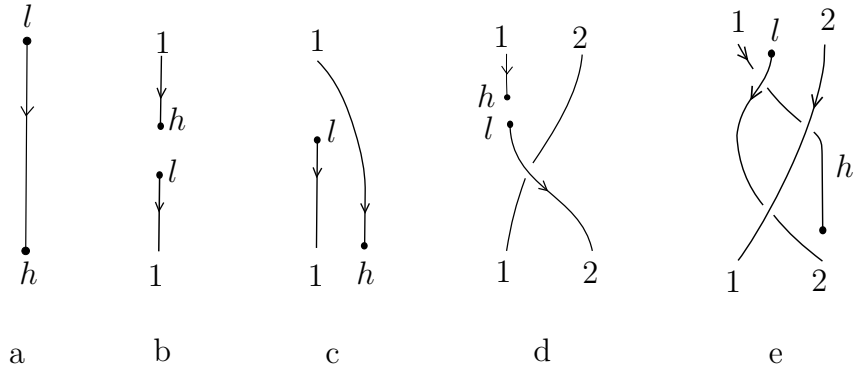

Figure 3.1: Some examples of braidoid diagrams

We assume that the braidoid ends lie equidistantly on the lines $\{t = 0\}$ and $\{t = 1\}$. It is clear that the number of braidoid ends that lie at the top line is equal to the number of braidoid ends that lie at the bottom line of the diagram and the number of braidoid ends on top/bottom line is $n - 1$ for a braidoid diagram with n strands. The braidoid ends are arranged in pairs that are vertically aligned, called *corresponding ends*, and they are numerated with integers according to their order on the lines from left to right, as seen in the examples illustrated in Figure 3.1.

The endpoints of B differ conceptually from its braidoid ends. As we shall see, the endpoints are subject to special isotopy moves unlike the braidoid ends which are assumed to be fixed at the top and the bottom line of the diagram and they

do not participate in the closure. To distinguish the endpoints from the braidoid ends, we denote them by graphical nodes. See Figure 3.1 for some basic examples of braidoids.

Definition 3.2. A braidoid diagram is a *piecewise-linear* braidoid diagram if all of its strands are formed by consecutive linear segments.

As any braid diagram can be approximated by a piecewise-linear braid diagram [92], any braidoid diagram can be approximated by a piecewise-linear braidoid diagram. We shall be considering piecewise-linear braidoid diagrams in the rest of the discussion although we give some figures in smooth category for easiness and aesthetics.

3.1.2 Braidoid isotopy

Moves on segments of strands

As for classical braids, the following moves are allowed on segments of braidoid strands.

Definition 3.3. A Δ-*move* is defined on braidoid diagrams similarly for knotoid diagrams as follows. A Δ-*move* on a braidoid diagram is defined on a local region that does not contain any of the endpoints and it replaces a segment of a strand with two segments passing only over or only under the arcs intersecting the triangular region of the move while the downward orientation of the strands is preserved (recall Figure 3.2). The oriented Reidemeister moves, Ω_2 and Ω_3, which keep the arcs in the move patterns directed downward, are defined on braidoid diagrams as special cases of Δ-moves.

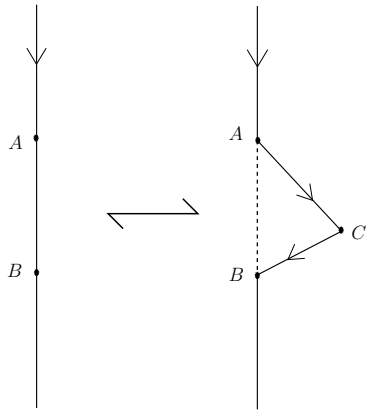

Figure 3.2: A planar Δ-move on a braidoid diagram

Moves of endpoints

As for knotoid diagrams, we forbid the pulling of the leg and the head over or under a strand, as shown in Figure 3.3. These are the *forbidden moves* of braidoid diagrams and they are denoted Φ_+ and Φ_-, respectively. It is clear that allowing both forbidden moves can cancel any braiding of the free strands.

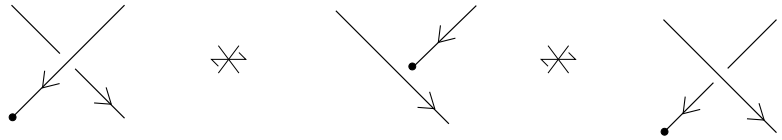

Figure 3.3: Forbidden braidoid moves

The following moves are allowed on segments of braidoid strands containing endpoints.

1. *Vertical Moves:* As shown in Figure 3.4, the endpoints of a braidoid diagram can be pulled up or down in the vertical direction as long as they do not violate any of the forbidden moves (that is crossing through or intersecting any strand of the diagram). Such moves are called *vertical move*.

2. *Swing Moves:* An endpoint may also swing to the right or the left like a pendulum as long as;
   i. the downward orientation on the arc moving, is preserved,
   ii. the endpoint does not cross through or intersect any strand of the diagram,
   iii. the endpoint cannot cross to right and left across the vertical line determined by a pair of corresponding braidoid ends. See Figure 3.5.

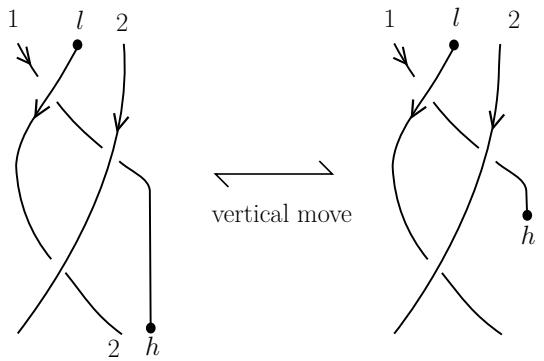

Figure 3.4: A vertical move on h

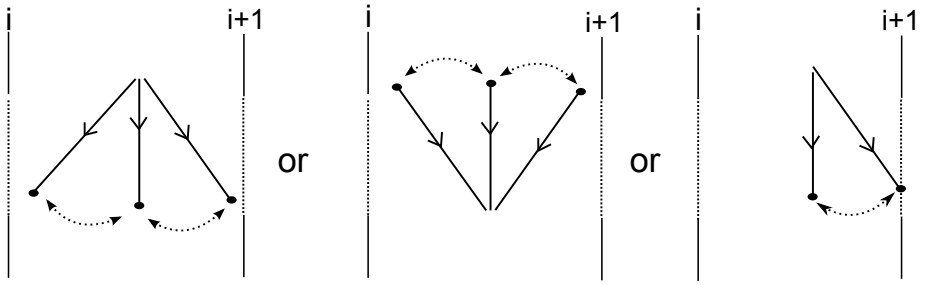

Figure 3.5: Swing moves

Definition 3.4 (braidoid isotopy)**.** It is clear that assuming braidoid ends fixed at the top and bottom lines ($t = 0$ and $t = 1$, respectively), the Ω- moves together with the swing and vertical moves for the endpoints generate an equivalence relation on braidoid diagrams in $\mathbb{R}^2$. Two braidoid diagrams are said to be *isotopic* if one can be obtained from the other by a finite sequence of Ω-moves, vertical and swing moves. An equivalence (or isotopy) class of isotopic braidoid diagrams is called a *braidoid*. Note that isotopy moves of braidoid diagrams do not change the number of strands. Thus isotopic braidoid diagrams have the same number of strands.

3.2 From braidoids to knotoids - the closure operation

In this section we define a closure operation on braidoid diagrams in analogy with the closure of braids in handlebodies [21], in order to obtain planar knotoid or multi-knotoid diagrams [18, 19]. In order to do this we further require to introduce a labeling on braidoid diagrams. Also, we assume that the endpoints of a braidoid diagram are not aligned vertically with any braidoid ends. Indeed, this can be achieved by a swing move moving the endpoint to the left hand side of the vertical line of the related corresponding ends (recall Figure 3.5).

Definition 3.5. A *labeled braidoid diagram* is a braidoid diagram such that every pair of its corresponding ends is labeled either by o or u, standing for 'over' or 'under', respectively. A label indicates an *overpassing* or an *underpassing* arc, accordingly, which will take place in the closure (see Definition 3.6). We attach the labels next to the braidoid ends lying at the top line.

Clearly, braidoid isotopy moves, described in Definition 3.4 do not change the labeling. Two labeled braidoid diagrams are called *isotopic* if they are isotopic as unlabeled braidoid diagrams and their braidoid ends admit the same labeling. The corresponding isotopy classes are called *labeled braidoids*.

Definition 3.6. Let B be a labeled braidoid diagram with $n > 1$ strands. The *closure* of B, denoted $\widehat{B}$, is a planar (multi-)knotoid diagram obtained by the following topological operation. Every pair of corresponding braidoid ends of B is connected by an embedded arc (with slightly tilted extremes) that lies on the right-hand side of the vertical line of the corresponding braidoid ends (the vertical line passing through the pair of corresponding ends) and within a distance d_j, $d_j < min\{\rho(leg, l_j), \rho(head, l_j)\}$ for each $1 \leq j \leq n-1$, where l_j denotes the vertical line passing through the pair of the j^{th} braidoid ends and ρ is the usual metric of $\mathbb{R}^2$. Such a connection arc goes entirely over or under the rest of the diagram accordingly to the label of the ends and is oriented upward following the orientation of the connected strands. Finally, the labels are forgotten in the resulting diagram that is a knotoid or a multi-knotoid diagram. See Figure 3.6 for an abstract illustration of the closure of a labeled braidoid diagram and Figures 3.7 and 3.8 for concrete examples.

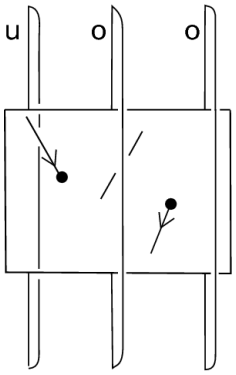

Figure 3.6: The closure of an abstract labeled braidoid diagram

Notes on the closure

1. The endpoints of B do not participate in the closure and they become the endpoints of the resulting (multi-) knotoid diagram $\widehat{B}$.

2. One reason that a joining arc is required to lie in a distance less than the distances of the endpoints to the line of the related corresponding ends is that, otherwise, forbidden moves may obstacle an isotopy of $\widehat{B}$ between any two joining arcs.
   The other reason for choosing the connection arc in relation with the distances of the endpoints to the braidoid ends and the vertical lines passing through them will get clear after introducing our braidoiding algorithm.

3. A connection arc can lie on the right or on the left of the line of the corresponding ends. It is a matter of preference that in this setting it is assumed to lie on the right. Clearly both choices result in isotopic knotoids since, by definition, the closure takes place sufficiently away from the endpoints avoiding the forbidden moves and we assume the endpoints are not aligned with any of the braidoid ends.

4. The resulting multi-knotoid depends on the labeling of the braidoid ends. See Figure 3.8 for an example of two non-isotopic labeled braidoid diagrams with the same underlying braidoid diagram, which give rise to non-equivalent knotoids. This is again due to the presence of the endpoints and forbidden moves of them. In fact we cannot simply carry connection arcs out of the strip containing the multi-knotoid diagram so that the closure is free of labeling. To obtain a well-defined map, we define the closure on the set of labeled braidoid diagrams.

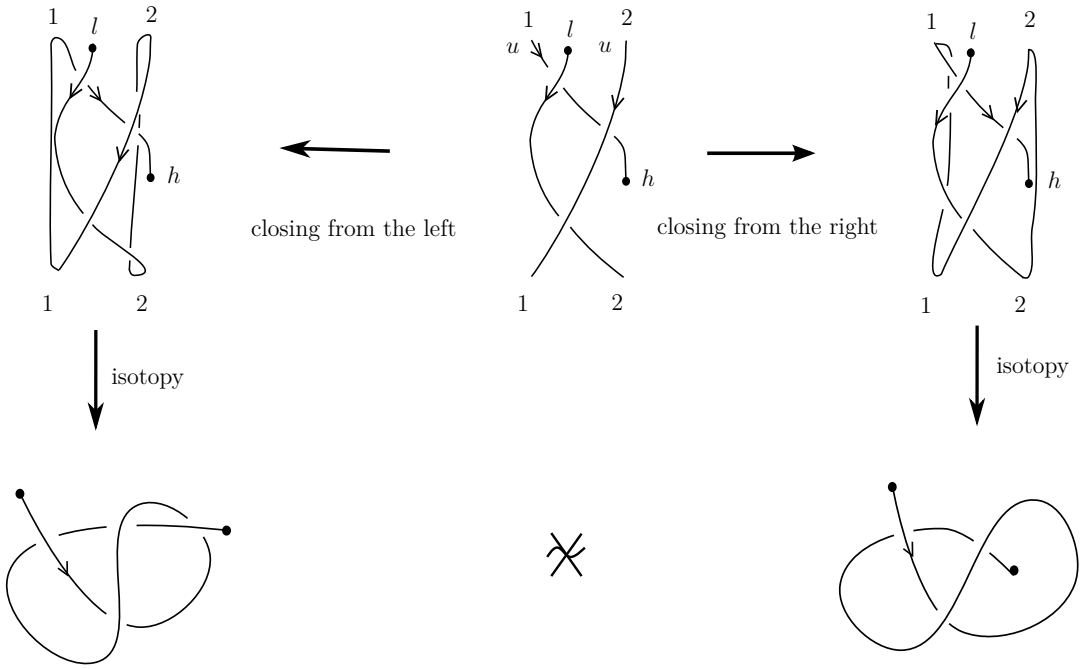

Figure 3.7: Non-isotopic closures in the presence of endpoint alignment

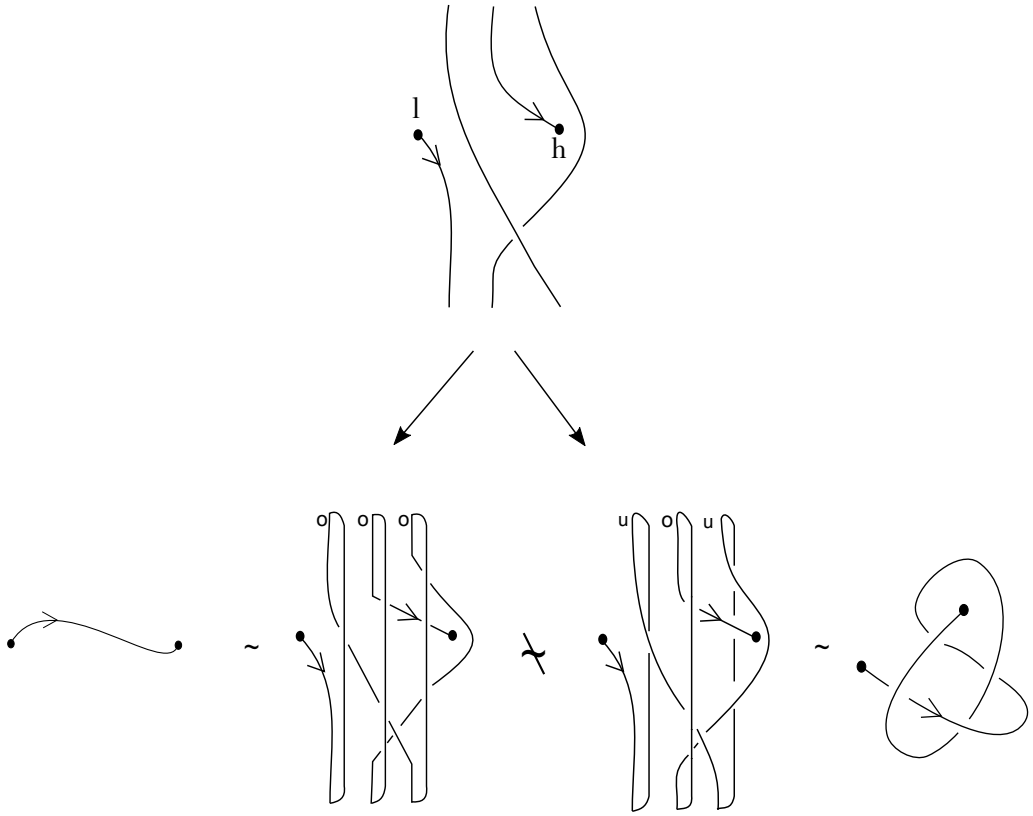

Figure 3.8: An example of non-equivalent closures resulting from different labelings

Proposition 3.7. *The closure operation induces a well-defined map from the set of labeled braidoids to the set of planar multi-knotoids.*

Proof. It is clear that labeled braidoid isotopy moves transform into isotopy moves on the resulting multi-knotoid diagrams. □

3.3 From knotoids to braidoids - two braidoiding algorithms

In analogy with the braiding moves [83–85], in this section we define the braidoiding moves and provide two algorithms that turn a planar (multi-) knotoid diagram into a braidoid diagram. More precisely we obtain the following theorem.

Theorem 3.8. *(An analogue of the Alexander theorem for knotoids) Any (multi-)knotoid diagram in* $\mathbb{R}^2$ *is isotopic to the closure of a labeled braidoid diagram.*

Let K be a (multi-)knotoid diagram. We shall describe below how to manipulate K in order to obtain a labeled braidoid diagram, after equipping the plane on which K lies with the top-to-bottom direction.

3.3.1 Preparatory concepts for braidoiding algorithms

The basic idea of braidoiding

The basic idea in order to turn K into a braidoid diagram is to keep the arcs that are oriented downward, with respect to the top-to-bottom direction, and to eliminate the ones that are oriented upward (up-arcs), producing at the same time pairs of corresponding braidoid strands, so that the resulting diagram is a (labeled) braidoid diagram whose closure is a knotoid isotopic to K. The elimination of the up-arcs is done by utilizing the braidoiding moves illustrated abstractly in Figure 3.9. A *braidoiding move* consists of cutting an up-arc at a point and pulling the resulting ends to top and bottom lines preserving the alignment with the cut-point. As can be seen in Figure 3.9, closing the pair of corresponding ends obtained, according the label of QP, results in a closed strand that is isotopic to the initial up-arc QP. Precisely, the closed strand can be contracted back to QP by utilizing Ω- moves.

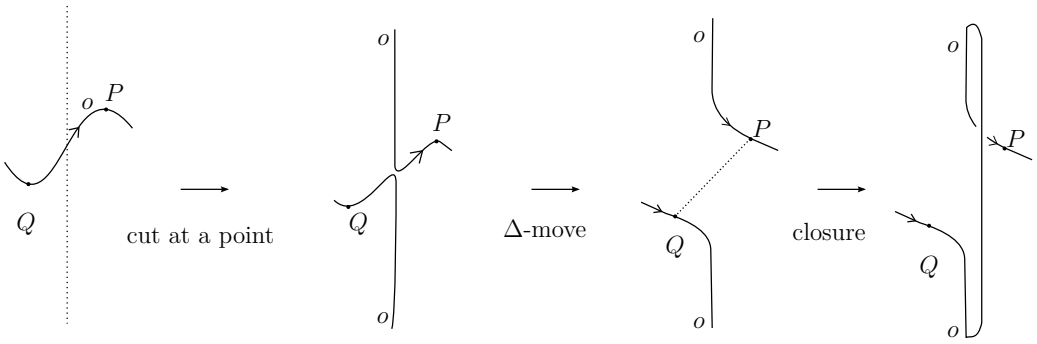

Figure 3.9: The germ of the braidoiding move and its closure

In order to implement this idea into a rigorous algorithm we need first to take care of a few technical points.

Up-arcs and free up-arcs

It is clear that by small Δ-moves K can be assumed to be a diagram without any horizontal arcs. Thus K consists of a finite number of arcs oriented either upward or downward, and these arcs are separated by finitely many local maxima or minima. The arcs of K that are oriented upward are called *up-arcs* and the ones oriented downward are called *down-arcs* of K. An up-arc may contain crossings of different types (over/under-crossings) or no crossing at all. See Figure 3.10. An up-arc that contains no crossing is called a *free up-arc*.

Figure 3.10: Two up-arcs containing crossings and a free up-arc

Subdivision

Subdivision is the addition or deletion of a subdividing point (recall Section 2.1.3). Subdivision can be considered as a special Δ-move, as shown in Figure 2.6. We start by marking the local maxima and minima of K with points, which we name *subdividing points*. In the process we may need to subdivide further some up-arcs of K.

Sliding triangles and cut-points

Let QP be an up-arc of K, with respect to a given subdivision of K where Q denotes the initial and P denotes the top-most subdivision point. A *cut-point* of an up-arc is defined to be the point where the up-arc is cut to initiate a braidoiding move. We choose the point $P \in QP$ as the cut-point of QP.

Definition 3.9. There is a unique right angled triangle associated to QP with vertices Q, P and R, where R is the point in the plane having the same x-coordinate with P and t- coordinate with Q, respectively. This triangle is called the *sliding triangle* of the up-arc QP. We denote the sliding triangle by $T(P)$. For an illustration of $T(P)$ see Figure 3.11.

The triangular region bounded by the sliding triangle $T(P)$ is utilized after cutting QP, for sliding the resulting lower sub-arc across the region to complete the braidoiding move. See Figure 3.11.

Note that, if QP is itself vertical, then the sliding triangle degenerates into QP for both cases.

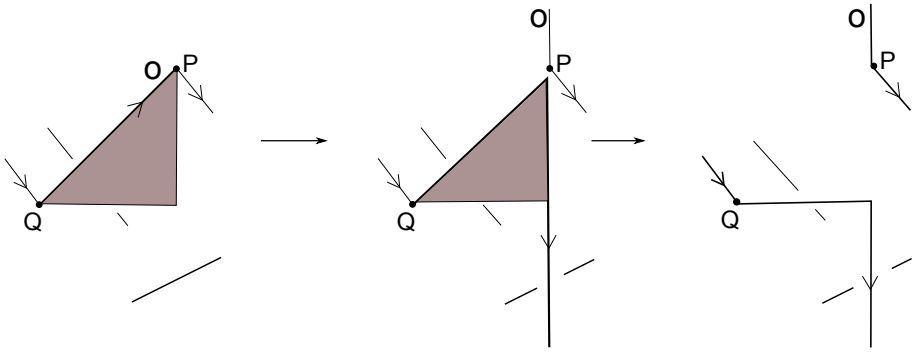

Figure 3.11: The sliding triangle of the up-arc QP

The endpoints triangle condition

In the process of the preparation of a knotoid diagram for braidoiding one may come across the situation where one (or two) of the endpoints lies in the region of some sliding triangle as in Figure 3.12. This is an unwanted situation since sliding a resulting arc across such a triangle will cause a forbidden move. We impose the following condition on a knotoid diagram.

The endpoints triangle condition: A sliding triangle of a knotoid diagram is not allowed to contain an endpoint.

To satisfy this condition we introduce a subdivision of up-arcs into smaller up-arcs by adding extra subdividing points. See Figure 3.12. More precisely, we have the following proposition.

Proposition 3.10. *Let K be a knotoid diagram and $T(P)$ be the sliding triangle corresponding to an up-arc QP . If $T(P)$ contains the leg or the head of K in its interior or boundary edges then there is a further subdivision of QP with new sliding triangles that are disjoint from the endpoint.*

Proof. We can assume that QP has a positive slope since the other case follows by symmetry. There is unique horizontal and vertical line passing through the endpoint in question and each intersecting QP exactly at one point, since $x_Q \leq x_{(endpoint)} \leq x_P$ and $t_P \leq t_{endpoint} \leq t_Q$. One can choose any point in the line segment whose boundary is the union of the two intersection points as the new subdividing point on QP. Let P^* denote the chosen point. The corresponding sliding triangles to this new subdivision produces smaller sliding triangles that do not contain the endpoint. In the case that $T(P)$ contains two of the endpoints, we introduce two new subdividing points on QP accordingly to the choice above. □

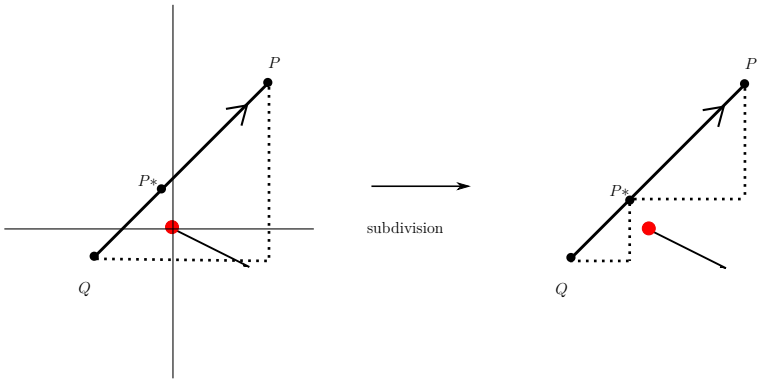

Figure 3.12: Further subdivision of QP to satisfy the endpoints triangle condition

3.3.2 Braidoiding algorithm I

Let K be a (multi-)knotoid diagram lying in the xt-plane. Since K is compact we can assume that it lies in the region $[0,1] \times [0,1]$. For turning K into a labeled braidoid diagram with isotopic closure we follow the steps below. These steps set the braidoiding algorithm I.

Step 1: Arranging the crossings

Rotate all crossings that are contained in at least one up-arc to turn the neighboring up-arcs into down-arcs. More precisely, if a crossing is contained in two up-arcs then rotate it by 180 degrees inside a small disk neighbourhood of the crossing intersecting K at four local strands around the crossing. See Figure 3.13. If a crossing is contained in only one up-arc then rotate it by 90 degrees in such a small disk. See Figure 3.14. The (multi-) knotoid diagram K' resulting from rotating each such crossing in this way is isotopic to K since rotations in the plane can be expressed as combinations of Δ-moves. Clearly, K' contains only free up-arcs.

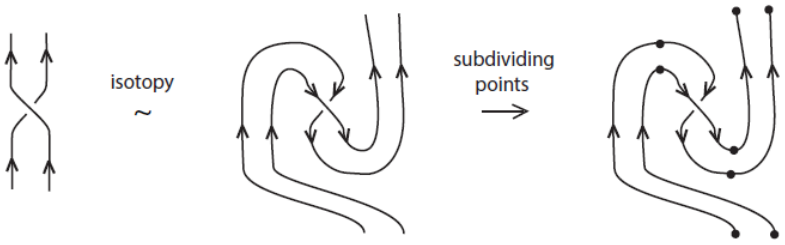

Figure 3.13: Eliminating up-arcs with a full twist

Figure 3.14: Eliminating an up-arc with a half twist

Step 2: Arranging the endpoints

For any knotoid diagram, by small perturbations, it can be assumed that the emanating arcs from the leg and the head are straight vertical arcs pointing downward with respect to a chosen top-to-bottom direction of the plane of the knotoid. We assume the endpoints of K lie on vertical and downward directed arcs. See Figure 3.15.

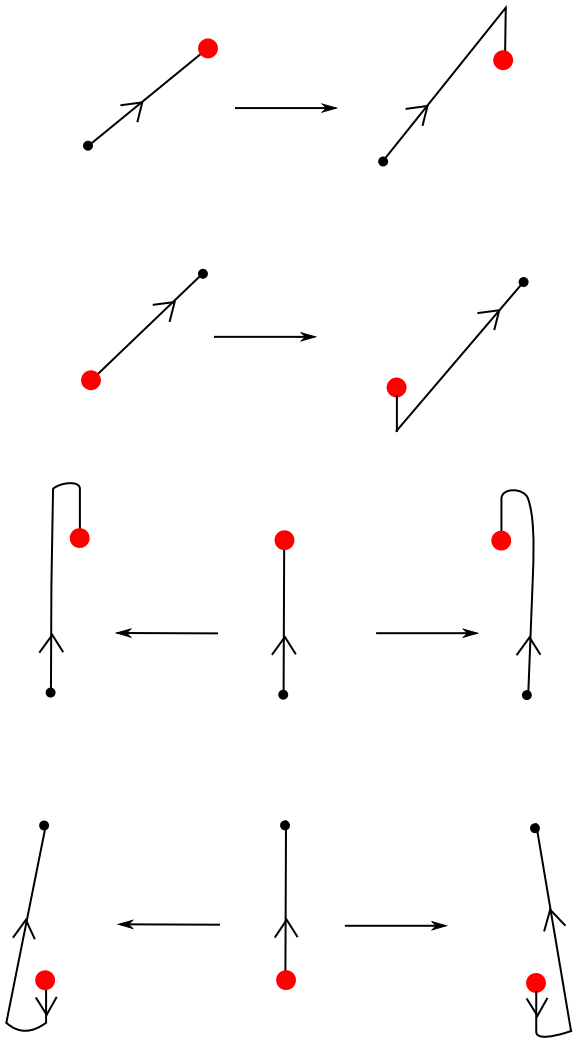

Figure 3.15: Arranging the endpoints

Step 3: Preparation for eliminating the free up-arcs

We first mark the up-arcs of K' with subdividing points, starting from the local minima and maxima. Then we shall continue with eliminating the free up-arcs of K'. For doing this, we first make some general positioning requirements on K'. Namely, we require K' to have no horizontal arcs, none of subdividing points are vertically aligned with each other unless they share a common edge, or with the endpoints or with any of the crossings, also none of the endpoints intersects with a sliding triangle. Clearly, any (multi-)knotoid diagram can be isotoped to such a diagram by Ω-moves including subdivision. Finally, we attach to each free up-arc either of the labels; o or u , and we give them an order for elimination.

Step 4: Applying the braidoiding moves

We start applying the braidoiding moves with respect to an order given to free up-arcs. Without loss of generality, let QP be a free up-arc of K' that is chosen as the first to be eliminated. We cut QP at its cut-point, namely at the point P.

If QP is labeled with o we pull the resulting two pieces, the upper upward to the line $t = 1$ and the lower downward to the line $t = 0$, both entirely *over* the rest of the diagram, by sliding them across the sliding triangles. The resulting pieces are pulled so that their ends are kept aligned vertically with the cut-point and by applying small planar isotopies we turn the lower and upper pieces into down-arcs. See Figure 3.9. This operation eliminates the up-arc QP and results in a pair of corresponding braidoid strands vertically aligned with the cut-point. For the purpose of closure, this pair of strands is labeled o. If QP is labeled with u, the resulting ends are pulled passing *under* the rest of the diagram and the new pair of strands is labeled by u for the purpose of closure. The algorithm continues with the elimination of remaining free up-arc as explained above. Since there is a finite number of free up-arcs the algorithm terminates in finite step. See Figure 3.16 for an illustration of the process of the algorithm.

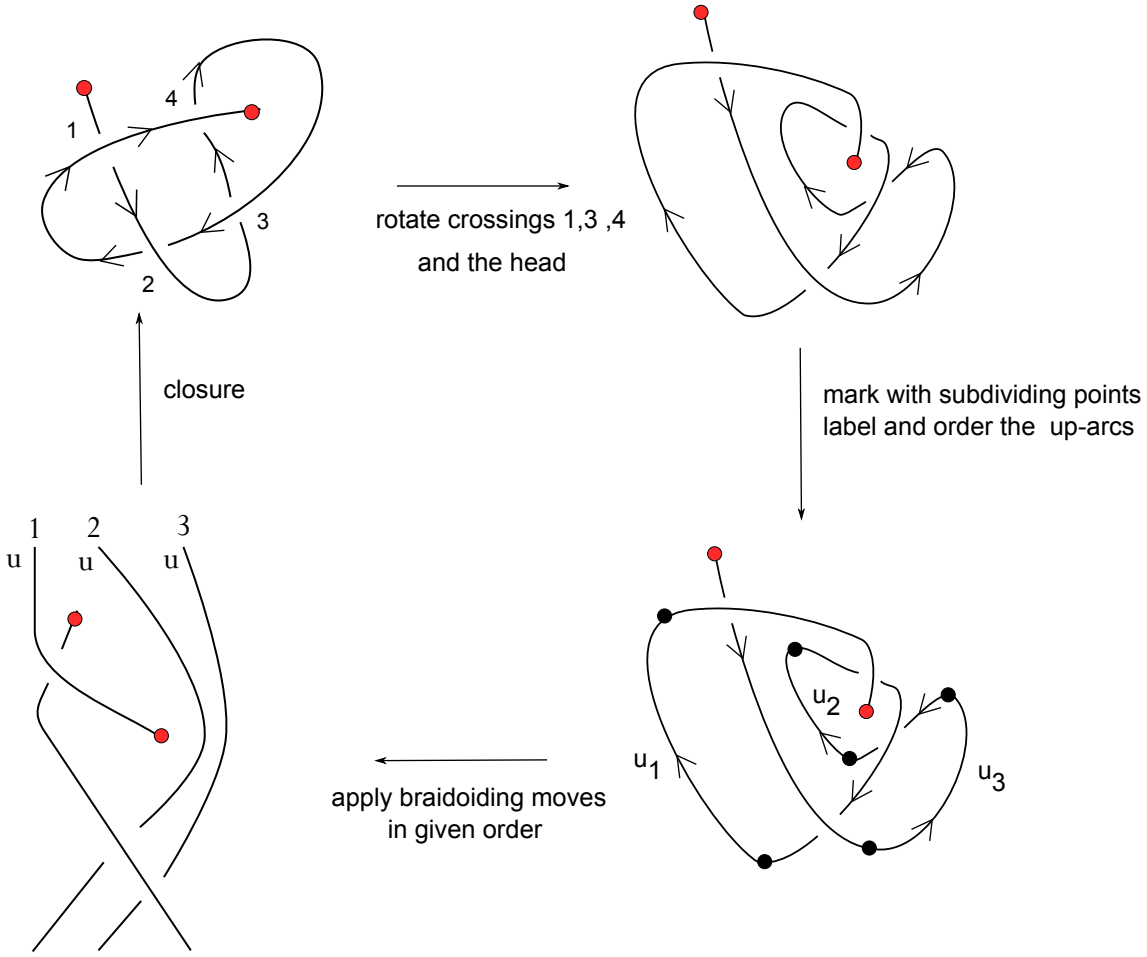

Figure 3.16: An illustration for the braidoiding algorithm I

The first proof of Theorem 3.8

Proof. It can be verified similarly as in [84, 85] that none of the orderings or the labeling of free up-arcs can cause an obstruction for elimination. Then the algorithm terminates at finite steps and results in a labeled braidoid diagram for any ordering and labeling. By the discussion regarding Figure 3.9, if we close all resulting strands accordingly to the labels assigned to them, we obtain a multi-knotoid diagram that is isotopic to K. This comprises a proof of Theorem 3.8. □

A corollary of the braidoiding algorithm I

The braidoiding algorithm I starts with rotating the crossings of a knotoid diagram that appear on up-arcs. The up-arcs resulting by rotation of each crossing are only free up-arcs that can be labeled either with o or u freely. Assuming that all free up-arcs are labeled the same, it is clear that the labeled braidoid diagram obtained by the braidoiding algorithm I contains only one type of label on its strands, say u.

Let us call a labeled braidoid diagram whose strands are labeled only with u (or o) a *u-labeled braidoid diagram* (o-labeled braidoid diagram, respectively). Then clearly we have a bijection,

$$Label_u : \{\text{Braidoids}\} \to \{\text{u-labeled braidoids}\},$$

induced by assigning to a braidoid diagram B the u-labeled braidoid diagram B_u obtained by attaching u labels to each braidoid end of B. Since the map $Label_u$ is a bijection, we can define a closure operation for braidoid diagrams without labels as follows. Connect each pair of corresponding braidoid ends with an underpassing arc in a distance arbitrarily close to the vertical lines of the corresponding ends. We call this closure *uniform closure* of a braidoid diagram. Then Theorem 3.8 is sharpened as follows.

Theorem 3.11. *Any multi-knotoid diagram is isotopic to the uniform closure of a braidoid diagram.*

3.3.3 Braidoiding algorithm II

We shall now give another algorithm for obtaining a labeled braidoid diagram from a (multi-)knotoid diagram K that once more utilizes the braidoiding moves. This algorithm is more 'rigid'than the previous one which makes it more appropriate for proving a braidoid equivalence result analogous to the classical Markov theorem. The algorithm runs as follows.

Step 1: Arranging the endpoints

As in Step 1 of the first braidoiding algoritm, the endpoints of K are assumed to lie on vertical arcs that are directed downwards. This can be ensured by Ω-moves.

Step 2: Arranging the up-arcs

Subdivide the resulting up-arcs starting from local maxima and minima. If an up-arc contains two types of crossings; both over- and under-crossings, then we subdivide the up-arc into smaller up-arcs each containing only one type of crossings (see Figure 3.17.

Figure 3.17: Subdividing an up-arc to contain one type of crossings

Step 3: Preparation for eliminating the up-arcs

The diagram is isotoped to satisfy the general positioning requirements given for braidoiding algorithm I including the endpoints triangle condition. We attach a label to each up-arc accordingly to the crossing type it contains: we attach o if the up-arc contains over-crossing(s), u if the up-arc contains under-crossing(s). Free up-arcs are labeled with o or u.

Step 4: Applying the braidoiding moves

We finally apply the braidoiding moves to each up-arc of K in a given order. The resulting braidoid strands are labeled with o or u accordingly to the label of the initial knotoid up-arcs, and give an order to them for elimination.

Obstructions for the braidoiding algorithm II and Resolutions

Now, we discuss on some bugs of the braidoiding algorithm II, as also discussed in [84, 85]. In some cases, as exemplified in Figure 3.18, the algorithm is obstructed by a clasp occuring in the sliding triangle of an up-arc. More precisely, we see in the figure that the braidoding move applied on the second-ordered up-arcs labeled with o and u respectively, cannot be completed, due to the clasps in their sliding triangles. It can be verified by checking all possible positioning and labeling/ordering of any two up-arcs that this type of obstruction may occur only if:

i. the top-most point of the first ordered up-arc intersects the sliding triangle of the second-ordered up-arc and,
ii. two up-arcs with intersecting sliding triangles, are labeled the same.

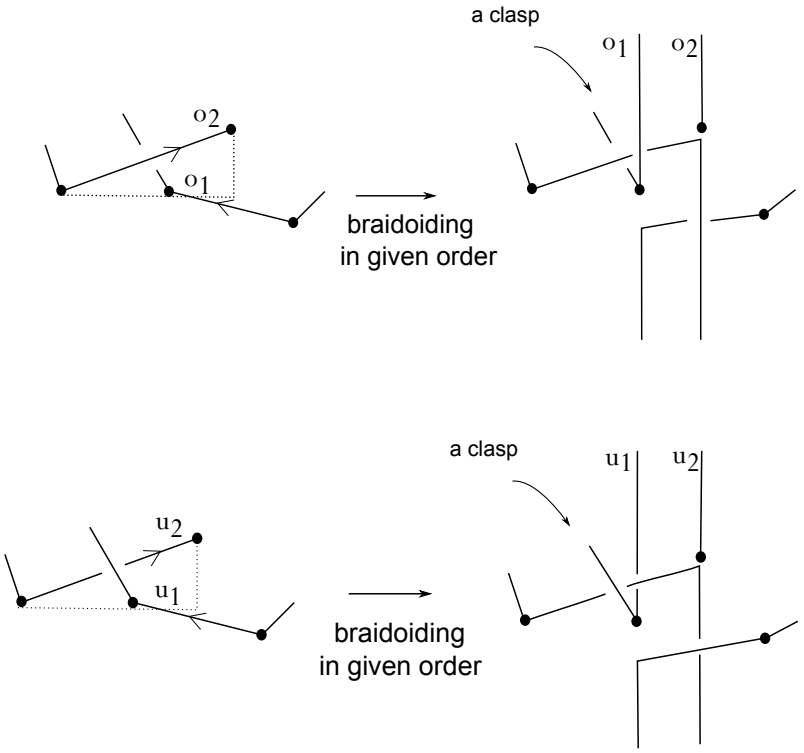

Figure 3.18: Obstructions for applying braidoiding moves

Due to the conditions creating obstructions, the resolutions for them may be:

i. swapping the ordering of the up-arcs; see Figure 3.19,

ii. changing the label of the free up-arc if there is a free up-arc involved in an obstruction; see Figure 3.20, **iii.** subdividing the up-arcs further to have disjoint sliding triangles; see Figure 3.21.

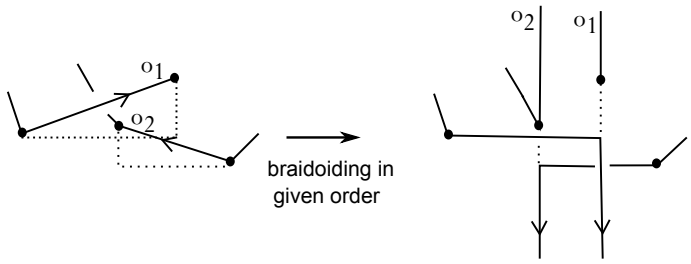

Figure 3.19: Swapping the order of up-arcs repairs the obstruction

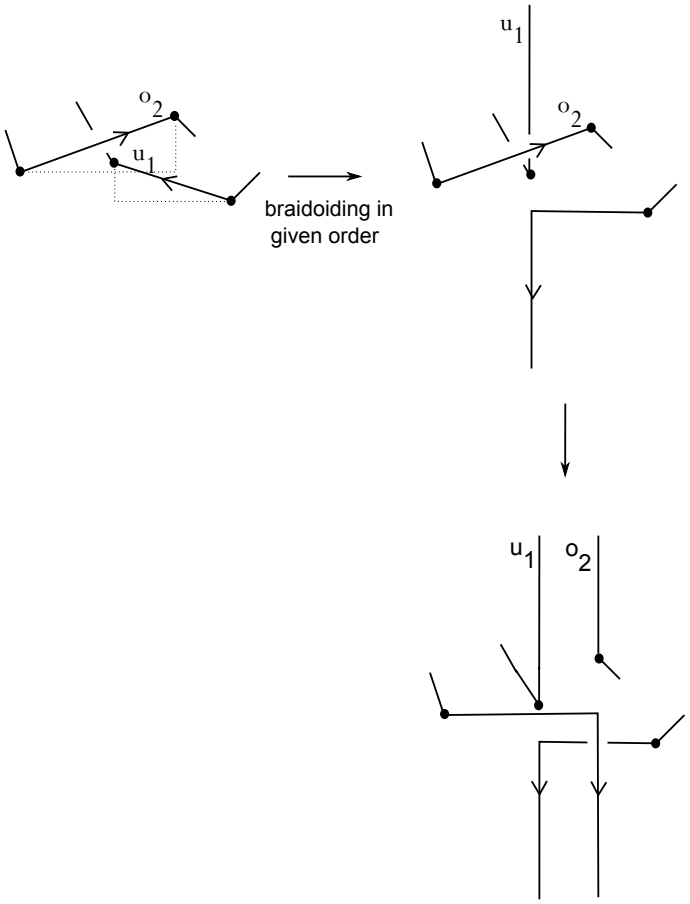

Figure 3.20: Changing the label of the free up-arc repairs the obstruction

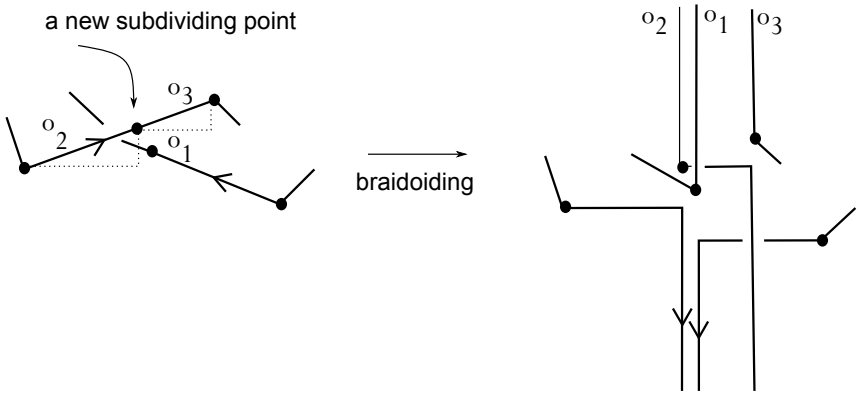

Figure 3.21: Adding a subdividing point the the upper up-arc repairs the obstruction

Moreover, the addition of subdividing points can result also that the elimination of up-arcs takes place independently of ordering, so even simultaneously. More precisely we can impose the following condition on knotoid diagrams which provides a simultaneous braidoiding algorithm.

The classical triangle condition

Two sliding triangles are said to be *adjacent* if the corresponding up-arcs have a common subdidiving point, and *non-adjacent* otherwise.

The classical triangle condition says that non-adjacent sliding triangles are allowed to intersect only if the up-arcs of the triangles have different labels. This condition can always be satisfied by the following lemma.

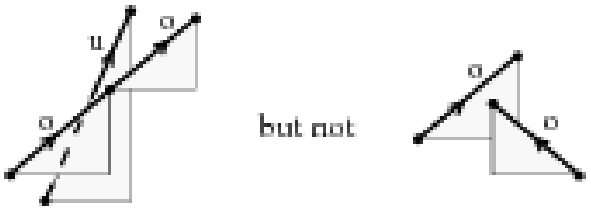

Figure 3.22: The classical triangle condition

Lemma 3.12. *Let K be a knotoid diagram. There exists a subdivision of K, for appropriate choices of labels for the free up-arcs, satisfying both classical triangle condition and the endpoints triangle condition.*

Proof. This lemma is proved similarly with Lemma 1 in [84]. We adapt the proof here, for completeness. We want to subdivide all up-arcs of K in a way that none of two having the same labels, have intersecting sliding triangles. Let d_1 be the minimum distance between any two crossings appearing on the up-arcs of K. Choose some r, $0 < r < d_1$ so that the disk of radius r centered at a crossing contained in an up-arc, intersects the up-arc at only four local strands around the crossing. Let d_2 be the minimum distance between any two disjoint points that are located outside the disks of radius r around the crossings and on different segments. Letting $\epsilon < 1/2 min\{d_1, d_2\}$ be the distance between any two subdivision points on K provides a subdivision of K satisfying the classical triangle condition and the endpoints triangle condition. Each sub-arc of length ϵ is also labeled according to the crossing type it contains, or if some become free, they are labeled freely. □

Second proof of Theorem 3.8

Proof. The proof follows similarly with the first proof. With the discussion above we know that there is always a choice for ordering and labeling up-arcs of a (multi)-knotoid diagram and, moreover, we can impose the classical triangle condition to make the algorithm free of ordering. This is sufficient for ensuring that the algorithm II terminates at a finite step and always results in a labeled braidoid diagram. See

Figure 3.23 for an illustration of the algorithm II. It is clear from Figure 3.9 that if the strands obtained when the algorithm terminates are closed accordingly to their label, then they can be contracted back to initial up-arcs all over or under the rest of the diagram, depending on the label of the strand. Such contraction utilizes the Ω-moves of knotoids, thus the closure of the resulting braidoid diagram is isotopic to K. $\square$

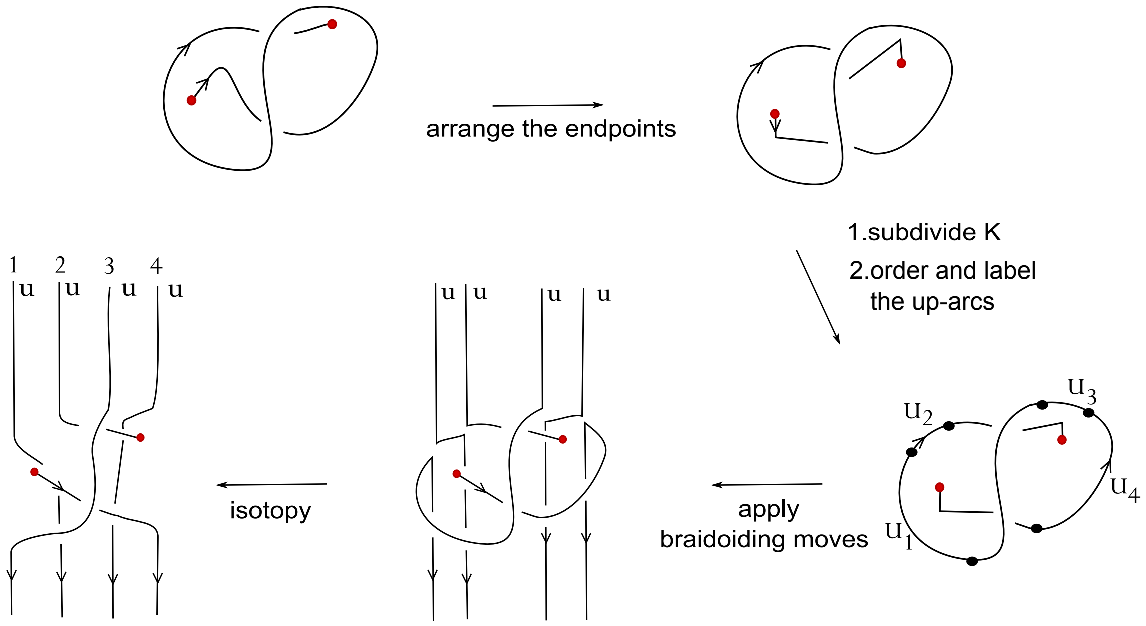

Figure 3.23: An illustration for the algorithm II

3.4 *L*-equivalence on braidoid diagrams

The *L*-moves were originally defined in 1993 by Lambropoulou for classical braids [83–85]. They were used for proving a one-move analogue of the classical two-move Markov theorem [2, 71, 72, 87, 88, 91, 94], which relates braids that close to isotopic knots or links. The *L*-moves are defined on braidoid diagrams analogousl and we shall use them for formulating a geometric analogue of the classical Markov theorem, even though we do not have an algebraic structure for braidoids.

3.4.1 L-moves

Definition 3.13. An *L-move* on a braidoid diagram B is the following operation.

1. Cut a strand of B at some point which could be an interior point or an endpoint, that is not vertically aligned with a braidoid end or an endpoint or a crossing of B. This can be ensured by small braidoid isotopies.

2. Pull the resulting ends away from the cut-point to the top and bottom lines of B respectively, keeping them vertically aligned with the cut-point, so as to create a new pair of strands with corresponding braidoid ends, and so that the new strands run both entirely over or under the rest of the braidoid diagram. In the case that an endpoint is contained in a vertical segment of a strand and the strand is cut at the endpoint then the resulting strands are created in a distance arbitrarily close to the vertical line of the endpoint, either on the right or the left of this line. See Figures 3.24 and 3.25 for abstract illustrations of L-moves.

3. From the above, there are two types of L-moves, namely L_{over} and L_{under}-moves, denoted by L_o and L_u, respectively. An L_o-move comprises pulling the resulting sub-strands entirely over the rest of the diagram. An L_u-move comprises pulling the sub-strands entirely under the rest of the diagram. See Figure 3.24. Moreover, an L-move applied on an interior point can be isotoped to having a small crossing on the resulting strands [84, 85]. See Figure 3.26.

The L-moves can be applied on labeled braidoid diagrams by labeling a pair of corresponding strands with 'o' if they are resulting from an L_o-move and with 'u' otherwise. As can be seen by Figure 3.24 the closure of the labeled braidoid strand resulting from an L-move is isotopic to the closure of the initial arc.

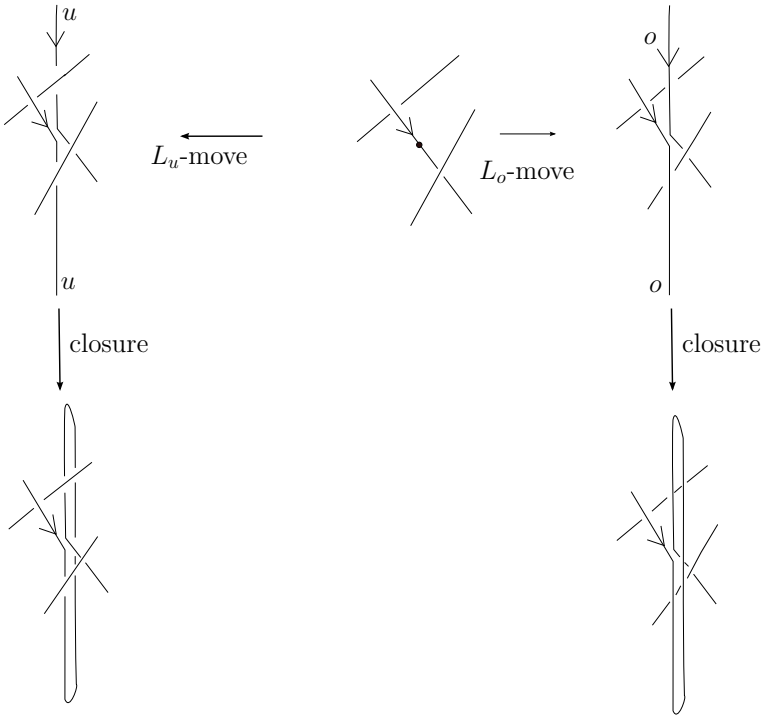

Figure 3.24: The closure of strands resulting by L-moves are isotopic to the initial strand

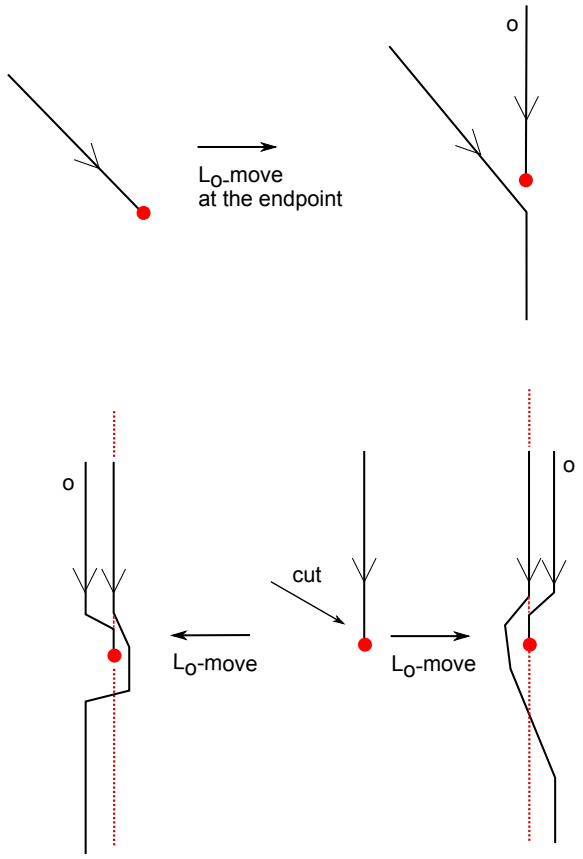

Figure 3.25: L-moves applied at the endpoints

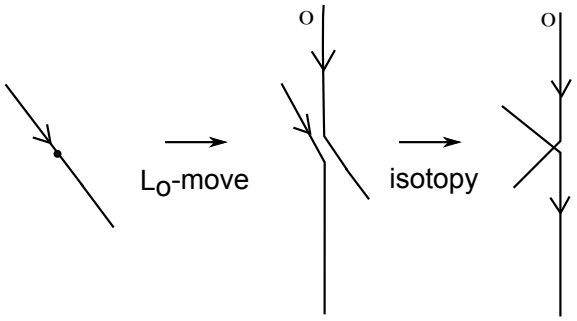

Figure 3.26: A crossing on the resulting strands

Definition 3.14. The L-moves together with labeled braidoid isotopy generate an equivalence relation on labeled braidoid diagrams that is called the *L-equivalence*. The L-equivalence is denoted by $\sim_L$.

Clearly, the L-equivalence does not preserve the number of strands or labels on the strands. Figure 3.27 illustrates a sequence of L-equivalence on labeled braidoid diagrams and how the L-equivalence affects the labeling.

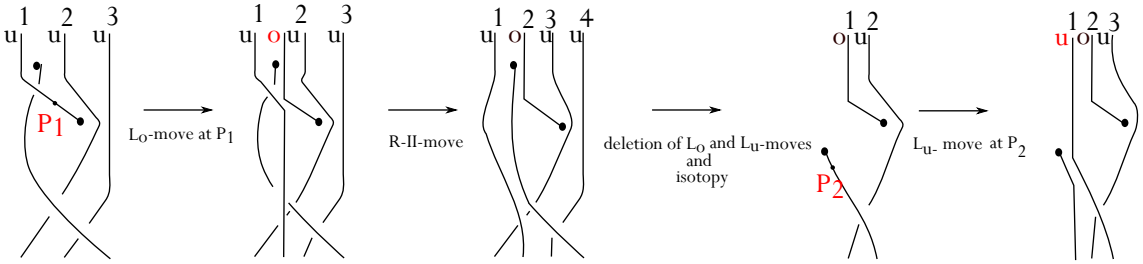

Figure 3.27: L-equivalence

It is also clear that a labeled braidoid diagram obtained by applying a braidoding algorithm to a knotoid diagram depends on the choices made for bringing the knotoid diagram to satisfy the general position requirements before starting the braidoiding algorithms, such as: arrangement of the endpoints, subdivision chosen and labeling of up-arcs. In other words, the labeled braidoid diagram associated to a knotoid via a braidoiding algorithm, is not unique up to the braidoid isotopy. Moreover, a knotoid diagram may also change by isotopy. Yet, the L-equivalence provides a one-to-one correspondence of multi-knotoids to labeled braidoids as we show in the sequel. More precisely, we will prove now the following theorem.

Theorem 3.15. *[18](An analogue of the Markov theorem for braidoids) The closures of two labeled braidoid diagrams are isotopic (multi-)knotoids in $\mathbb{R}^2$ if and only if the labeled braidoid diagrams are L-equivalent.*

The part of the proof of Theorem 3.15 not involving the endpoints are analogous to the case of classical knots and braids [83, 84]. We adapt these parts here and focus on the situations involving the endpoints. Before starting the proof we give the following definition.

Definition 3.16. A multi-knotoid diagram K in the xt-plane, with a subdivision and labeling on its up-arcs, is said to be in *general position* if
i. it has no horizontal arcs,
ii. no two disjoint subdividing points are vertically aligned with each other or a crossing or an endpoint,
iii. the arcs adjacent to the endpoints of K are vertical down-arcs.
*iv.*no sliding triangles intersect with an endpoint,
*v.*sliding triangles satisfy the classical triangle condition.

Note that a multi-knotoid diagram can always be perturbed to take its in general position by small Ω-moves. For the proof of Theorem 3.15, we assume that multi-knotoid diagrams are in general position.

Proof. If part:
Let B_1, B_2 be any two labeled braidoid diagram such that $B_1 \sim_L B_2$. Let the arc, illustrated in Figure 3.24, be a segment of a strand of B_1 on which an L-move is applied. It can be observed by the same figure that the closure of the resulting strands labeled accordingly to the type of the L-move applied, is isotopic to this arc. More precisely, the resulting closed strand can be contracted over the rest of the diagram back to the initial arc as seen in Figure 3.24. This suffices to tell that the closures of B_1 and B_2 are isotopic. This also shows that the closure map extends to a well-defined map cl_L on the set of of all L-equivalence classes of labeled braidoids.

cl_L : {L-classes of labeled braidoid diagrams}$\rightarrow$ {Multi-knotoids}.

Only if part:
For showing the only if part, we need to show that the map cl_L is a bijection.

The braidoiding algoritm II induces a mapping br,

br: {(Multi-)knotoids in $\mathbb{R}^2$} $\rightarrow$ {L-classes of labeled braidoid diagrams},

that associates a (multi-)knotoid K in $\mathbb{R}^2$ to the L-class of the braidoid diagram obtained from K by the algorithm II. We call this map the *braidoiding map*.

Now we show the map *br* is well-defined, that is, up-to the L-equivalence, the labeled braidoid assigned to K, is independent of the choices of subdivision of up-arcs and labeling of free up-arcs, and also invariant under the Ω-moves of knotoids.

Lemma 3.17. *Let K be a (multi-)knotoid diagram. Addition of subdividing points to K yields L-equivalent braidoid diagrams.*

Proof. Let QP denote an up-arc of K as depicted in Figure 3.28. First, let us assume that the vertical line passing through one of the endpoints of K intersects QP. Let P_1 denote the new subdividing point on QP that is chosen so that it is not vertically aligned with another subdivision point, a crossing, or an endpoint, and also it does not lie on the local component of the plane containing P that is determined by the vertical line passing through the endpoint. We label the sub-arcs resulting from the new subdivision according to the initial labeling, here in the figure they are free up-arcs and are labeled with o. It can be verified by Figure 3.28 that the braidoid diagram resulting from the initial subdivision on K (that is by applying a braidoiding move at P) can be turned into the braidoid diagram resulting from the latter subdivision (that is by applying braidoiding moves at the points P and P_1) by an L-move that is applied at the point Q^* , where Q^* denotes the intersection point of the vertical line passing through P_1 and the lower strand containing Q that has been obtained by the initial braidoiding of QP. Note that an arbitrarily small neighborhood of Q containing Q^* is perturbed to slope slightly downwards for applying the L-move. For the case of adding a subdividing point that is located on the same local component with P with respect to the vertical line of an endpoint, the proof follows similarly as for classical knots and braids [84]. □

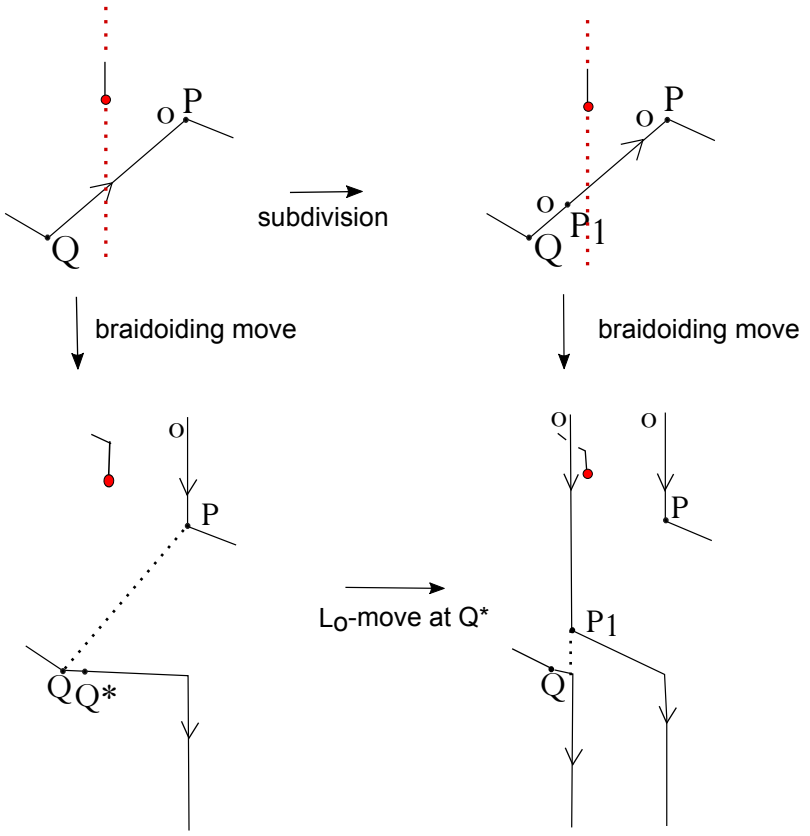

Figure 3.28: Adding a subdividing point on the up-arc yields L-equivalence

Lemma 3.18. *The choice of labeling a free up-arc does not change the resulting braidoid diagram up to the L-equivalence.*

Proof. This is verified in Figure 3.29. For simplicity we illustrate a case where the sliding triangle of the up-arc does not intersect with any other arcs of the diagram. Note also that the L_o-move is applied (at the top line) at a point that is arbitrarily close to P so that there is no other vertical strands between the vertical lines passing through P and P^*. Note that the point Q^* in the figure denotes a point that is the vertical projection of the point P on the lower sub-strand containing Q, and the L-move is applied at Q^* when a small neighborhood of it is assumed to slope downwards.

If the sliding triangle of QP intersects with other arcs of the diagram then we subdivide QP into small enough sub-arcs to ensure the corresponding sliding triangles are all clear of arcs. We label each small up-arcs in the same way with QP, say o. Then from the discussion above we can change the labeling of each up-arc to u and by Lemma 3.17 we delete all further subdividing points and have Q and P as subdividing points for the up-arc labeled now with u. See Figure 3.30.

□

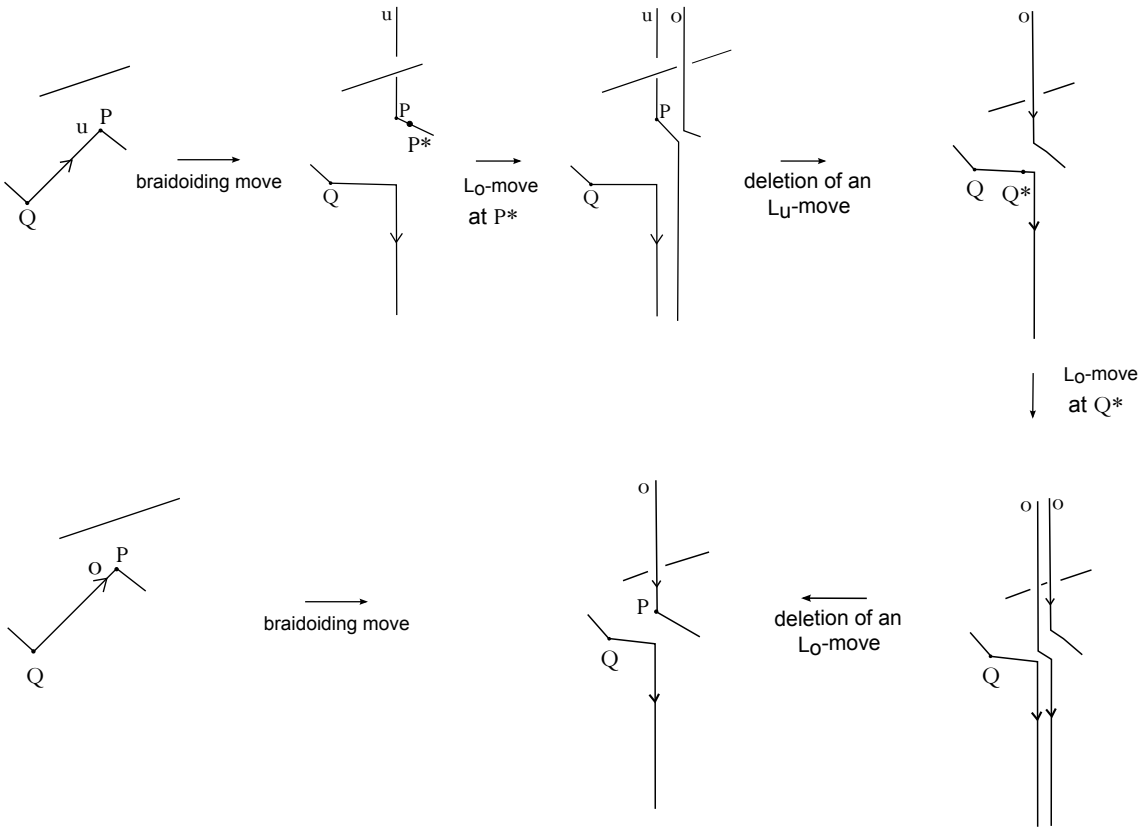

Figure 3.29: The L-class of the resulting braidoid is independent of labeling of free up-arcs

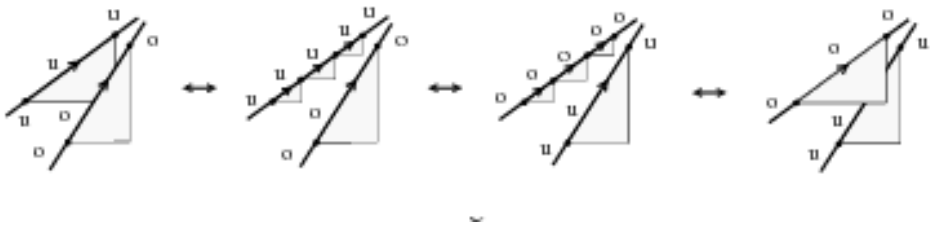

Figure 3.30

Proposition 3.19. *Given any two subdivision S_1, S_2 of a knotoid diagram K the resulting braidoid diagrams are L-equivalent.*

Proof. It is clear that any subdivision further than S_1 or S_2 satisfies both triangle conditions. Consider the further subdivision $S_1 \cup S_2$ of both S_1 and S_2 on K. By Lemma 3.17 that takes care of the choices of labels for the resulting free up-arcs, the resulting braidoid diagram by the subdivision $S_1 \cup S_2$ is L-equivalent to the braidoid diagrams resulting from the subdivision S_1 and S_2. Since the L-equivalence is an equivalence relation, the proposition follows. □

Now we shall show the invariance under the Ω-moves.

Lemma 3.20. *Planar isotopy moves and the Reidemeister moves on knotoid diagrams correspond to the L-moves on the braidoid diagrams obtained.*

Proof. Let us starting with the observation that by imposing the classical triangle condition, we can assume the isotopy moves to take place locally without affecting or conflicting with the braidoiding of the rest of the diagrams that lie outside the regions of the moves. In fact we can assume the rest of the diagram is already to be already turned into a braidoid and the arcs taking place in an isotopy move are left for elimination.

The examination of planar isotopy moves on up-arcs that do not contain any of the endpoints and the Reidemeister moves that take place away from the endpoints, follows similarly with the examination of these moves on classical knots/links, that appears in [84, 85]. Here in Figure 3.31 we give an illustration for an Ω_1- move.

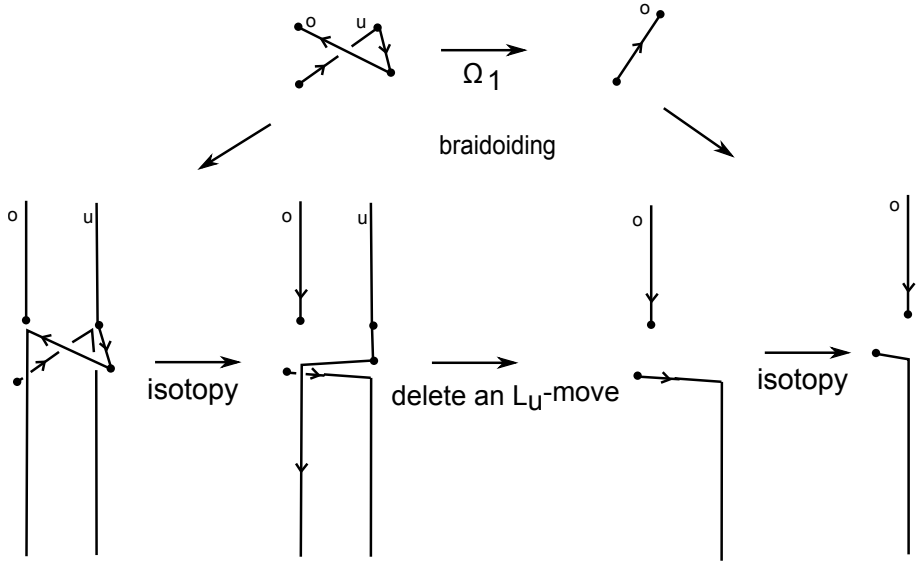

Figure 3.31: An Ω_1-move under braidoiding

The choices of planar isotopies applied for preparation to turn a vertical up-arc adjacent to an endpoint are realized as L-equivalence as seen in Figure 3.32.

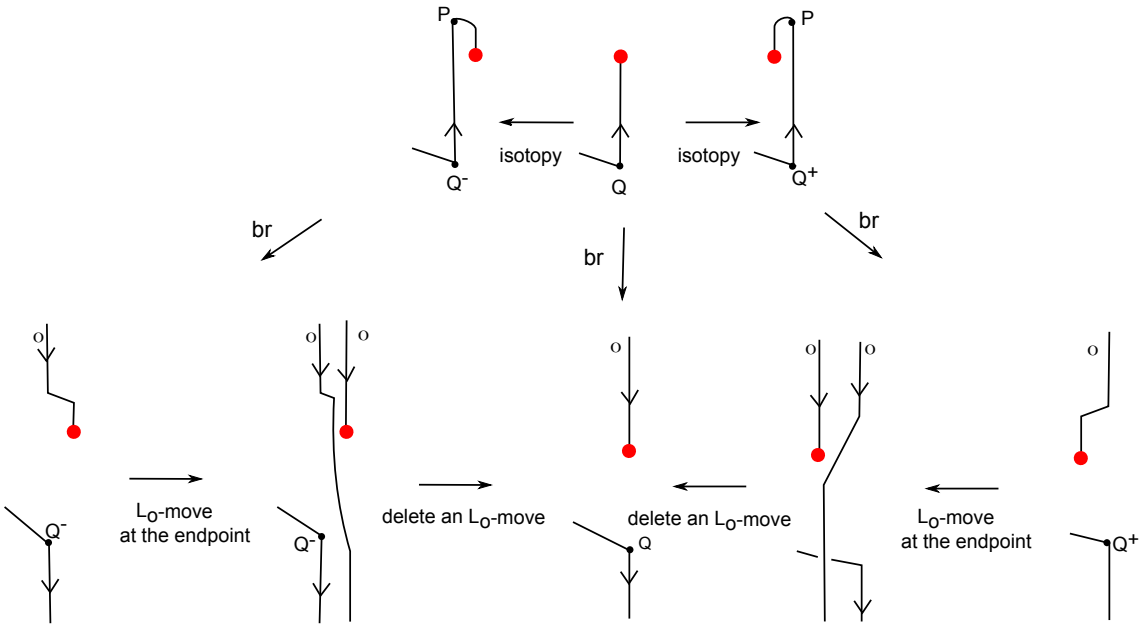

Figure 3.32

□

Corollary 9. *The braidoing map is a well-defined map.*

Lastly it needs to be showed that br is the inverse map of cl_L.
Let B be a labeled braidoid diagram. It is clear that the closure diagram of B, $\widehat{B}$, is a knotoid diagram in general position whose only up-arcs are the connection arcs taking place in closing B. Then the braidoding algorithm II turns $\widehat{B}$ into a braidoid diagram which is L-equivalent to the braidoid diagram B. Thus,

$$br \circ cl_L = id$$

.
Given a knotoid diagram K in general position, applying the braidoiding algorithm II, we obtain a labeled braidoid diagram B. It is clear from the discussion above that the closure of the the diagrams in the L-class of B is isotopic to K. From this, it follows

$$cl_L \circ br = id$$

.

By the above the proof of Theorem 3.15 is completed. □

Corollary 10. *The braidoiding algorithm I utilizes rotation of crossings which can be expressed as a combination of planar isotopy moves and the rest of the algorithm*

follows the same with braidoiding algorithm II. Then by Lemma 3.18 and Lemma 3.20 , the two braidoiding algorithms given in Section 3.3 result in L- equivalent labeled braidoid diagrams.

Proposition 3.21. *Any labeled braidoid diagram is L-equivalent to a u-labeled braidoid diagram.*

Proof. Let B a labeled braidoid diagram and $\widehat{B}$ be its closure. The braidoiding algorithm I turns $\widehat{B}$ to a u-labeled braidoid diagram B_u by the choice of labeling all free up-arcs with u (recall discussion in Section 3.3.2). Since the L-equivalences of labeled braidoids are in one-to-one correspondence with multi-knotoids, by Theorem 3.15, it follows that B and B_u are L -equivalent. □

Then Theorem 3.15 can be reformulated according to the discussion above, as follows.

Theorem 3.22. *The closures of two u-labeled braidoid diagrams are isotopic (multi-)knotoid diagrams if and only if these braidoid diagrams are L-equivalent.*

From braidoids to classical braids

Two endpoints of a braidoid diagram can be joined to obtain a (classical) braid diagram in the following way. Let B be a braidoid diagram with n strands. The two endpoints of B can be connected with an embedded arc or a pair of strands in the plane, resulting in a classical braid diagram. There are two cases for the connection.

If the head of B appears before the leg (as t increases), then a downward directed embedded arc is chosen to connect them, running *under* each piece of the strands which it meets during the connection. Two such embedded arcs are clearly isotopic. The resulting diagram is a classical braid diagram on n strands. See the top of Figure 3.33 for an abstract illustration of this case.

If, however, the leg of B appears before the head, then any arc connecting them is oriented upward in order to be consistent with the orientation of the free strands. That is, it is an 'up-arc' in the resulting tangle diagram. We apply a braiding move (which is also available for tangle diagrams, see [83–85]) on such a connection arc to turn the resulting up-arc into a pair of braid strands. The resulting diagram is a classical braid diagram on $n + 1$ strands.

We call this closure defined on braidoid diagrams the *underpass connection* of a braidoid diagram, in analogy with the underpass closure of a knotoid diagram that results in a knot diagram.

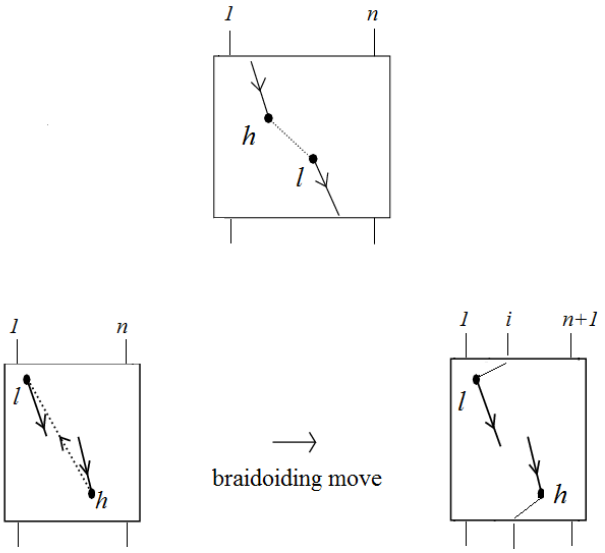

Figure 3.33: Underpass connection

Proposition 3.23. *[18,19] The operation of turning a braidoid diagram into a braid diagram induces a surjective map from the set of braidoids to the set of L-equivalence classes of braids. Furthermore, this map is not injective.*

Proof. We examine the isotopy moves on braidoid moves under the underpass connection. The Ω-moves take place away from the endpoints so it is clear that they are transformed to the Reidemeister moves on the resulting braid diagram. The swing moves of the endpoints are transformed to braid isotopy moves in which a connecting arc is involved. The vertical move can cause a change in relative positioning of the endpoints so a connecting arc may change direction. In this case resulting braid diagrams are L- equivalent to each to other as it is shown in Figure 3.34. The map is surjective since cutting any underpassing arc from a braid diagram results in a braidoid diagram which will be taken to the braid diagram via the map. Further, the fact that the underpass connection is not an injective map is evident by the fact that joining the endpoints with an underpassing arc corresponds to allowing the braidoid forbidden move that slides the free up-arc under transversal strands. □

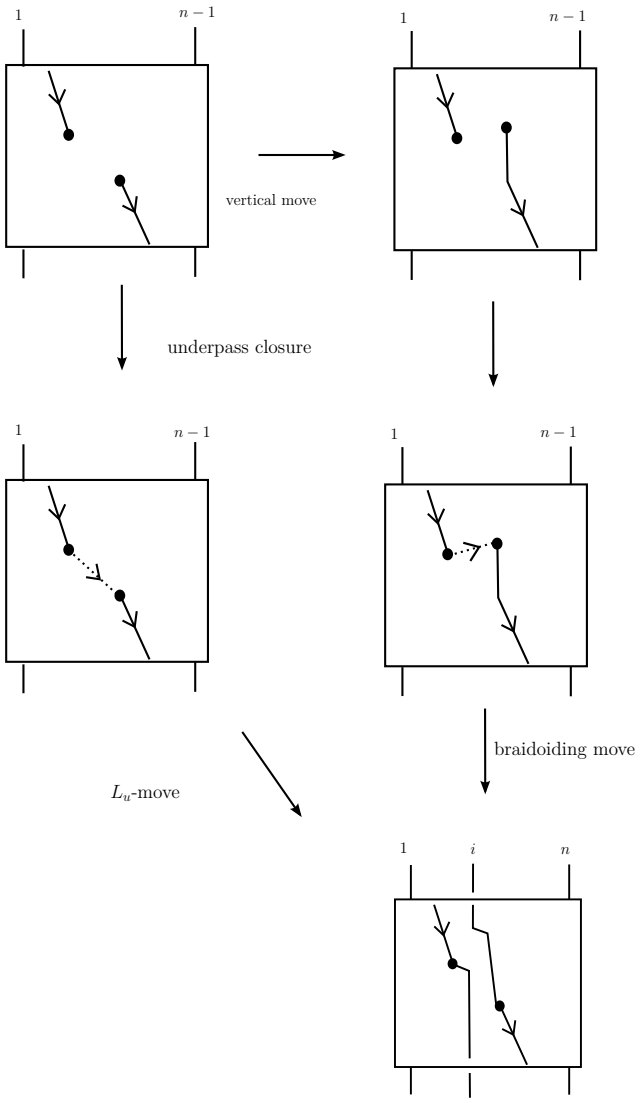

Figure 3.34: The choice of the arc connecting the endpoints does not affect the resulting braid up to L-equivalence

3.5 On the way to an algebraic structure

3.5.1 Combinatorial braidoid diagrams

In order to express braidoids in terms of basic generating blocks, we introduce an auxiliary combinatorial structure for braidoid diagrams so called the implicit points [18, 19].

Implicit points and indexing

It is clear that right after or just before an appearance of an endpoint, the number of points on the horizontal levels of a braidoid diagram (that is, intersections of

the diagram with lines $t = t_i$, $0 \leq t_i \leq 1$) may increase or decrease by one. In order to regard a braidoid diagram as a composition of blocks we fill the braidoid diagram at discrete horizontal levels with the *implicit points*, denoted by empty dots. Implicit points hold the positions of braidoid ends and the endpoints along their vertical line. Assuming that the endpoints and braidoid ends occupy different vertical positions, it is clear that a braidoid diagram with n strands can determine at least n vertical positions in the case that the endpoints can be brought to be aligned vertically, and at most $n+1$ vertical positions in the case that the endpoints appear in different vertical alignments. In this setting we require that the endpoints lie on vertical segments of the free strands which can be achieved by the braidoid swing moves and if both endpoints can be brought to be aligned vertically with each other without violating the braidoid isotopy, we assume them aligned before filling a braidoid diagram to minimize the number of points in blocks.

See Figure 3.35 for the braidoid diagrams of Figure 3.1 completed with implicit points.

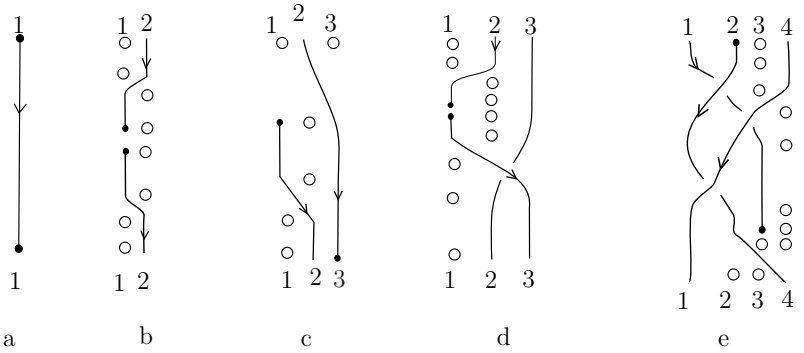

Figure 3.35: Filling braidoid diagrams with implicit points

After the completion of the diagram with implicit points, all points appearing in a horizontal level (braidoid ends, endpoints, implicit points) get indexed by consecutive natural numbers, starting from 1, according to their horizontal positions from left to right. Note that some indices of braidoid ends may now be shifted from the previous numbering with the appearance of the implicit points. Clearly the number of strands or crossings do not change. See Figure 3.35.

Definition 3.24. A braidoid diagram filled in with implicit points and indexed accordingly shall be called a *combinatorial braidoid diagram*.

Elementary k-blocks of braidoid diagrams

Definition 3.25. Let B be a combinatorial braidoid diagram with k points at each horizontal level. An *elementary k-block* of B is a union of $2k$-points positioned at

top and bottom lines parallel to each other, k of which at the top and $k$of which at the bottom, together with descending strands connecting top points to bottom ones accordingly to the following rules. A top point is connected to at most one bottom point that lies at the same position or at a successive position. There may be points both at top and bottom lines that are not connected to a point; the number of isolated points can be at most two at each line. The isolated points correspond to implicit points of B. See Figure 3.36.

The elementary blocks fall into the following four types.

1. The *identity and crossing k- blocks*: They consist of blocks 1_k and $\sigma_i^{\pm 1}$ that are the identity braid on k strands and the *elementary braidings*, respectively, and augmentations of these blocks with one or two pairs of vertically aligned implicit points as shown in Figure 3.36. The position of implicit points are indicated inside a parenthesis on the right upper part of the corresponding symbol.

2. The *endpoints k-blocks*: These are identity blocks augmented with a graphical node at the top/bottom i^{th} position that is connected to the i^{th} bottom/top row. The graphical nodes are regarded as the endpoints of B and these elementary blocks are denoted by h_i and l_i, respectively. The endpoint blocks may be augmented with one pair of vertically aligned (at top and bottom row) implicit points whose positions are denoted inside a parenthesis on the right upper part of the corresponding symbol.

3. The *shifting k-blocks*: They are denoted by λ_{i+1i} and λ_{ii+1}. In the shifting block λ_{i+1i}, $k-2$ points at the top row is connected to their corresponding points at the bottom row and the top i^{th} point is connected to the bottom $(i+1)^{st}$ point, while the top $(i+1)^{st}$ and the bottom i^{th} points are not connected to a point, left as implicit points. The shifting block λ_{ii+1} similarly comprises identity braid on $k-2$ strands but this time the top $(i+1)^{st}$ point is connected to the bottom $(i+1)^{st}$ point and the top i^{th} point together with the bottom $(i+1)^{st}$ are left as implicit points. The shifting elements represent the shifting of the index of a strand adjacent to a free strand that may happen before or after the appearance or disappearance of an endpoint. The set of shifting k-blocks may be augmented by elementary blocks containing one pair of vertically aligned implicit points.

It is clear that, by small braidoid isotopies we can arrange B, so that it is divided into finitely many horizontal stripes, each containing exactly one of the elementary

k - blocks. Note that, unlike the case of braids, an elementary block of a braidoid

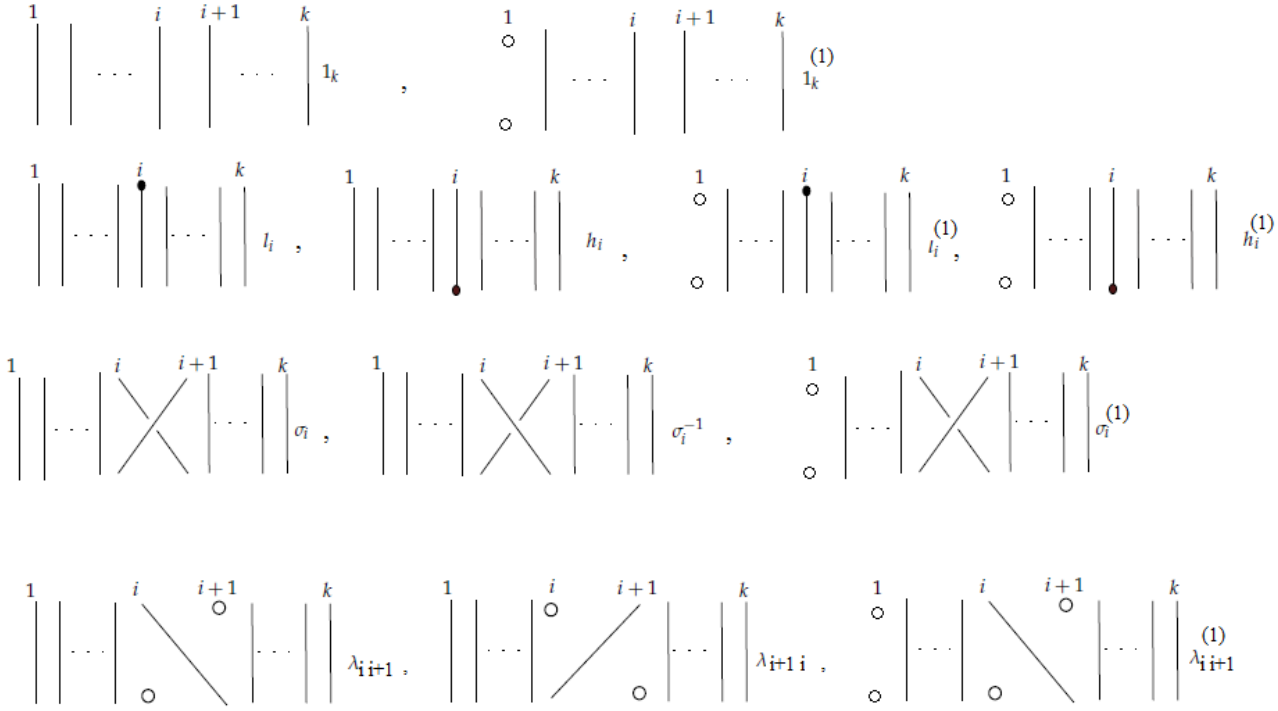

Figure 3.36: Elementary k-blocks

A product of elementary blocks

We define a product operation on the set of elementary k-blocks to obtain combinatorial braidoid diagrams. This product is induced by placing one elementary k-block below another elementary k-block and concatenating the ends of the blocks in the following way [18, 19]:

1. We call the ends of strands in elementary blocks *usual ends* if they are not the endpoints. Usual ends can be concatenated with only usual ends at the same position so that the resulting diagram contains strands emanating from top to bottom row. See top illustration of Figure 3.37.

2. An endpoint can be multiplied with either another endpoint or with implicit points. Two multiplied endpoints remain at their vertical position as two disjoint endpoints. See the middle and the bottom illustrations of Figure 3.37. When an endpoint is multiplied with an implicit point, the endpoint remains as itself, while the implicit point is annihilated.

3. Two implicit points meeting in the middle row annihilate each other.

4. Exactly two endpoints block take place in final products; one is h_i, the other one is l_j, for some $1 \leq i, j \leq k$. The usual ends in a final product appear in pairs at the same vertical position, at top and bottom rows.

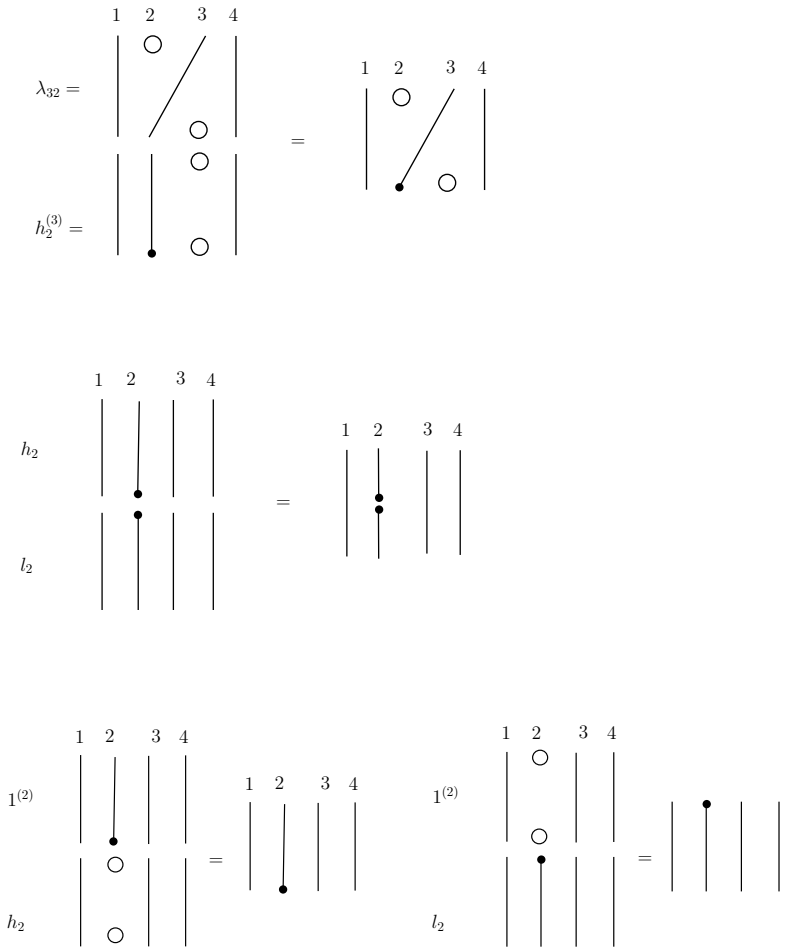

Figure 3.37: The product of 4-blocks containing endpoints and implicit points

It is clear that any such product of elementary blocks is a combinatorial braidoid diagram. Since any combinatorial braidoid diagram uniquely defines a braidoid diagram by forgetting its implicit points, any braidoid diagram with n strands can be seen as a finite product of elementary n- or $(n+1)$-blocks. By regarding a braidoid diagram as a product of elementary blocks one can read the diagram from top to bottom, as a word consisting of symbols corresponding to factor elementary blocks. To give an example, the braidoid diagram in Figure 3.35(d) is a product of 3-blocks and the corresponding word is $1_3^{(1)}\lambda_{21}h_1^{(2)}l_1^{(2)}\lambda_{12}(\sigma_2^{(1)})^{-1}$.

Relations on the product

The product operation defined on the elementary blocks is subjected to the following relations that extends the braid group relations and corresponds to braidoid isotopy moves. More precisely, one can verify by simply drawing the diagrams, that the relations 1, 2, 3, and 4 correspond to Ω_2 and Ω_3 moves, relations 5, 6, 7 correspond to the vertical moves of braidoids, relations 8, 9, 10, 11, and 12 are due to planar isotopy moves.

1. $\sigma_i\sigma_i^{-1} = 1_k = \sigma_i^{-1}\sigma_i$ for all $1 \leq i \leq k-1$
2. $\sigma_i^{(j)}(\sigma_i^{(j)})^{-1} = 1_k^{(j)}$ for some j such that, $1 \leq j \leq i-1$ or $i+2 \leq j \leq k$.
3. $\sigma_i\sigma_{i+1}\sigma_i = \sigma_{i+1}\sigma_i\sigma_{i+1}$ for $1 \leq i < k$.
4. $\sigma_i^{(j)}\sigma_{i+1}^{(j)}\sigma_i^{(j)} = \sigma_{i+1}^{(j)}\sigma_i^{(j)}\sigma_{i+1}^{(j)}$ for some j such that $1 \leq j \leq i-1$ or $i+3 \leq j \leq k$.
5. $\sigma_i^{\pm 1}l_j = l_j(\sigma_i^{(j)})^{\pm 1}$, for some j, $i+2 \leq j \leq k$ or $1 \leq j \leq i-1$.
6. $\sigma_i^{\pm 1}h_j = h_j(\sigma_i^{(j)})^{\pm 1}$, for some j, $i+2 \leq j \leq k$ or $1 \leq j \leq i-1$.
7. $h_i^{(j)}l_j^{(i)} = l_j h_i$, for $|i-j| \geq 1$.
8. $\lambda_{ii+1}\lambda_{i+1i} = 1_k^{(i+1)}$.
   $\lambda_{i+1i}\lambda_{i+1i} = 1_k^{(i)}$.
9. $\lambda_{i+1i}^{(j)}\lambda_{j+1j}^{(i+1)} = \lambda_{j+1j}^{(i)}\lambda_{i+1i}^{(j+1)}$, for $|j-i| \geq 2$.
10. $\lambda_{ii+1}^{(j+1)}\lambda_{jj+1}^{(i)} = \lambda_{jj+1}^{(i+1)}\lambda_{ii+1}^{(j)}$, for $|j-i| \geq 2$.
11. $\lambda_{i+1i}^{(j+1)}\lambda_{jj+1}^{(i+1)} = \lambda_{jj+1}^{(i)}\lambda_{i+1i}^{(j)}$, for $|j-i| \geq 2$.
12. $\lambda_{ii+1}^{(i+2)}\lambda_{i+1i+2}^{(i)}\sigma_{i+2}^{(i,i+1)}\lambda_{i+2i+1}^{(i)}\lambda_{i+1i}^{(i+2)} = \lambda_{ii+1}^{(i+2)}\lambda_{i+3i+2}^{(i)}\sigma_{i+1}^{(i,i+3)}\lambda_{i+1i}^{(i+3)}\lambda_{i+2i+3}^{(i+1)}$
13. $\lambda_{ii+1}^{(i+2)}\lambda_{i+1i+2}^{(i)}\sigma_{i+2}^{(i,i+1)}\lambda_{i+2i+1}^{(i)}\lambda_{i+1i}^{(i+2)} = \lambda_{i+3i+2}^{(i+1)}\lambda_{i+2i+1}^{(i+2)}\sigma_{i}^{(i+2,i+3)}\lambda_{i+1i+2}^{(i+3)}\lambda_{i+2i+3}^{(i+1)}$.

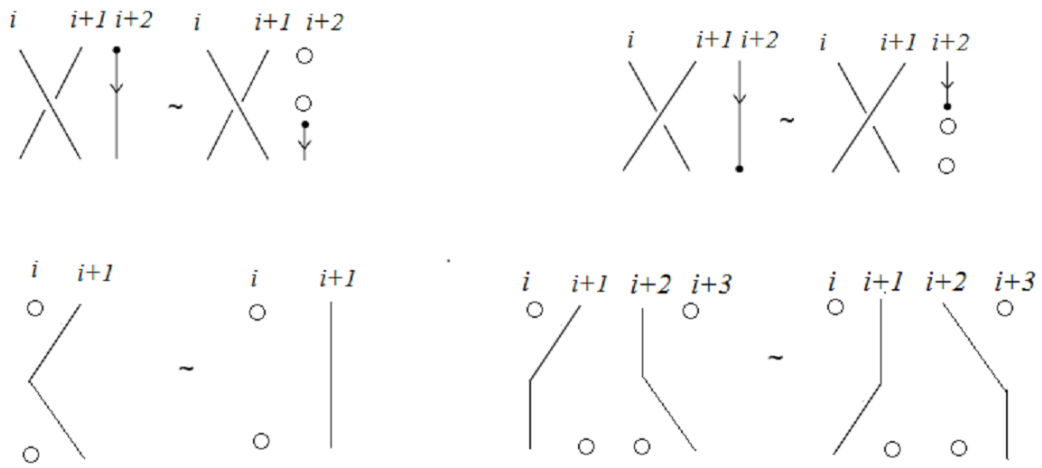

Figure 3.38: Diagrammatic pictures of relations; 5, 6, 8 and 10

We can conclude that the set of all final products of elementary blocks taken up to the relations above is in one-to-one correspondence with the set of braidoid diagrams taken up to braidoid isotopy.

3.5.2 Discussion/ further questions on braidoids

1. One natural way of closing a braidoid diagram is to connect each pair of corresponding ends with an embedded arc that lies away from a disk containing the braidoid diagram. This closure can be illustrated as in Figure 3.39. Let us name this closure as *classical closure* of a braidoid diagram. It is clear that the classical closure of a braidoid diagram is a (multi-)knotoid diagram. However, the braidoid algorithms that we have discussed previously, may turn a knotoid diagram into a braidoid diagram whose end-to-end closure is not isotopic to the knotoid diagram we started with. See Figure 3.39 again for an example. This is once more due to the presence of the endpoints and restricted moves of them.

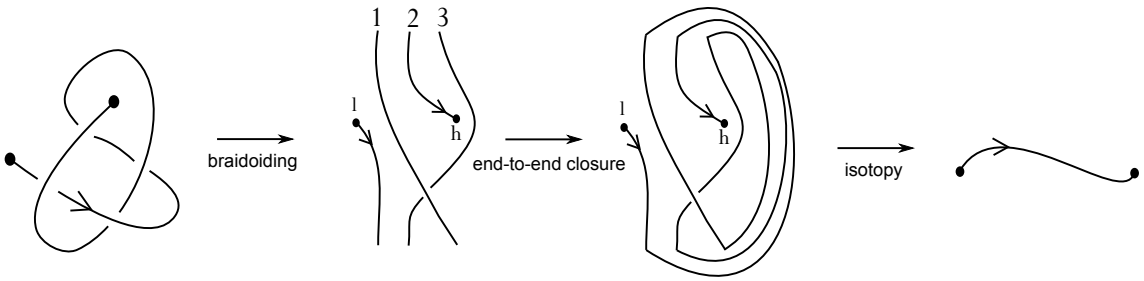

Figure 3.39: Classical closure does not induce an inverse map for the braidoiding

A natural question arising here is: *Is there an algorithm turning a (multi-)knotoid diagram into a braidoid diagram whose classical closure is isotopic to the (multi-)knotoid diagram?* This question is left open for now.

2. There is also the question of understanding the algebraic structure on the set of braidoid diagrams. Defining a multiplication operation on set of braidoid diagrams with n strands that yields an algebraic structure on the set is not yet visible due to the endpoints. The question of a possible algebraic structure of braidoid diagrams will be worked within the context of a future work.

3. The elementary blocks of a braidoid diagram are in resemblance with Rook diagrams [3, 89] with an extension by the endpoint blocks. The question follows: *Is there an association of the set of braidoids with a diagram algebra such as Rook or, Motzkin algebras [2, 3] ?*. This question is left as a proposal for a future work.

4. As we mentioned before, the notion of a knotoid extends the notion of a $1-1$-tangle by having its endpoints that are not necessarily fixed at top and bottom lines. In fact, a new category extending the category of tangles can be defined via the notion of a tangloid. A tangloid can be defined as in the following.

   Definition 3.26. Let I denote the unit interval in $\mathbb{R}$. An (unoriented) tangloid diagram T is a generic immersion of $k > 0$ intervals and a number of disjoint unit circles in $I \times I \subset \mathbb{R}^2$ such that $0 \leq n \leq k$ of them have fixed ends on $I \times \{0\}$ and $I \times \{1\}$ and $k - n$ of them can have their ends anywhere in $I \times I$ as disjoint from each other and from other points and not necessarily fixed at their position. T has only a finite number of singular points that are transversal double intersection points each endowed with under-/over-data. The ends of immersed arcs which that are not necessarily fixed on $I \times \{0\}$ and $I \times \{1\}$ are denoted by a graphical node as for braidoid endpoints.
   A oriented tangloid diagram is a tangloid diagram with an orientation assigned for each of its arcs.

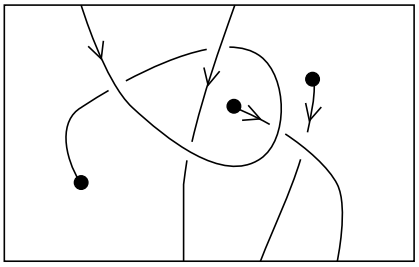

Figure 3.40: An oriented tangloid

Examples. (a) An (n, m)- tangle is a tangloid that has $n + m$ ends fixed on the top and m points fixed on the bottom and a number of circular components.

(b) A knotoid diagram is an oriented tangloid diagram with one arc whose ends do not necessarily lie on $I \times \{0\}$ and $I \times \{1\}$.

(c) A braidoid diagram with n usual strands and two free strands is an oriented (with descending orientation) tangloid with $n + 2$ arcs, n of which have their ends fixed on $I \times \{0\}$ and $I \times \{1\}$ and two of which have one of its ends fixed on $I \times \{0\}$ or $I \times \{1\}$ and the other ends appearing anywhere in $I \times I$ and also a braidoid diagram does not have any cups or caps (see Figure 3.41 for cups and caps).

The Δ-moves defined for tangle diagrams can directly be applied to tangloid diagrams under the condition that no ends of arcs can slide across (over or under) some other transversal arc. We can define the isotopy relation for tangloid diagrams as generated by these moves.

A composition on tangloid diagrams extending the composition of tangles, can be defined as follows. The composition of the ends that lie fixed on top and bottom line are concatenated and the composition of the ends that are denoted by graphical nodes (that are necessarily fixed on top and bottom lines) can be defined by leaving them disjoint, see Figure 3.42.

A tangloid diagram T can be arranged with respect to the height function of the plane so that, each horizontal line intersects T at a finite number of points. According to the definition above, a tangloid diagram can be then regarded as the composition of basic tangloids that are shown in Figure 3.41.

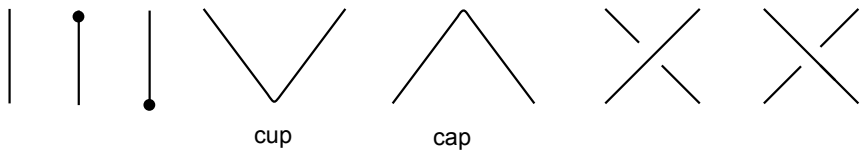

Figure 3.41: Basic tangloids

Figure 3.42: Composition of tangloid ends specified with graphical nodes

Constructing a category for tangloids and working on topological properties of tangloids will be the subject of a future work.

Chapter 4

On Applications

4.0 Introduction

Given a smooth open oriented curve C embedded in $\mathbb{R}^3$. We define $\mathscr{P}(C)$ to be the set of all knotoid equivalence classes obtained from the generic projection of C onto planes in $\mathbb{R}^3$ that are outside a sufficiently large radius ball containing C. We suggest [15] to take $\mathscr{P}(C)$ as a measure of the knottedness of C. This proposes a new and more realistic way to measure the knottedness of an open curve and may have significant applications in the study of tangled physical systems. In the direction of this proposal, this chapter inclues our results obtained by the topological modeling of knotted and bonded linear protein chains by using knotoids and bonded knotoids. The results of this chapter appear in [18, 23].

4.1 Studies on protein chains

A *protein* is a linear bio-polymer chain composed of different amino-acid residues covalently linked together by peptide bonds arranged in order from the N-terminus to the C-terminus (a terminus is an end of the protein chain) [81]. Proteins appear in various and quite often in very complicated conformations. In order to determine the entanglement type of a protein in terms of topology, one usually considers its backbone as an open polygonal curve and then simplifies it by applying an algorithm that preserves the underlying topology. One of the the most well-known techniques in the literature is the triangle elimination or KMT algorithm [11, 42, 43]. Up to time, the entanglement type of protein

chains has been tried to be understood by relating the chain with classical knots. In this direction, many suggestions have been made on how to close an open 3D curve and they all fall into two big categories [43, 60–64, 78, 79]. First are the single closure techniques, such as the direct closure [43] and the out of the center of mass closure [78], where the chain is closed by a single arc that connects the endpoints. These methods are computationally fast but depending on the particular closure recipe the same protein may end up forming different knots. The second category comprises the probabilistic methods such as the uniform closure technique [61, 63, 64], where the chain is first placed inside a large enough ball (usually a radius of twice the length of the chain will be sufficient) and a simplification algorithm is applied. Each point of the sphere is now a possible closure point of the open chain. The closure is achieved by picking a point and then extending two rays, one from each endpoint of the chain, towards the chosen point and connecting them. Such methods are less biased but they are more computationally intensive as the knot type of each closure has to be computed. Both categories have the disadvantage of altering the geometry of the studied object.

4.1.1 Analyzing open protein chains using knotoids

In the direction of the geometric interpretation of planar knotoids that was discussed in Section 2.1.3, one can study the entanglement of the protein backbone by knotoids as follows.

Similarly to the case of the uniform closure, the protein chain is assumed to lie into a 3- ball of sufficiently large radius, but in this case each point of the boundary of the ball corresponds to a projection direction on a plane that lies outside the ball. When the projection direction is determined, two lines that pass through the termini of the protein chain and are perpendicular to the determined plane are introduced. A simplification algorithm that eliminates the triangular regions is applied on the chain in a way that the lines introduced are never crossed. Notice that such a simplification on the chain corresponds to the line isotopy on space curves we introduce in Section 2.1.3. Finally the protein chain is projected to the plane and the projection is regarded as a planar knotoid diagram that is subject to knotoid equivalence moves. The diagrams resulting from projecting a protein chain can be considered also as spherical knotoids as it is studied in [22]. See [7] for another recent study suggesting to consider the 'virtual closure"' of the projections of a protein

chain.

The results then can be summarized on an atlas that identifies regions on a sphere and each distinct region corresponds to the projection directions in spherical coordinates that produce the same knotoid type. Moreover, each distinct region is color coded according to the knotoid type it carries. We shall call such a map the *projection globe* of a protein.

Coming back to the discussion in Section 2.1.2, one can obtain a wider spectrum of knotoid types by considering projections of the chain on a plane instead of a 2-sphere. This allows projections that were previously detected as unknotted to emerge as non-trivial planar knotoids. In [23], we apply this approach to the protein with PDB entry 3KZN (N-acetyl-L-ornithine) [74], see Figure 4.1. This protein is known to form a trefoil knot via closures or a $k3.1^{\circ}$ knot-type knotoid when projected as a knotoid in S^2. Recall that knot-type knotoids have both endpoints in the same region of the diagram and if one decides to close the diagram with an arc, the newly introduced arc may not create any additional crossings to the diagram, we apply this definition for planar knotoids as well. In our notation, a knotoid is represented by $kX.Y$, where X is the number of crossings of the knotoid diagram in question and Y corresponds to the position of the knotoid in our table among knotoids with the same number of crossings. Moreover, an exponent $^{\circ}$ indicates a knot-type knotoid, an exponent ^{p} a planar knotoid, and an exponent $^{-}$ a knotoid with its crossings inverted. Comparing now the projection globe obtained from the planar knotoids approach to the one derived from the spherical knotoids approach, as well as to the one that is derived from the uniform closure technique, we can see that new regions are gradually emerging as we move from knots to spherical knotoids and then to planar knotoids (see Figure 4.2). In fact, we observe that the grey regions of the uniform closure globe corresponding to trivial results are replaced by red regions corresponding to non-trivial knotoids with two crossings and as we go from the spherical knotoids globe to the planar knotoids globe, there are more knotoid types corresponding to 3KZN are captured. The reason behind this is that the number of classes of planar knotoids is larger than the number of classes of spherical knotoids due to the restricted isotopy in the plane, as discussed in Section 2.1.2. Figure 4.3 shows equirectangular projections of each projection globe shown in Figure 4.2. From this study we can conclude that following.

Corollary 11. *Analyzing open protein chains as planar knotoids reveals more details of their topology.*

Figure 4.1: The protein chain with entry 3KZN and its simplified backbone

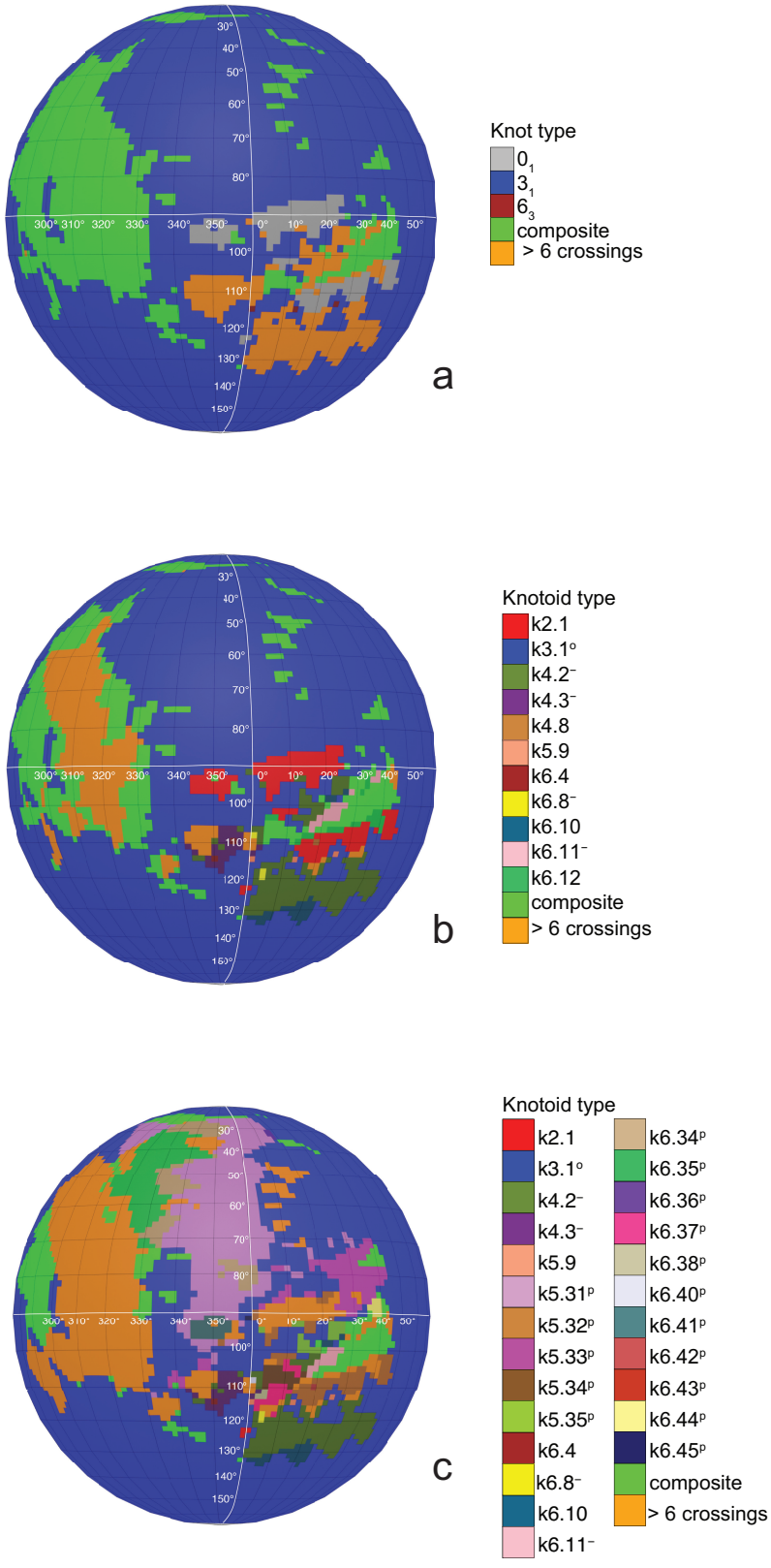

Figure 4.2: Projection globes obtained by uniform closure, spherical knotoid projection and planar knotoid projection; figure taken from [23].

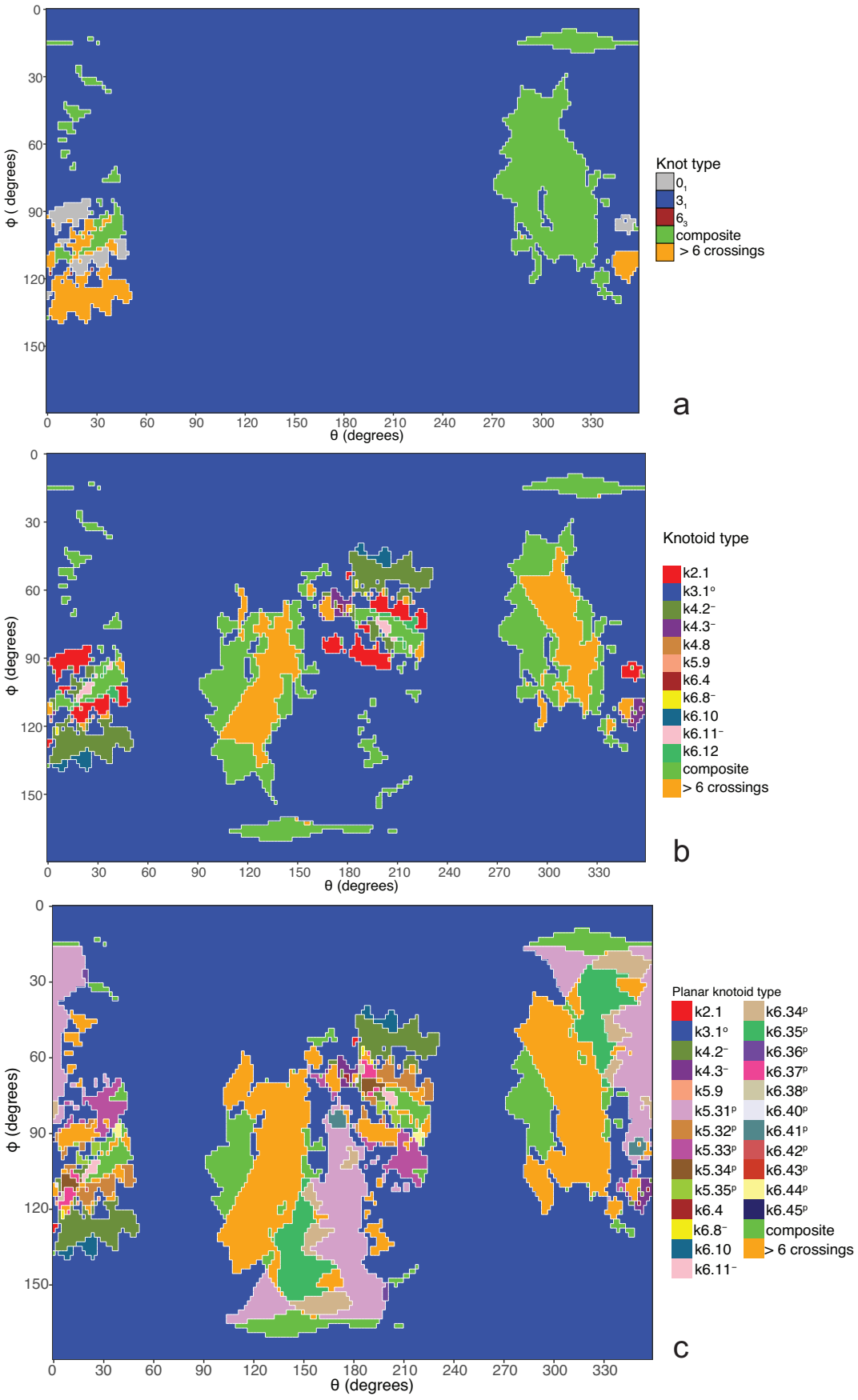

Figure 4.3: Equirectangular projections of each projection globe, figure taken from [23].

4.1.2 A topological model for bonded open protein chains

Motivated by the ideas in [80], we introduce a purely topological model for analyzing the topology of bonded open protein chains in terms of planar (multi-) knotoids [23].

A bonding site of a protein chain consists of two local strands of the chain and a bonding arc with its ends based on these strands, as illustrated in Figure 4.4. We adapt the projection of a space curve into planes resulting in knotoid diagrams, to a projection for a bonded protein chain. More precisely, we choose a projection direction determined by two parallel (infinite) lines passing through the termini of the chain and we project the protein chain into the plane that is orthogonal to these lines. We only consider projection directions that give a generic diagram, in the sense that we have only finitely many transversal self-crossing points and that a bonding site is represented in the projection in parallel or in anti-parallel fashion. The information of each bond is represented with dotted segments connecting the two ends involved. Endowing each self-intersection point with the weaving information of the chain in the space, we obtain an open-ended knotted diagram in the projection plane with the extra information of bonds. We call such a diagram a *bonded knotoid diagram*.

We consider each bonding site in a bonded knotoid diagram locally as a rigid planar formation. As such, a bonding arc in a diagram is not subjected to any topological deformations in the plane such as bending, shrinking or enlarging, and any twisting of the bonding arc is avoided. On the other hand, local strands of bonding sites are topologically flexible. More precisely, we allow on bonded knotoid diagrams, the usual Reidemeister moves for knotoids away from the bonds and away from any of the endpoints, and also we allow the bonded moves illustrated in Figure 4.4, each of which is realized in bonding sites. As seen in Figure 4.4a-d, the first two moves, namely bonded twist moves 1 and 2, introduce a twisting in the strands neighboring the bonds. These moves are resulting from a 180-degree turn of the bond, about a vertical and a horizontal axis, respectively. The bonded Reidemeister three move allows an edge of the diagram to slide over or under a bond as a whole without any other change in the bonded knotoid diagram. An edge may be located over or under a bonding arc. The bonded slide moves illustrated in Figure 4.4e,f allow the movement of such an edge located in between the local strands of the bonding site, so that the bonding site is free from any edges other than the bonding arc. The above moves generate an isotopy relation for bonded

knotoid diagrams and an isotopy class of bonded knotoid diagrams is a *bonded knotoid*. The isotopy moves of bonded knotoid diagrams are analogous to what is known in graph theory as rigid vertex isotopy moves [75], if one replaces a bonding site with a rigid vertex.

In order to obtain a (multi-)knotoid diagram from a bonded knotoid diagram, we substitute each bonding site by a chosen full twist (a 360-degree twist) using the following convention. If the local strands are directed anti-parallel then we substitute the bonding site by a full twist of the strands along the bonding arc, as illustrated in Figure 4.5a,b, and the substitution is called of type D. If the local strands are directed parallel then we substitute the site by a full twist of the strands, as shown in Figure 4.5c,d, and the substitution is called of type C. Note that insertions of type D make disconnections in the diagram, while of type C retain connectivity. Either type of full twists can be positive (right-handed) or negative (left-handed). In this paper, all full-twist substitutions are of positive type. After replacing all bonding sites we end up with a planar (multi-) knotoid diagram. Besides, the isotopy moves defined on bonded knotoid diagrams are consistent with the isotopy moves defined on knotoid diagrams after making the twist substitutions. It follows that if two bonded knotoid diagrams are isotopic then the corresponding fknotoid diagrams obtained by full-twist substitutions are isotopic. This means that any topological invariant of knotoids can be used for analyzing the topological type of a knotted bonded open protein chain modeled by bonded knotoid. There are mainly three types of protein bonds: sequential, nested and pseudoknot-like type bonds, as illustrated in Figure 4.5e,f,g. As we see in the figure, all these types of bonds are detected by type D substitutions as compared to the same formations with the bonds ignored. This fact can be proved by applying knotoid invariants such as the Turaev loop bracket polynomial and the arrow polynomial.

An application of our model is illustrated in Figure 4.6 where we consider the protein with PDB entry 2LFK (NMR solution structure of native TdPI-short) [96]. This protein contains two cysteine bridges that appear between residues 24 and 51 (shown as green beads), and between 52 and 69 (shown as red beads) in Figure 4.6a,b. For demonstrative reasons we will discuss the application of our model on a single fixed projection, however one has to have in mind that, following Section 4.1.1, several projections of the backbone have to be analyzed in order to obtain an accurate overview of the topology of the chain. We consider the projection of the protein chain that is shown in

Figure 4.6c, which is a bonded knotoid diagram with two bonding sites. Notice that in the green bonding site an arc of the diagram crosses over the bonding arc and so an immediate application of a full-twist is not possible at this state. An application though of a bonded Reidemeister III move, pushes the arc to the left allowing now the application of a type $C+$ full-twist since the green bonding site is in parallel fashion. The situation for the red bonding site is straight forward. Here we observe that the bonding site is in anti-parallel fashion and so a type $D+$ full-twist substitution is immediately applied giving rise to a multi-knotoid diagram with two components that can be evaluated with any invariant for knotoids such as the Turaev loop bracket polynomial or the arrow polynomial. The vital notice here is that if one drops the bonding information, the structure becomes unknotted. We note here that the same protein has been analyzed in [76,77] for the existence of links where the cysteine bridges are closed with a direct line instead of a full-twist substitution. This explains the difference in the detected link type.

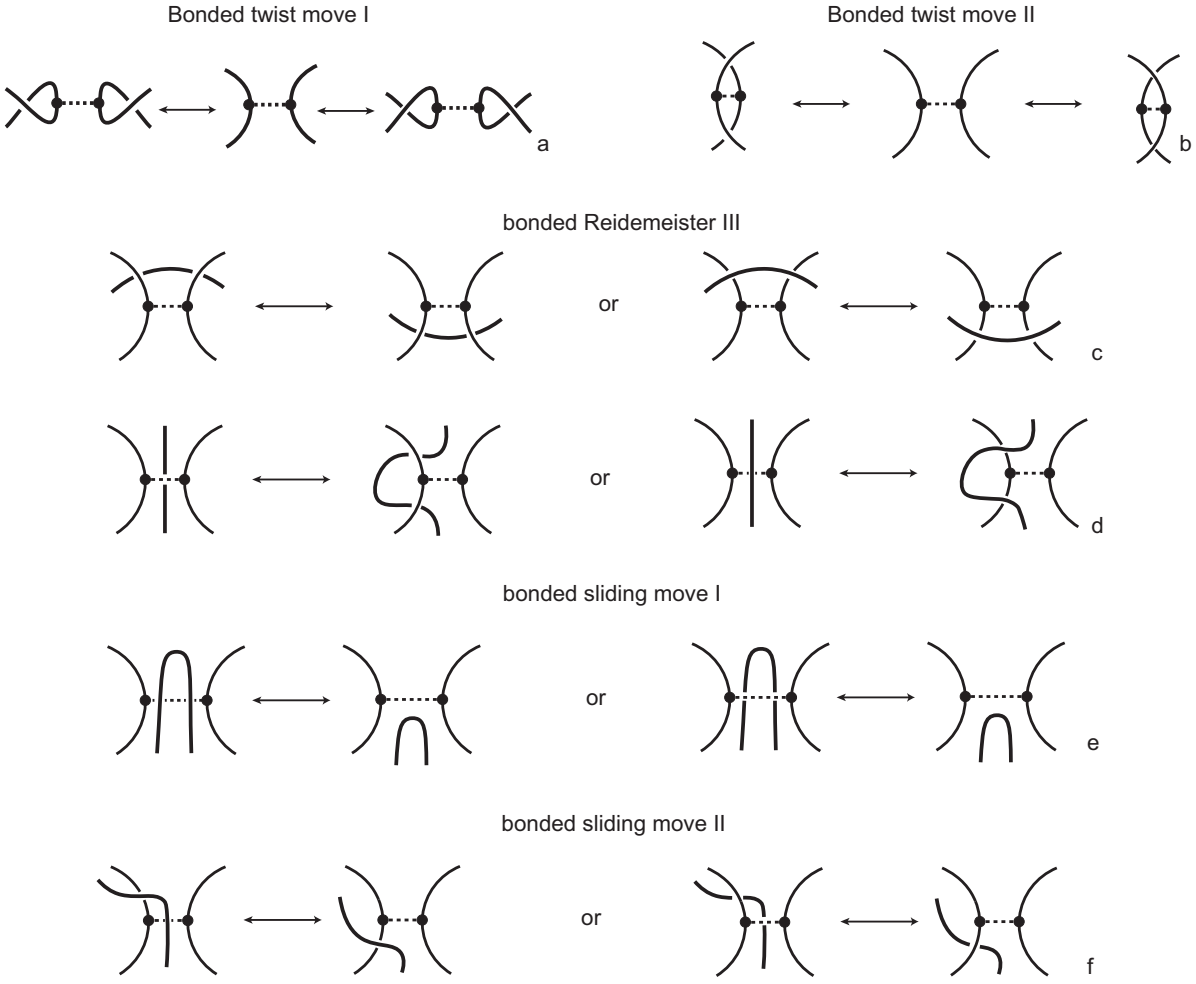

Figure 4.4: The bonded moves, figure taken from [23].

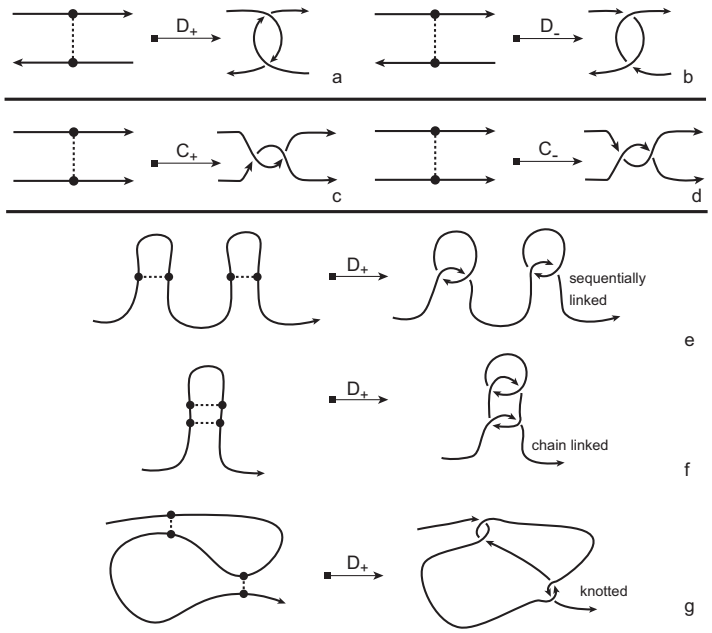

Figure 4.5: Type D (a and b), and type C (c and d) substitutions. Type D substitutions distinguish (e) sequential, (f) nested and (g) pseudoknot-like bonds by applying to the substitution a polynomial invariant for knotoids like the Turaev loop bracket polynomial or the arrow polynomial, figure taken from [23].

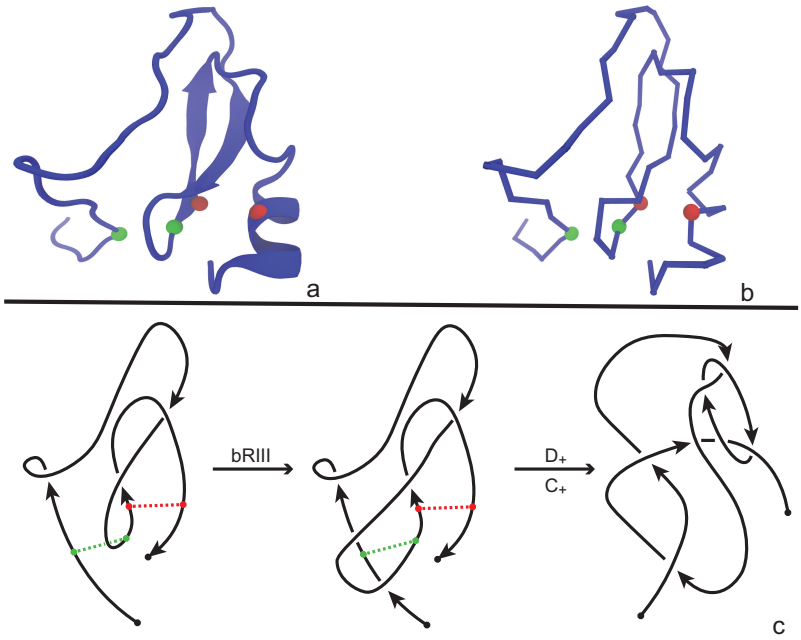

Figure 4.6: The Protein 2LFK as (a) a cartoon, (b) a polygonal curve. A pair of same coloured beads indicate the bonding site . More precisely, the green dots correspond to the pair of residues with indices 24 and 51, while the red to the pair 52 and 69. Below (c) is the corresponding bonded knotoid diagram and the appropriate substitutions. In the diagram the bonds are represented by colored dashed lines; figure taken from [23].

Corollary 12. *[23] Twist substitutions at bonding sites of a bonded protein chain provides detection of sequential, nested and pseaudoknot-like bonds by using a knotoid invariant such as the Turaev loop bracket polynomial or the arrow polynomial.*

4.1.3 An algebraic encoding of protein chains

We finalize this chapter with a proposal for a possible application of braidoids in direction of the above discussion.

As we showed in Section 3.3, any knotoid diagram can be turned into a labeled braidoid diagram. The resulting braidoid diagram can be made algebraic by braidoid isotopy, and can be represented by an expression in terms of elementary blocks. This suggests a possible algebraic encoding for open protein chains or, in general, of linear polymer chains as follows. A polymer chain can be projected to a plane as a knotoid diagram then can be turned into braidoid diagrams by utilizing one of the braidoing algorithms. Finally, one can read the algebraic expression given in terms of the elementary blocks corresponding to the resulting braidoid diagram. An example is illustrated in Figure 4.7, where the knotoid corresponding to the protein 3KZN is turned into a braidoid diagram, which is represented by the word $l_2\sigma_1^3 h_2$ in elementary blocks.

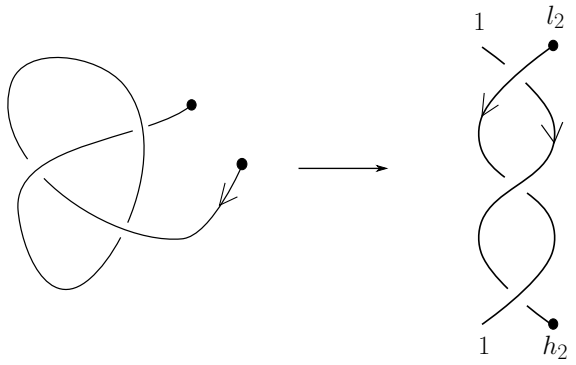

Figure 4.7: A corresponding braidoid diagram to the protein 3KZN

An important topological and computational project is to enumerate all braidoid forms related to a protein form, up to braidoid isotopy and cyclic permutation (preserving braidoid closure). Having such an algebraic tabulation available, would prove useful in the study of proteins, and elements in the protein database could be encoded in this formalism. This project would have a strong impact both on the theory and applications of braidoids.

More precisely, the implementation of such a project would require the following steps:

Step 1: A protein is taken from the Protein Database (PDB) [70]. It is converted to xyz-coordinates and its backbone is extracted (namely, the coordinates of the $C\alpha$ atoms).

Step 2: The reconstructed protein chain is placed inside a large enough sphere and it is projected to, say, 100 different planes perpendicular to corresponding fixed directions evenly distributed on the sphere. The projections are planar knotoid diagrams. We take the dominant knotoid diagram, which is the one with the highest probability of appearance. The steps so far have been implemented in [23].

Step 3: We turn the dominant knotoid diagram into a dominant braidoid diagram using the most efficient braidoiding algorithm for the specific knotoid diagram. It would be very useful to automatize this step through a computer program. We then fill in the braidoid diagram with implicit points and we index accordingly, obtaining the combinatorial dominant braidoid diagram.

Step 4: We list all combinatorial braidoid diagrams that are obtained from the dominant braidoid diagram by braidoid isotopy and cyclic permutation (that preserves braidoid closure). These all have isotopic closures. We then note all words in elementary blocks that our combinatorial braidoid diagrams stand for. This list of words is associated to the original protein form.

Step 5: Any given protein can be then identified by comparing its associated set of algebraic words against the tabulated lists that we produce. The last two steps can be easily implemented to a computer program.

It would be meaningful to generalize the above to the mathematical project of tabulating planar knotoids through their corresponding sets of algebraic expressions. Using braidoids instead of knotoids gives more control and offers the possibility of employing more algebraic techniques in the topological study of proteins and in general of knotoids, as supposed to the diagrammatic methods used so far.

Appendix A

Appendix

A.1 Classical Knots and Braids

In this section, we recall the fundamental definitions/notions of classical knots/links, braids and tangles.

A.1.1 Classical knots and links

Definition A.1. A *classical link* is a smooth embedding of a finite number of disjoint circles in $\mathbb{R}^3$ or S^3.
Specifically, a *classical knot* is a smooth embedding of one circle in $\mathbb{R}^3$ or S^3.

Definition A.2. Two (classical) links are said to be *equivalent* if there is an orientation preserving homeomorphism of $\mathbb{R}^3$ taking one link to the other.
Equivalently, two classical knots/links are said to be isotopic if there is an ambient isotopy of $\mathbb{R}^{\not\vdash}$ taking one knot to the other.

Definition A.3. A *knot/link diagram* is a projection of a knot/link to a plane that is generic in the sense that only transversal double points are allowed as intersection points. The intersection points are endowed with over/under-data accordingly to the weaving of the link in 3-dimensional space.

It is well-known that any classical knot/link admits a diagram. Moreover, the Reidemeister theorem allows us to work with knots/links by their diagram representations in planes.

Theorem A.4. *(Reidemeister theorem) Two knot/link diagrams represent equivalent classical knots/links if and only if they can be obtained by from each*

other by a finite sequence of Reidemeister moves and planar isotopy moves (see Figure 2.2b).

A.1.2 Classical braids

Definition A.5. An n- *strand geometric braid* is a union of n disjoint arcs $\gamma_1, ..., \gamma_n$ in $\mathbb{R}^2 \times [0,1]$ such that γ_i connects $(i, 0, 1)$ to $(f(i), 0, 0)$ where f is a permutation of $\{1, ..., n\}$, and for every z_0 in $[0, 1]$, the intersection of γ_i with the plane $t = t_0$ is exactly one point.

Definition A.6. Two n- strand geometric braids, b, b' are said to be *equivalent* or *isotopic* if there is a continous map $F : b \times I \to \mathbb{R}^2 \times I$ such that for each $s \in I$, the map $F_s : b \to \mathbb{R}^2 \times I$ taking $x \in b$ to $F(x, s)$ is an embedding whose image is an n- strand braid, $F_0 = id_b$ and $F_1(b) = b'$.

A braid whose projection has only double transversal crossings is a *regular braid*. Any geometric braid is isotopic to a regular one.

Definition A.7. A *braid diagram* is the y- projection of a regular n- strand gometric braid satisfying the following:

- The projections of strands are topological intervals each of which is also called a *strand*.
- Every point of $\{1, ..., n\} \times \{0, 1\}$ is the endpoint of a unique strand.
- Every point in $\mathbb{R} \times [0, 1]$ belongs to at most two strands. The strands may intersect each other at a finite number of transversal points that are endowed with over-/under- data accordingly to the weaving of the braid. The intersection points are called *crossings* of the braid diagram.

The oriented Ω_2 and Ω_3 moves (all arcs in the region of moves are directed downward) together with planar isotopies generate an equivalence relation on braid diagrams. We have an analogue of the Reidemeister theorem for braids. That is, two braid diagrams represent isotopic geometric braids if and only if these diagrams are related to each other by a finite sequence of oriented Ω_2, Ω_3, and planar isotopy moves.

Any braid diagram is equivalent to a braid diagram in general position that is, a braid diagram with top-to-bottom direction and, in addition no crossings

are on the same horizontal level. A n-braid diagram in general position can be sliced up so that it can be seen as a word on the basic crossings $\sigma_i^{\pm 1}$ for $i = 1, 2, ..., n-1$ at every horizontal strip. The set of n-braids modulo isotopy gives rise to the braid group B_n with presentation:

$$B_n =< \sigma_1, ..., \sigma_{n-1} | \sigma_i \sigma_j = \sigma_j \sigma_i for |i-j| > 1, \sigma_i \sigma_{i+1} \sigma_i = \sigma_{i+1} \sigma_i \sigma_{i+1} > .$$

The group operation in the group is concatenation (we place one braid on top of the other), and the identity element is the n-braid with no braiding among its strands.

A.1.3 Braids vs Links

The closure of a braid diagram

Any braid diagram determines a link when its ends are connected with embedded arcs in the plane. J. W. Alexander proved in 1923 that in fact any knot/link can be represented as the closure of a braid diagram.

Theorem A.8. *(Alexander theorem) [65] Any oriented classical knot/link can be represented by an isotopic knot/link diagram in braided form.*

Various proofs of the Alexander theorem can be found in [65,71,82,83,85,88,93, 95]. The proof appearing in [85] utilizes *braiding moves* that were introduced by Lambropoulou [83, 84].

Theorem A.9. *(Markov theorem) [87] The closures of two braid diagrams b, b' in $\cup_{n=1}^{\infty} B_n$, represent isotopic links in $\mathbb{R}^3$ if and only if these braids are equivalent by the following operations.*

- *Conjugation: For $b, b' \in B_n$, $b' = gbg^{-1}$ for some $g \in B_n$.*
- *Stabilization: For $b \in B_n$, $b' \in B_{n+1}$, $b' = \sigma_n^{\pm} b$.*

Theorem A.10. *(One move Markov theorem) [84, 85] There is a bijection between the set of L-equivalence classes of braids and the set of isotopy classes of (oriented) link diagrams.*

Bibliography

[1] A. Bartholomew, *Andrew Bartholomew's Mathematics Page: Knotoids*, `http://www.layer8.co.uk/maths/knotoids/index.htm`, January 14, 2015

[2] G. Benkart, T. Halverson, it Motzkin Algebras, European Journal of Combinatorics, **36**, (2014).

[3] S. Bigelow, E. Ramos, R. Yi, *The Alexander and Jones polynomials through representations of Rook Algebras*, Journal of Knot Theory and its Ramifications, **21(12)**, (2012), 18 pages.

[4] J. Scott Carter and S. Kamada and M. Saito, *Stable Equivalence of Knots and Virtual Knot Cobordisms*,Knots 2000 Korea, Vol. 1 (Yongpyong). J. Knot Theory Ramifications, **11**, (2002), no. 3, 311-322

[5] Z. Cheng and H. Gao, *A polynomial invariant of virtual links*, J. Knot Theory Ramifications, **22**, (2013), no:12, 33 pp.

[6] S. Chumutov and S.Duzhin and J. Mostovoy, *Introduction to Vassiliev Knot Invariants*, Cambridge University Press, Cambridge, (2012)

[7] K. Alexander, A.J. Taylor, M.R. Dennis, *Proteins analysed as virtual knots*, Scientific Reports 7, Article Number: 42300, (2017), doi:10.1038/srep4

[8] H.A. Dye and Louis H. Kauffman, *Minimal Surface Representations of Virtual Knots and Links*, Algebr. Geom. Topol., **5**, (2009):509-535

[9] H.A. Dye and A. Kaestner and L.H. Kauffman, *Khovanov Homology, Lee Homology and a Rasmussen Invariant for Virtual Knots* (to appear in Journal of Knot Theory and Ramifications)

[10] H.A. Dye and L.H. Kauffman, *Virtual Crossing Number and the Arrow Polynomial*, J. Knot Theory Ramifications, **18**, (2009), no.10, 1335-1357

[11] S.F. Edwards, *The theory of rubber elasticity*, Br. Polym. J., **9**,**1977**, 140-143.

[12] R. Fenn, M.J-Santana, L. Kauffman, *Biquandles and Virtual Links*, Topology and its Applications, 145 (2004) 157â“175

[13] N.D.Gilbert and T.Porter, *Knots and Surfaces*, Oxford University Press, (1994)

[14] J. Green, *A table of Virtual Knots*, `https://www.math.toronto.edu/drorbn/Students/GreenJ/`, August 10, 2004

[15] N.Gügümcü and L.H.Kauffman, *New invariants of knotoids*, European Journal of Combinatorics, 65C, 2017, pp.

[16] N.Gügümcü and L.H.Kauffman, *On the height of knotoids*, Springer Proceedings in Mathematics Statistics (PROMS) titled: Algebraic Modeling of Topological and Computational Structures and Applications (2017)

[17] N.Gügümcü and L.H.Kauffman, *Parity in Knotoids*, in preparation

[18] N.Gügümcü and S. Lambropoulou, *Braidoids*, in preparation

[19] N.Gügümcü and S. Lambropoulou, *Knotoids, Braidoids and Applications*, Symmetry 2017, 9(12), 315

[20] M. Goussarov, M.Polyak, O. Viro *Finite type invariants of classical and virtual knots*, Topology, **39**, (2000), 1045-1068.

[21] R. H.-Oldenburg and S. Lambropoulou, *Knot theory in handlebodies*, Journal of Knot Theory and its Ramifications, **11**, (2002)

[22] D. Goundaroulis, J. Dorier, F. Benedetti, A. Stasiak, *Studies of global and local entanglements of individual protein chains using the concept of knotoids*, Scientific Reports **7**, Article number: 6309 (2017)

[23] D. Goundaroulis , N. Gügümcü, S. Lambropoulou , J. Dorier , A. Stasiak , L.H. Kauffman, *Topological models for open knotted protein chains using the concepts of knotoids and bonded knotoids*, Polymers, Polymers Special issue on Knotted and Catenated Polymers, Dusan Racko and Andrzej Stasiak Eds. **2017**, 9(9), 444, DOI;10.3390/polym9090444.

[24] Gilbert, N.D. and Porter, T. *Knots and Surfaces*, Oxford Science Publications, (1994), p. 8

[25] N.Kamada and S.Kamada, *Abstract Link Diagrams and Virtual Knots*, J. of Knot Theory and Its Ramifications, **9**,(2000), no.1, 93-106

[26] A. Kaestner, *On Applications of Parity in Virtual Knot Theory*, PhD thesis, University of Illinois at Chicago, USA, (2011)

[27] A. Kaestner and L.H. Kauffman, *Parity, Skein Polynomials and Categorification*, J. of Knot Theory and Its Ramifications, **21**, (10/2011), no.13, 56 pp.

[28] L.H. Kauffman, *Virtual Knot Theory*, European Journal of Combinatorics, **20**, (1999), 663-690

[29] L.H. Kauffman, *Introduction to Virtual Knot Theory*, J. of Knot Theory and Its Ramifications, **21**, (2012), no.13, 37 pp.

[30] L.H.Kauffman, *Detecting virtual knots*, Atti. Sem. Mat. Fis. Univ. Modena, **49**, (Suppl.), (2001), 241-282

[31] L.H.Kauffman, *Knot Diagrammatics*, Handbook of Knot Theory, edited by W.Menasco and M.Thistlethwaite, Elsevier B. V., Amsterdam, (2005), 233-318

[32] L.H. Kauffman, *Knots and Physics*, Fourth edition, Series on Knots and Everything, **53**, World Scientific Publishing Co. Pte. Ltd., Hackensack, NJ, (2013), xviii+846 pp.

[33] L.H. Kauffman, *An affine index polynomial invariant of virtual knots*, J. of Knot Theory and Its Ramifications, **22**, (2013), no.4, 30 pp.

[34] L.H. Kauffman, *New Invariants in the Theory of Knots*, Amer. Math. Monthly, **95**, (1988), 195-242

[35] L.H.Kauffman, *State Models and the Jones Polynomial*, Topology, **26**, (1987), 395-407

[36] Louis H. Kauffman, *A self-linking invariant of virtual knots*, Fund. Math., **184** (2004), 135–158.

[37] L.H. Kauffman and V. Manturov, *Virtual Biquandles*, Fund. Math., **188**, (2005), 103-146

[38] A. Kawauchi, *A Survey of Knot Theory*, Birkhäuser Verlag,Basel, (1996)

[39] Ph. Korablev, Ya. K. May *Knotoids and knots in the thickened torus*, Siberian Mathematical Journal, Vol. 58, No.5. pp. 837-844, 2017

[40] P.B. Kronheimer and T.S. Mrowka, *Khovanov Homology is an Unknot Detector*, Publications mathematiques de l'IHES, **113**, June 2011, , Issue 1, pp. 97-

[41] G. Kuperberg, *What is a Virtual Link?*, Algebraic&Geometric Topology, **3**, (2003), 587-591

[42] Koniaris, K.; Muthukumar, *M. Self-entanglement in ring polymers*, J. Chem. Phys., **1991**, *95(4)*, 2873-2881.

[43] Taylor. W.R. *A deeply knotted protein and how it might fold*, Nature, **2000**, *406*, 916-919.

[44] C. Livingston and J.C. Cha, *A table of Knot Invariants*, `http://www.indiana.edu/~knotinfo/`

[45] V. O. Manturov, *Parity in knot theory*, (Russian) Mat. Sb., **201**, (2010), no.5, 65-110; translation in Sb. Math., **201**, (2010), no. 5, 693-733

[46] V. O. Manturov, *Parity and projection from virtual knots to classical knots*, *Journal of Knot Theory and its Ramifications*, **22**, (2013), (20 pages)

[47] V. O. Manturov, *Knot Theory*, Chapman & Hall/ CRC Press, Boca Raton, FL, (2004)

[48] V. O. Manturov, *Long Virtual Knots and Their Invariants*, J. Knot Theory Ramifications, **13**, (2004),1029-1039

[49] V.O. Manturov and D.P.Ilyutko, The State of Art: Virtual Knots, Series on Knots and Everything:**51**, World Scientific Publishing Co.Pte. Ltd., Hackensack, NJ, (2013)

[50] Y. Miyazawa, *A multivariable polynomial invariant for unoriented virtual knots and links*, Journal of Knot Theory and Its Ramifications, **17**, (2008), no.11, 1311-1326

[51] S. Nelson,*Unknotting virtual knots with Gauss diagram forbidden moves*, J. Knot Theory Ramifications, **10**, (2001), no.6, 931-935.

[52] M. Polyak, *Minimal Generating Sets Of Reidemeister Moves*, Quantum Topology, **1**, (2010), 399-411

[53] R. C. Read and P.Rosenstiehl, *On the Gauss crossing problem* Combinatorics (Proc. Fifth Hungarian Colloq., Keszthely, (1976), Vol.**II**, 843-876, Colloq. Math. Soc. J'anos Bolyai, **18**, North-Holland, Amsterdam-New York

[54] C. Rourke, *What is a welded link?*, Intelligence of low dimensional topology, (2006), 263-270, Ser. Knots Everything, **40**, World Sci. Publ., Hackensack, NJ, (2007)

[55] S. Satoh, *Virtual knot presentation of ribbon torus-knots*, J. Knot Theory Ramifications, **9**, (2000), no. 4, 531-542.

[56] D. Silver, S. Williams, *On a class of virtual knots with unit Jones polynomial*, Journal of Knot Theory and its Ramifications, Vol. 13, No.3, (2004), p.367-371

[57] V. Turaev, *Knotoids*, Osaka Journal of Mathematics, **49**, (2012), no.1 195-223

[58] V. Turaev, *Cobordisms of knots in surfaces*, Journal of Topology, **1(2)**, (2008), 285-305

[59] V.A. Vassiliev, *Cohomology of knot spaces*, Theory of singularities and its applications, Adv. Soviet Math.,**1**, Amer. Math. Soc., Providence, RI, (1990), 23-69

[60] K. Millett, E. Rawdon, A. Stasiak, J. Sulkowska, *Identifying knots in proteins*, Biochem Soc Trans., **41** (2013) , 533–537.

[61] J. Sulkowska, E. Rawdon, K. Millett, J. N. Onuchic, A. Stasiak, *A Conservation of complex knotting and slipknotting patterns in proteins*, **109**, Proc. Natl. Acad. Sci. U. S. A., (2012) E1715.

[62] R. Lua, A. Grosberg, *Statistics of knots, geometry of conformations, and evolution of proteins.* PLoS Comput. Biol., **2** (2006), 350–357.

[63] K.C Millett, A. Dobay, A. Stasiak, *Linear random knots and their scaling behavior*, Macromolecules, (2004) **38**.

[64] M. Jamroz, W. Niemyska, E.J. Rawdon A. Stasiak, K.C. Millett, P. Sulkowski, J.I. Sulkowska *Knotprot: a database of proteins with knots and slipknots*, Nucleic Acids Research, 2015 **43(D1)**, D306-D314.

[65] Alexander, J.W. A lemma on systems of knotted curves. *Proc. Nat. Acad. Sci. U.S.A.* **1923**, *9*, 93–95.

[66] Artin E. Theorie der Zöpfe. *Abh. Math. Sem. Hamburg Univ.* **1926** , **4**, 47–72.

[67] Artin, E. Theory of braids. *Annals Math.* **1947**, *48*, 101-126.

[68] Bartholomew A. Andrew Bartholomew's Mathematics Page: Knotoids. `http://www.layer8.co.uk/maths/knotoids/index.htm`, January 14, 2015.

[69] D. Bennequin, Entrlacements et équations de Pfaffe, *Asterisque* **107-108** (1983) 87–161.

[70] Berman, H.M.; Westbrook, J., Feng, Z., Gilliland, G., Bhat, T.N., Weissig, H., Shindyalov, I.N., Bourne, P.E. The Protein Data Bank. *Nucleic Acids Res.* **2000**, *28*, 235â“242.

[71] Birman J.S. Braids, links and mapping class groups. *Annals of Mathematics Studies* **1974**, *82*, Princeton University Press, Princeton.

[72] Birman J.S.,Menasco W.W. On Markov's Theorem. *J. Knot Theory and Ramifications***2002**,**11** no.3, 295–310.

[73] Brunn H. Über verknotete Curven. *Verh. des intern. Math. Congr.* **1897**, **1**, 256–259.

[74] Shi, D.; Yu, X.; Roth, L.; Morizono, H; Tuchman, M; Allewell, N. M. *Structures of N-acetylornithine transcarbamoylase from Xanthomonas campestris complexed with substrates and substrate analogs imply mechanisms for substrate binding and catalysism*, Proteins: Structure, Function, and Bioinformatics **2006 64**(2),pp. 532-542.

[75] Kauffman L.H., *Invariants of Graphs in Three-Space*, Trans. Amer. Math. Soc., (1989), **311**, pp. 697-710.

[76] Dabrowski-Tumanski, P; Sulkowska, J. I. *Topological knots and links in proteins*, Proc. Natl. Acad. Sci. U. S. A.,(2017), 201615862.

[77] Dabrowski-Tumanski, P.; and Jarmolinska, A.; I and Niemyska, W.; and Rawdon, E. J.; and Millett, K. C.; and Sulkowska, J. I. *LinkProt: a database collecting information about biological links*, Nucleic Acids Res., **2017**, *45*(D1), pp. D243-D249.

[78] Virnau, P.; Mirny, L. A.; Kardar, M. Intricate knots in proteins: Function and evolution. *PLoS Comput. Biol.*, (2006) **2**, 1074–1079.

[79] Mansfield, M. L.*Are there knots in proteins?* Nat. Struct. Biol., (1994) **1**, pp. 213-214.

[80] Tian, W.; Lei, X.; Kauffman, L.H.; and Liang, J. *A knot polynomial invariant for analysis of Topology of Rna Stems and Protein Disulfide Bonds. DeGruyter Mol.Based Math.Bio.*(2017)**5**, pp.21-30.

[81] N. Lim, S. Jackson, *Molecular knots in biology and chemistry*, Journal of Physics, Condens. Matter 27 (2015)

[82] Kauffman, L. H., Lambropoulou, S. Virtual braids. *Fundamenta Mathematicae* **2004**, *184*, 159-186.

[83] Lambropoulou, S. Short proofs of Alexander's and Markov's theorems. Warwick preprint **1990**.

[84] Lambropoulou, S. A study of braids in 3-manifolds. PhD thesis, University of Warwick, **1993**.

[85] Lambropoulou S., Rourke C. P. Markov's theorem in 3-manifolds. *Topology and its Applications* **1997**, *78*, 95-122.

[86] Lambropoulou S. Braid equivalences and the *L*-moves. In Introductory Lectures on Knot Theory with subtitle Selected Lectures presented at the Advanced School and Conference on Knot Theory and its Applications to Physics and Biology, ICTP, Trieste, Italy, 11 - 29 May 2009; L.H. Kauffman, S. Lambropoulou, J.H. Przytycki, S. Jablan, Eds.; Ser. Knots Everything, vol. 46; World Scientific Press, 2011; pp. 281-320. See also ArXiv.

[87] Markov, A. A. Über die freie Äquivalenz geschlossener Zöpfe. *Rec. Math. Moscou* **1936**, *1* (43), 73-78.

[88] Morton, H. R. Threading knot diagrams. *Mathematical Proceedings of the Cambridge Philosophical Society* **1986**, *99*, 247-260.

[89] L.Solomon, *Representations of Rook monoid*, Journal of Algebra, **256**, (2002), 309- 342.

[90] Shi, D., Yu, X., Roth, L., Morizono, H., Tuchman, M., Allewell, N.M. Structures of N-acetylornithine transcarbamoylase from Xanthomonas campestris complexed with substrates and substrate analogs imply mechanisms for substrate binding and catalysis. *Proteins* **2006**, *64*, 532-542.

[91] Traczyk, P. A new proof of Markov's braid theorem. *Banach Center Publications* **1992**, *42*, Institute of Mathematics Polish Academy of Sciences, Warszawa (1998).

[92] Kassel C., Turaev V. *Braid groups*. Volume 247 of Graduate Texts in Mathematics, Springer, New York, 2008.

[93] Vogel P. Representation of links by braid: A new algorithm. *Commentarii Mathematici Helvetici* **1990**, *65*, 104-113.

[94] Weinberg N. Sur l' equivalence libre des tresses fermée. *Comptes Rendus (Doklady) de l' Académie des Sciences de l' URSS* **1939**, **23**(3), 215–216.

[95] Yamada S. The minimal number of Seifert circles equals the braid index of a link. *Invent. Math.***1987**, **89**, 347–356.

[96] S. Bronsoms, D. Pantoja-Uceda, D. Gabrijelcic-Geiger,L. Sanglas, F. X. Aviles, and J. Santoro, C. P. Sommerhoff, J. L. Arolas, *Oxidative folding and structural analyses of a kunitz-related inhibitor and its disulfide intermediates: functional implications*, *J. Mol. Biol.*, **414**(3), 2011, pp. 427-441.